

NAVAL POSTGRADUATE SCHOOL
Monterey, California



THESIS

**PREDICTION OF WIRELESS COMMUNICATION SYSTEMS
PERFORMANCE IN SHIPBOARD COMPARTMENTS IN THE
2.4 GHz ISM BAND**

by

John Martinos

March 2001

Thesis Advisor:
Co-Advisor:

Jovan Lebaric
David Jenn

Approved for public release; distribution is unlimited.

20010612 006

REPORT DOCUMENTATION PAGE			Form Approved OMB No. 0704-0188	
Public reporting burden for this collection of information is estimated to average 1 hour per response, including the time for reviewing instruction, searching existing data sources, gathering and maintaining the data needed, and completing and reviewing the collection of information. Send comments regarding this burden estimate or any other aspect of this collection of information, including suggestions for reducing this burden, to Washington headquarters Services, Directorate for Information Operations and Reports, 1215 Jefferson Davis Highway, Suite 1204, Arlington, VA 22202-4302, and to the Office of Management and Budget, Paperwork Reduction Project (0704-0188) Washington DC 20503.				
1. AGENCY USE ONLY (Leave blank)		2. REPORT DATE March 2001		3. REPORT TYPE AND DATES COVERED Master's Thesis
4. TITLE AND SUBTITLE Prediction of Wireless Communication Systems Performance in Shipboard Compartments in the 2.4 GHz ISM Band			5. FUNDING NUMBERS	
6. AUTHOR(S) Martinis, John				
7. PERFORMING ORGANIZATION NAME(S) AND ADDRESS(ES) Naval Postgraduate School Monterey, CA 93943-5000			8. PERFORMING ORGANIZATION REPORT NUMBER	
9. SPONSORING / MONITORING AGENCY NAME(S) AND ADDRESS(ES)			10. SPONSORING / MONITORING AGENCY REPORT NUMBER	
11. SUPPLEMENTARY NOTES The views expressed in this thesis are those of the author and do not reflect the official policy or position of the Department of Defense or the U.S. Government.				
12a. DISTRIBUTION / AVAILABILITY STATEMENT Approved for public release; distribution is unlimited.			12b. DISTRIBUTION CODE	
13. ABSTRACT (maximum 200 words) A physical understanding and consequent mathematical modeling of RF energy in naval indoor environments is of vital importance to the usability and effectiveness of communication systems used by Navy. Over the last few years, there is a growing interest in placing Wireless Local Area Networks (WLANs) in ships and submarines. Especially large ships yet to be constructed, are designed with increased electronic systems but limited personnel. Reliable electronic systems will be crucial for efficient ship operation and survivability. This thesis investigates the feasibility of deploying a physical model called Numerical Electromagnetic Code-Basic Scattering Code (NEC-BSC) to simulate confined naval compartments in the 2.4 GHz Industrial Scientific Medical (ISM) band. More specifically, using NEC-BSC the coverage area, the number and positions of transmitters and observation points and the statistics of Radio Frequency (RF) signal distribution were described. The area specifically targeted for this research was a typical two-story missile room. Additionally, some important conclusions regarding the validity of NEC-BSC for indoor applications are presented and some recommendations for future research are provided.				
14. SUBJECT TERMS Simulation of signal propagation, indoor radio propagation, NEC-BSC			15. NUMBER OF PAGES 246	
			16. PRICE CODE	
17. SECURITY CLASSIFICATION OF REPORT Unclassified	18. SECURITY CLASSIFICATION OF THIS PAGE Unclassified	19. SECURITY CLASSIFICATION OF ABSTRACT Unclassified	20. LIMITATION OF ABSTRACT UL	

THIS PAGE INTENTIONALLY LEFT BLANK

Approved for public release; distribution is unlimited.

**PREDICTION OF WIRELESS COMMUNICATION SYSTEMS PERFORMANCE IN
SHIPBOARD COMPARTMENTS IN THE 2.4 GHz ISM BAND**

John Martinos
Lieutenant J.G., Hellenic Navy
B.S., Hellenic Naval Academy, 1993

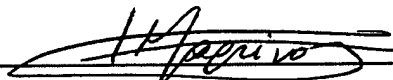
Submitted in partial fulfillment of the
requirements for the degrees of

**MASTER OF SCIENCE IN ELECTRICAL ENGINEERING
and
MASTER OF SCIENCE IN SYSTEMS ENGINEERING**

from the

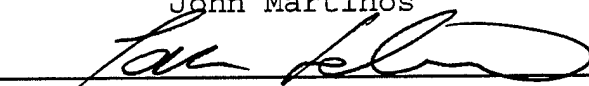
**NAVAL POSTGRADUATE SCHOOL
March 2001**

Author:

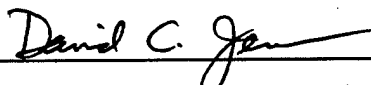


John Martinos


Approved by:



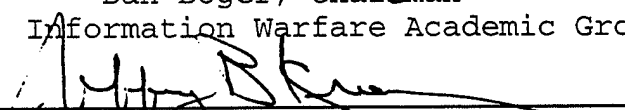
Jovan Lebaric, Thesis Advisor



David Jenn, Co-Advisor



Dan Boger, Chairman
Information Warfare Academic Group



Jeffrey B. Knorr, Chairman
Department of Electrical and Computer Engineering

THIS PAGE INTENTIONALLY LEFT BLANK

ABSTRACT

A physical understanding and consequent mathematical modeling of RF energy in naval indoor environments is of vital importance to the usability and effectiveness of communication systems used by Navy. Over the last few years, there is a growing interest in placing Wireless Local Area Networks (WLANs) in ships and submarines. Especially large ships yet to be constructed, are designed with increased electronic systems but limited personnel. Reliable electronic systems will be crucial for efficient ship operation and survivability.

This thesis investigates the feasibility of deploying a physical model called Numerical Electromagnetic Code-Basic Scattering Code (NEC-BSC) to simulate confined naval compartments in the 2.4 GHz Industrial Scientific Medical (ISM) band. More specifically, the coverage area, the number and positions of transmitters and observation points and the statistics of Radio Frequency (RF) signal distribution were described. The area specifically targeted for this research was a typical two-story missile room. Additionally, some important conclusions regarding the validity of NEC-BSC for indoor applications are presented and some recommendations for future research are provided.

THIS PAGE INTENTIONALLY LEFT BLANK

TABLE OF CONTENTS

I. INTRODUCTION	1
A. WIRED VS WIRELESS COMMUNICATION	1
B. WIRELESS PROPAGATION BACKGROUND	2
C. THE PHYSICS OF PROPAGATION	6
D. FUNDAMENTALS OF ANTENNAS	10
1. Radiation Pattern	10
2. Near Field and Far Field Regions	12
E. OBJECTIVE AND APPROACH	14
F. THESIS OUTLINE	15
II. INDOOR PROPAGATION MODELS AND THESIS OBJECTIVES	17
A. COMPARISON BETWEEN INDOOR AND OUTDOOR MODELS	17
B. MODELS FOR INDOOR PROPAGATION	18
C. POTENTIAL BENEFITS FOR THE NAVY	22
D. OPERATION, IMPLEMENTATION AND SAFETY ISSUES	23
III. NEC-BSC SOFTWARE OVERVIEW	25
A. INTRODUCTION OF NEC-BSC	25
B. NEC-BSC MODELS AND LIMITATIONS	25
C. MODELING THE STRUCTURE	29
D. MAJOR COMPONENTS OF NEC-BSC MAIN PROGRAM	31
E. TABLE OF COMMANDS	32
IV. DEVELOPMENT OF BASIC EXAMPLES	33
A. COMPARISON OF NEC-BSC AND "PATCH" CODE RCS PREDICTIONS	33
B. SIMPLE ROOM WITH METALLIC WALLS	36
C. COMPLEX ROOM WITH METALLIC WALLS	39
D. OPENINGS	44
V. TYPICAL MISSILE ROOM	51
A. GENERAL DERSCRIPTION	51
B. NEC-BSC MODEL SPECIFICS	55
C. SIMULATION RESULTS	56
1. Antenna Located in the Middle of the Room	56
2. Results for the Antenna in an "Arbitrary" Location ...	60
3. Results for two Antennas in the Missile Room	63
4. Floor-to-Floor Propagation	65
D. PROPAGATION STATISTICS FOR THE MISSILE COMPARTMENT	68
1. Theoretical Background	68
2. Results	73
VI. UNRESOLVED ISSUES, RECOMMENDATIONS, AND CONCLUSIONS	95
A. UNRESOLVED PROBLEMS	95
1. Floor-to-Floor Propagation	95
2. Problematic PN Command	95
3. Running Time	96
B. RECOMMENDATIONS	96
C. CONCLUSIONS	98

APPENDIX A. MATLAB FILES	103
APPENDIX B. NEC-BSC INPUT FILES	107
APPENDIX C. MATHCAD FILES	171
LIST OF REFERENCES	223
INITIAL DISTRIBUTION LIST	229

ACKNOWLEDGEMENT

During this Thesis research, I had the privilege to receive assistance from many individuals who made the process a tolerable experience.

At first, I would like to thank Dr. D. Jenn for providing his support, guidance and advice to my efforts. I wish to express my appreciation to the author of NEC-BSC Dr R. Marhefka. The inherent nonideality of this deterministic model while it complicated the life of his scientists, actually simplified my work and quite often made it a pleasurable experience. Dr. R. Adler clarified many essential issues of the software. I felt honored to have been given the insightful instruction of the only person at NPS with prior exposure on NEC-BSC. I would also like to thank the outstanding professors and staff of NPS for their tutoring and assistance in my learning endeavors.

A very special thanks is extended to Hellenic Navy for giving me the chance to fulfill a lifetime dream. In addition, thanks are due Lt. Bolanis Ilias for his excellent partnership. It was a delight to work with a model partner whose cooperation was provoking, rewarding and enriching. I am thankful for having had the opportunity to work with Dr J. E. Lebaric. Not only had he been an excellent advisor, but also a collaborator, a

partner, a friend. His eagerness to impart knowledge was the driving power that kept me on the track to accomplish my goal.

I am also much appreciative of all advice, enduring faith and continuous support that my parents have given me from thousands of miles away. Through their example I was taught a good work ethic and I was encouraged in all my undertakings. I would like to acknowledge the love and patience of my wife, Zoi. Despite the loneliness she often tolerated as a Navy spouse, Zoi always unselfishly kept my well being and happiness as her primary concern. She put up with countless hours of neglect and inattention to family matters.

Most importantly, I wish to express my humble gratitude to my Heavenly Father and Savior Jesus Christ for blessing me with all the help necessary to accomplish this difficult task. "HE has turned all my sunsets into dawns".

EXECUTIVE SUMMARY

Indoor wireless systems are already used in a huge variety of office, residential and even military environments. Two types of models, the empirical and the physical ones, are powerful tools, capable of simulating a given confined area and collecting significant databases.

The Numerical Electromagnetic Code-Basic Scattering Code (NEC-BSC), developed at Ohio State University under government contract, is a well-known physical model in electromagnetic field theory. Over the last ten years it has been of great use in analyzing scattering and radiation problems and visualizing the flow of energy from antennas. Given that the code's applicability has recently been proved reliable for complex buildings [37], we tested its performance to a typical missile room of a military ship in the 2.4 GHz ISM band.

At first, the case of the electric field returned by a smooth perfectly conducting convex surface was investigated. Then, the results were compared to the ones obtained by the reliable software called "PATCH", within the framework and limitations of the Method of Moments (MOM). The comparison offered encouraging results. In addition, other simple geometries were simulated in order to gain familiarity with the code and its limitations. The

goals, however, were to construct a typical missile room with material (metallic) uniformity, examine the electric field strength coverage maps and perform a statistical analysis of the electric field strength variation.

To this end, the antenna was placed in four different positions and data were collected. Then the excess "room gain" over free space of the same volume was calculated within certain distances from the antenna, called "distance groups." Next, the probability density function (pdf) and cumulative distribution function (cdf) of the variation of the "room gain" variable was introduced. It appeared that the key parameter in defining the mean value of the excess gain was the relative number of observation points that were shadowed by the obstacles and thus experience non-line-of-sight propagation attenuation. In any case, however, the distribution followed the lognormal one and its pdf and cdf obeyed the Gaussian ones. Finally, the mean value of the "room gain" ranged from -0.1 dB to + 2.91 dB.

I. INTRODUCTION

A. WIRED VS WIRELESS COMMUNICATION

The last century has seen the rise of telephony, as well as the successful deployment of wireless communications. The introduction of these inventions underscored, without doubt, a fundamental change in the way people communicated and was a critical step toward shattering the barriers of time and space. To date, however, the hindrance of location has not been conquered, since most individuals are still confined to wired equipment for communications [1].

Rapid changes in word communications have been prompted by demand for more reliable and convenient ways to communicate. Especially during the past decade, wireless services proved to be cost effective solutions for providing data due to their inherent advantages over the conventional, wired services. These advantages include simplicity and ease of use, integrity and reliability, compatibility with existing networks without the need for expensive and time-consuming rewiring. In addition, there is more immunity to natural and man made disasters, flexibility of shifting terminals and equipment around, relatively easy maintenance, providing services for a

larger number of users, roaming and, finally, elimination of wiring around and inside buildings. The introduction of successful wireless systems is comparable in significance with that of any major invention made during the 20th century. The deployment of wireless systems is increasing, while the wired communications is holding steady if not decreasing.

All the aforementioned advantages of using wireless communication mainly in small or large offices, public services buildings and even military environments, have built a potential market of a very large number of users. In order to meet these demands, new systems have been and are being designed to provide services of the best possible quality in indoor and outdoor environment [2].

B. WIRELESS PROPAGATION BACKGROUND

Radio communication, to date, is enjoying the fastest growth period in history, since enabling technologies permit wide spread deployment. During the past decade, radio communications business has grown by orders of magnitude, fueled by large-scale circuit integration, digital and radio frequency (RF) circuit fabrication improvements and other miniaturization technologies which

make radio equipment smaller, less heavy and more affordable and reliable [3].

The Ultra High Frequency (UHF) electromagnetic spectrum ranges from 300 MHz to 3 GHz. There is much more frequency space available for communications in this band than in the entire spectrum below. Moreover, high directivity obtainable at microwave frequencies makes reuse of these frequencies possible in the same area.

The most basic model of radio wave propagation involves the ideal "free space" model which treats the region between the transmit and receive antennas as being free of all objects that might absorb, refract, reflect, diffract or scatter radio frequency energy. It thus follows that, within this region, the medium behaves as a perfectly homogeneous and nonabsorbent medium. Furthermore, earth is treated as being infinitely far away from the propagating signal (or, equivalently, as having a reflection coefficient that is negligible).

In free space the spreading of RF energy creates apparent attenuation between the transmitter and receiver according to an inverse-square law. In typical broadcasting applications radio waves emanate from a point source of radio energy, traveling in all directions along

straight lines, filling the entire spherical volume of space with radio energy that varies in strength with a $1/(\text{range})^2$ rule (or 20 dB per decade increase in range). The received power, expressed in terms of transmitted power, is attenuated by a factor called (free space) path loss.

Calculating free space loss is quite simple. Consider a transmitter with power P_t coupled to an antenna, which radiates equally in all directions (an isotropic antenna). At a distance d from the transmitter, the radiated power is distributed uniformly over an area of $4d^2$ (i.e. the surface area of a sphere of radius d), so that the power flux density is:

$$s = \frac{P_t}{4\pi d^2} \text{ Watts/m}^2 . \quad (1.1)$$

The transmission loss then depends on how much of this power is captured by the receiving antenna. If the capture area, or effective aperture of this antenna is A_e then the power, which can be delivered to the receiver (assuming no mismatch or feed line losses), is simply:

$$P_r = sA_e \text{ Watts.} \quad (1.2)$$

For the hypothetical isotropic receiving antenna and a wavelength λ we have:

$$A_e = \frac{\lambda^2}{4\pi} \text{ m}^2. \quad (1.3)$$

Combining all equations, we obtain:

$$P_R = P_t \left(\frac{\lambda}{4\pi d} \right)^2 \text{ Watts.} \quad (1.4)$$

The free space path loss between isotropic antennas is then P_t/P_r . For this case of idealized propagation, received signal power is very predictable.

In reality, however, propagation rarely follows the free space model. Three major mechanisms, which are going to be examined in the next pages, dominate in the radio propagation: (1) reflection, (2) diffraction and (3) scattering. All three of these phenomena result in radio signal distortions, additional losses, and cause signals to fade.

C. THE PHYSICS OF PROPAGATION

The phenomena, which govern radio propagation, can be very complex and diverse. However, we can categorize them according to the three major mechanisms of object interaction (reflection, diffraction and scattering).

Reflection occurs when a propagating electromagnetic wave impinges upon an object, which has very large dimensions compared to the wavelength of the propagating wave. Reflections occur from the surface of the earth and from buildings and walls, and reflected waves can interfere constructively or destructively at the receiver [3].

Diffraction occurs when the radio path between the transmitter and receiver is obstructed by an impenetrable surface. The secondary waves resulting from the obstructing surface are formed throughout the space and even behind the obstacle, giving rise to an apparent bending of waves around the obstacle, enabling reception even when a line-of-sight (LOS) path does not exist between transmitter and receiver. Diffraction is assumed to be a strictly local phenomenon; this means that the diffracted field depends only on the power of the incident field at the exact diffraction point, and on the local geometry of the diffracting object [3].

At high frequencies, diffraction, like reflection, depends on the geometry of the object, as well as the amplitude, phase, and polarization of the incident wave at the point of diffraction. Because of diffraction RF energy can be received, even though the source is "shadowed" by an obstacle [3].

Scattering occurs when the medium through which the wave travels contains objects ("obstacles") with dimensions that are small compared to the wavelength, and where the number of obstacles per unit volume is large. Scattered waves are produced by rough surfaces, atmospherics (rain and snow), or by other irregularities in the channel. Foliage, street signs, and lampposts induce scattering in a mobile communications system. Figure 1 shows the different propagation mechanisms in the presence of an arbitrary, impenetrable obstacle.

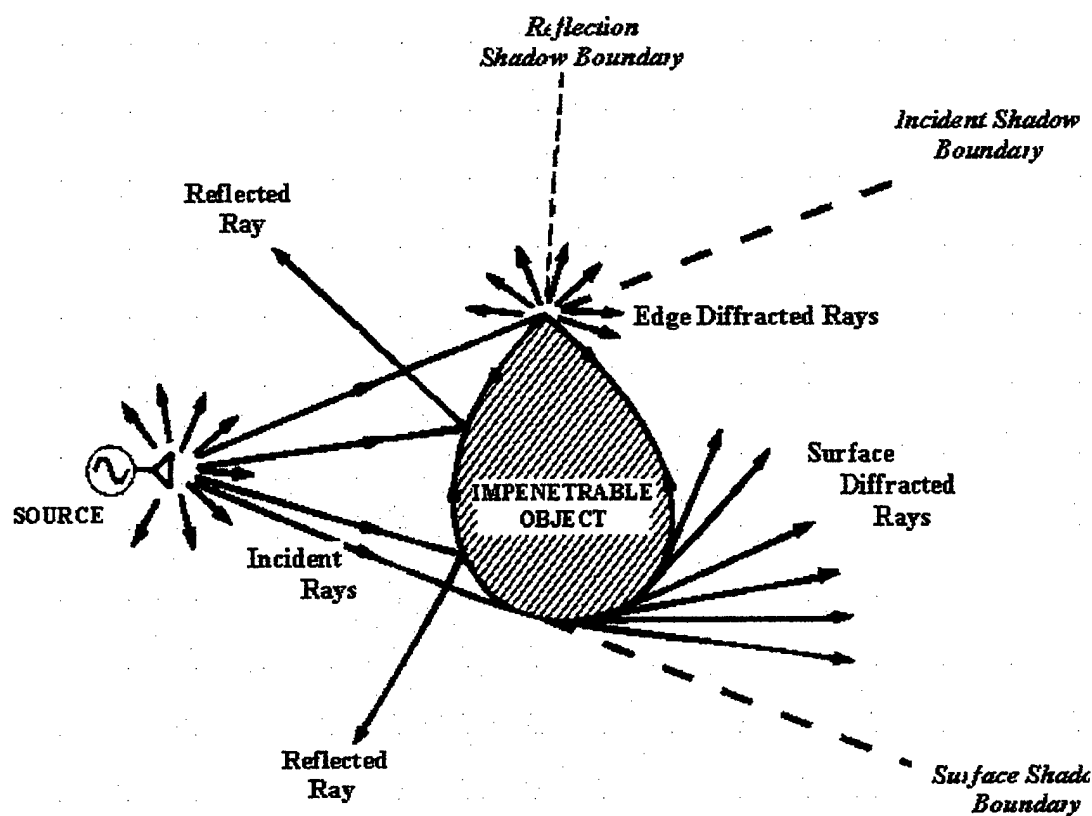


Figure 1. Different Propagation Mechanisms in the Presence of an Arbitrary, Impenetrable Obstacle (from [4]).

In practice, not only metallic materials cause reflections, but also dielectrics (or electrical insulators). Insulators are not as efficient at reflecting radio signals as metal surfaces, but even common insulating materials do cause some reflection of radio waves. Multipath occurs when all the radio propagation effects combine in a real world environment. In other words, when

multiple signal propagation paths exist, caused by whatever phenomenon, the actual received signal level is a vector sum of the all signals incident from all directions. Some signals will aid the direct path (assuming that the direct path exists), while other signals will subtract (or tend to vector cancel) from the direct signal path. The total composite phenomenon is called multipath.

As a mobile receiver moves through a specific indoor space, the three phenomena affect the instantaneous received signal in different ways. For a clear LOS path to the transmitter, diffraction and scattering will not dominate. On the other hand, in an environment where there are many obstacles of different sizes and constituent materials and the direct channel is blocked between the receiver and the transmitter, diffraction as well as scattering are most likely to dominate [5].

Two kinds of multipath exist: (1) specular multipath arising from discrete, coherent reflections from smooth metal surfaces, and (2) diffuse multipath arising from diffuse scatterers and sources of diffraction (the visible glint of sunlight off a choppy sea is such an example). Both forms of multipath are undesired for radio communications. Diffuse multipath provides a sort of

background "noise" level of interference, while specular multipath can actually cause complete signal outages and radio "dead spots" within a building.

Another phenomenon, called scintillation, describes the rapid fluctuation of the phase and intensity of a radio signal that has passed through the earth's ionosphere, typically on a satellite-to-ground propagation channel. This phenomenon is similar to the twinkling of stars in the night sky, except in this case the fluctuations are caused by small-scale variations (irregularities) in the ionospheric plasma density along the propagation path followed by the signal.

D. FUNDAMENTALS OF ANTENNAS

1. Radiation Pattern

The antenna's radiation pattern is the graphical representation of the radiation characteristics of the antenna as a function of space coordinates. The most usual representation is the three-dimensional spatial distribution of radiated energy along an observer's position at a constant distance from the antenna. The graph of the spatial variation of the electric field along that path is called a field pattern.

An isotropic antenna is defined as a hypothetical lossless antenna that radiates or receives equally in all directions. Clearly, an isotropic antenna is a fictitious entity, since even the simplest antenna has some degree of directivity. However, an isotropic radiator represents a convenient reference for comparing the directional properties of physical antennas. On the other hand, a directional antenna radiates or receives electromagnetic energy more effectively in some directions than in others. As an example, the radiation pattern of a half-wave linear dipole is shown in Figure 2.

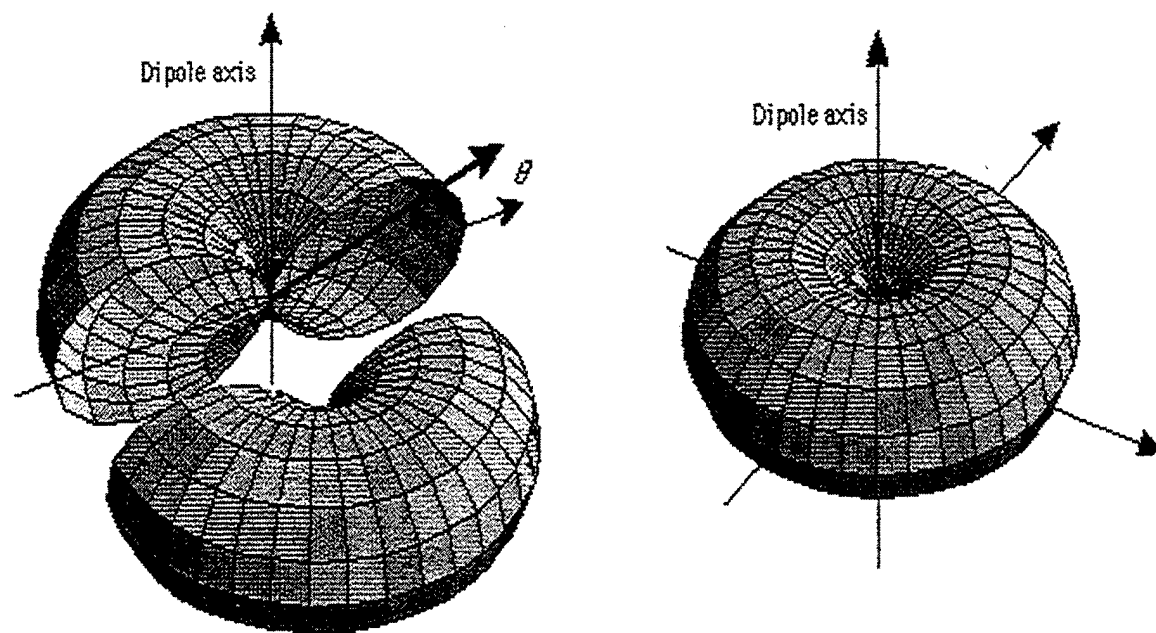


Figure 2. Power Pattern of a Half-Wave Dipole (from [6]).

2. Near Field and Far Field Regions

The antenna's electromagnetic (EM) field can be classified according to the relative (in terms of operating wavelength) distance to the antenna as:

- The reactive near field region adjacent to the antenna. In this case, the field patterns change rapidly and reactive energy is stored around the antenna
- The radiating near field region (for large antennas known as the Fresnel region). Again, the field patterns change rapidly, but radiating energy oscillates towards the antenna.
- The furthestmost, the far field region, commonly referred to as the Fraunhofer region, has no reactive energy and is represented by a spherical wave (for any realistic antenna of finite size) propagating away from the antenna.

Certain behavior characteristics of EM fields dominate at one range from the radiating antenna, while others, completely different, can dominate at another distance. In order to categorize characteristics of electromagnetic fields as a function of distance from the radiating source, we define the following boundaries: the "Near-Field

boundary," the "Far-Field boundary" and the "Transition Zone boundary," which has a combination of the characteristics found in both fields. The regional boundaries are usually categorized as a function of the operating wavelength (λ).

We must state, however, that these regions categorize behaviors, which may vary even within each region. In addition, the boundaries for these regions are approximate "rules of thumb" (more precise boundaries can be defined based primarily on antenna type and antenna size, and even then the experts differ). Figure 3 shows these regions and boundaries.

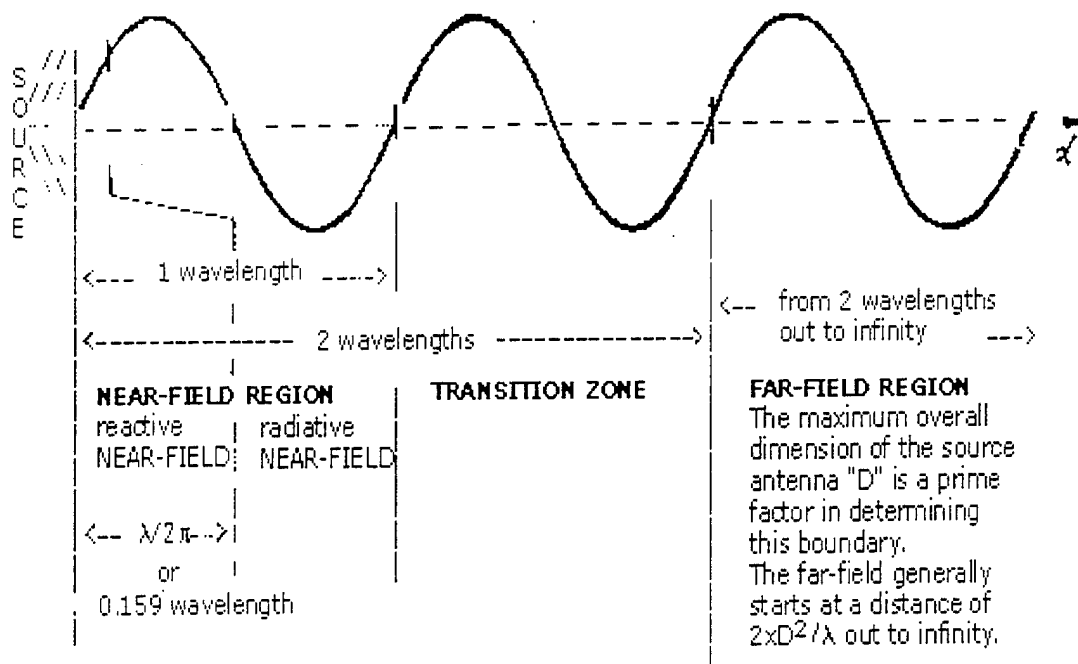


Figure 3. Antenna Field Regions for Typical Antennas (from Ref. [7]).

When placing an antenna, it is of vital importance to remove all objects from at least the near field, since their presence can alter the design radiation and impedance characteristics unpredictably.

E. OBJECTIVE AND APPROACH

The objective of this thesis is to evaluate the Numerical Electromagnetic Code - Basic Scattering Code (NEC-BSC), for shipboard (indoors) wireless propagation prediction. Using the code, we will predict the signal strength distribution for wireless communication in the 2.4

GHz Instrumentation-Scientific-Medical (ISM) band for a given antenna location in a shipboard compartment. Simulation results will be presented graphically and the signal strength statistics will be extracted from the results.

F. THESIS OUTLINE

This thesis consists of six chapters and is organized as follows. Chapter I compares the wired and wireless communication and provides the introduction of the RF propagation. Chapter II describes the theoretical principles of indoor propagation. Chapter III presents the NEC-BSC software overview. Chapter IV describes some basic examples and the associated results obtained by using NEC-BSC code. Chapter V provides the development of a realistic model of a shipboard compartment, the simulation results and the statistics for signal propagation. Finally, chapter VI concludes the thesis and present recommendations for future work.

THIS PAGE INTENTIONALLY LEFT BLANK

II. INDOOR PROPAGATION MODELS AND THESIS OBJECTIVES

A. COMPARISON BETWEEN INDOOR AND OUTDOOR MODELS

Outdoor environments are characterized by significant signal strength fluctuations caused by reflection, diffraction, and scattering. These signal strength variations may have a range of 30 to 40 dB at Ultra High Frequencies (UHF) and account for some of the difficulties that a designer of reliable radio communications systems has to cope with. For example, if we shift the receiver by a distance of a half-wavelength in a random direction, the received signal magnitude may change drastically. The basic signal attenuation with range noticed in the real world describes the so-called "large scale" effects, while the signal strength fluctuations with motion are reported "small scale" effects [8].

Outdoor propagation models presented by Ibrahim [Ref. 10], Okumura [11] and Hata [12], have been developed for large cells, whereas for indoor communications the suitable cell diameter is substantially smaller and such cells are usually termed as nanocells and picocells. Hence, the outdoor models are inadequate for accurate indoor propagation prediction.

Indoor propagation, although dominated by the same mechanisms, can not be treated as an extension of outdoor propagation. For example, signal levels depend on whether interior doors and windows are open or closed. Also, the location of antennas affects the large-scale phenomena, since an antenna mounted at a floor level in a partitioned room receives different signals than that same antenna mounted above the floor. Moreover, in a room crowded with obstacles, all propagation mechanisms become more and more complex and the smaller propagation range makes it even more difficult to ensure far-field radiation for all plausible types of antennas and receiver positions.

B. MODELS FOR INDOOR PROPAGATION

To make things more challenging, it is impossible to design an "RF friendly" building, free of multipath reflections from numerous smooth surfaces, diffraction around sharp corners or scattering from walls and ceilings. In addition, the RF signal is subject to temporal variations due to the motion of people, doors, etc. [13], [14], [15], [16].

Radio wave propagation inside metal-walled compartments such as a missile room of a military ship is dominated by strong reflections off the compartment walls.

In such an environment, signal strength at 2.4 GHz can vary dramatically over a distance of a few centimeters. Despite these problems, we are still capable of predicting radio propagation in a typical room or a shipboard compartment. To this effect a number of models have been developed and semi-empirical formulas for indoor signal propagation prediction developed from propagation studies. Figure 4 illustrates the results of a study of a signal at 1.8 GHz, penetrating a window of a typical room.

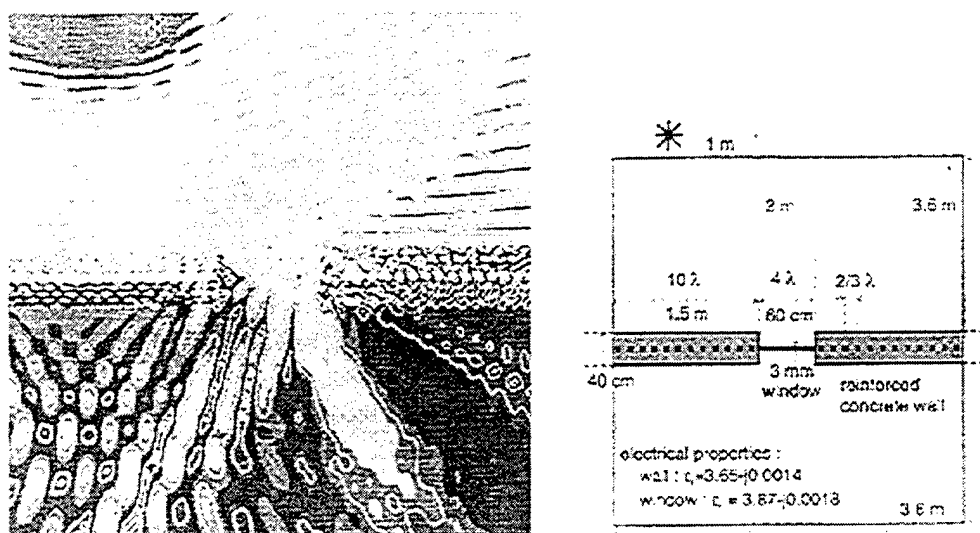


Figure 4. The Penetration of a Mobile Phone Signal at 1.8 GHz Through a Window in a Reinforced Concrete Wall is Studied by Means of a Two-Dimensional Model. Right: Geometry. Left: Field Levels in dB Due to the Line Source in the Left Upper Corner. (From [17]).

Generally, models can be classified as either statistical, based on empirical data, or deterministic, valid for the specific environment under consideration.

Some models do not belong in either category, since they are a combination of those two. These are referred to as *hybrid models*.

Statistical models [18] and [3], are based on fitting curves or analytical expressions to observed empirical data, such that the propagation mechanisms are accounted for in an average sense. Since reality seldom corresponds to relatively simple mathematical models, a certain range of error cannot be avoided. The accuracy of these models depends on the accuracy of the measurements taken, as well as the similarities of the room to be examined with the (usually simpler) room in which the results were collected. However, the statistical models are simple to implement and computationally efficient.

With *Deterministic models*, (also called *site specific (SISP) models* [19], [20], [21], [22], [23], [24], [25] specific environments are characterized individually (rooms, buildings, tunnels, shipboard compartments etc.). In this way the model accuracy is improved, as long as there is detailed database available for the geometry, materials, location/motion of people etc for the indoor environment under consideration. The obvious and very important drawback in this case is that even if the

geometry/media database is available, the algorithms for indoor propagation calculation are typically very complex and, depending on the accuracy desired, model calculations can be extremely time consuming.

In general, various "ray tracing" algorithms are employed for indoor propagation prediction. Such algorithms typically implement an exhaustive search of a "ray tree" as follows: first and foremost, a ray tracing code detects if there is a LOS path between the receiver and the transmitter and determines the RF energy received via the direct path. Then, depending on the source ray algorithm, the program detects if an object intersection occurs. If such is the case, code distinguishes the phenomenon as scattering or diffraction or reflection and computes the received signal, otherwise process stops and a new ray is "launched." Typically, as the number of rays encountered in the problem increases linearly, the number of required computation increases exponentially. Therefore, for given computational resources, there is a limit on the relative size of the indoor geometry that a particular code can be applied to.

Hybrid models [19], [26] can be a successful combination of the statistical and site-specific models by

trading accuracy for computational efficiency. A survey of field strength prediction models is presented in [27].

NEC-BSC utilizes ray-tracing technique based on the Uniform Theory of Diffraction (UTD) and the geometry and materials data for the specific environment to be analyzed. Therefore it can be classified as a physical model.

C. POTENTIAL BENEFITS FOR THE NAVY

As mentioned previously, the majority of materials used in a shipboard compartment are metals (good conductors) that can be approximated as Perfect Electric Conductors (PECs). However, the geometry of a shipboard compartment (on the scale of the operating wavelength) can be very complex and the behavior of the transmitted signals can be difficult to predict. Furthermore, very limited and often classified research and documentation is available for shipboard wireless propagation.

In 1998, a bistatic measurement system was developed for the 0.8 to 3 GHz frequency range [28]. Experiments took place onboard the former USS SHADWELL for a variety of types of confined rooms, locations of transmitters and receivers, as well as open or closed door configurations. The results led to the conclusion that the expected elimination of RF energy due to the ship's metallic

structure (bulkheads, tanks, overheads, watertight doors, etc.) did not apply. The major phenomenon observed, was an approximate 10-dB signal attenuation for each closed passageway door and/or bulkhead [28].

Let us now examine the motives that urged the Navy to sponsor these and other similar measurements. Over the last few years, there is a growing interest in placing Wireless Local Area Networks (WLANs) in ships and submarines. Future generations of large ships are being designed with more and more electronic systems but with fewer personnel. Currently, it is generally agreed that WLANs are more efficient than conventional LANs. First, WLANs can provide services almost everywhere on the ship, without the physical limitations that cables have. WLANs also mitigate problems due to physical damage to wires or fiber optic cables. Finally, a sophisticated WLAN can also offer installation flexibility, reduced cost and ability to transfer vast amounts of sensor data related to condition, operation and damage control of the majority of ship's departments.

D. OPERATION, IMPLEMENTATION AND SAFETY ISSUES

So far, the most common and convenient application has been the hand-held walkie-talkies that crewmembers use.

During state of readiness, communication can be established from various locations even if all intermediate watertight doors are closed. However, this application could lead to mild to severe Electromagnetic Interference (EMI) problems [28].

For all potential WLAN applications, EMI is the system "bottleneck." Therefore, WLANs have to be designed using the best combination of transmitter power, receiver performance and operating frequency. In 1985, the Federal Communication Commission (FCC) authorized license-free spread spectrum RF communications for low power (less than 1 watt) transmitters in the 910 MHz, 2.44 GHz, and 5.8 GHz ISM bands [29]. This enabled a rapid growth of spread spectrum WLAN industry, primarily for commercial applications. Lately, the technology is being applied to military use as well. Finally, since the transmitter power levels of WLAN systems are typically less than 1 Watt and radiated power density is attenuated at least 20 dB per decade increase in range, crewmembers present in a WLAN coverage area are not at risk to high RF exposure.

III. NEC-BSC SOFTWARE OVERVIEW

A. INTRODUCTION TO NEC-BSC

NEC-BCS, developed at Ohio State University under government contract, has been used over the last ten years for solving EM scattering and radiation problems [34]. More specifically, this user-oriented code is capable of analyzing near and far field radiation and scattering in an arbitrarily shaped room/compartment at UHF (300 MHz to 3 GHz) and above. Rooms and compartments can be modeled by combining a number of basic structural shapes: multi-sided flat plates and finite elliptic curved surfaces like cylinders, cone frustums, and finite composite ellipsoids.

Over the past years, NEC-BSC has been successfully used to predict scattering from superstructures of ships, wings of aircraft, large tanks and indoor compartments of space stations, simulated using perfectly conducting materials. The newest version of NEC-BSC (4.2) incorporates a thin dielectric slab option, hence the code can be used to model propagation within buildings with non-metallic walls [38].

B. NEC-BSC MODELS AND LIMITATIONS

NEC-BSC utilizes advanced formulations based on the Geometric Theory of Diffraction (GTD) and Uniform Theory of

Diffraction (UTD) [30], [31] to solve problems involving electromagnetic coupling, scattering, diffraction and computation of near- and far-field antenna patterns.

Geometrical Theory of Diffraction is a high-frequency technique suitable for the analysis of antennas that are large in terms of wavelength (λ) and located in a complex environment. Keller [32], [33] originally formulated GTD as an extension of Geometrical Optics (GO). GTD proved to be very reliable in calculating the non-zero fields in a shadow region. This was accomplished by introducing a set of diffracted rays analogous to the reflected and transmitted rays of GO.

In NEC-BSC, ray-tracing algorithms define the parameters of the field incident onto various obstacles. The diffracted rays are then defined by UTD for all incident rays, and added to the geometrical optics terms for the observation points of interest. Since most of the scattered and diffracted rays will encounter obstacles themselves, a rapidly increasing number of higher order scattered and diffracted rays will be created. In order to limit the number of computations for a solution with acceptable accuracy, a sophisticated code is required to "trace out" the various possible combinations that will not

contribute significantly to the total field at the selected observation points. In this manner only the components with the strongest contributions need to be calculated, thus increasing the code's computational efficiency.

There are, however, some limitations of this user-oriented code, which basically occur due to the very nature of the algorithms employed [34]. Since all diffracted components are calculated using UTD, each plate should have edges of at least a wavelength long. In terms of curved surfaces their major and minor radii and length should be at least a wavelength in extent. Furthermore, for dielectric (non-metallic) obstacles, the source has to be located at least a wavelength away from the surface and the incident field angle of incidence should not be too close to the grazing angle. Also, the dielectric layer must be thin, at most half of the operating wavelength. For example, at 2.4 GHz (12.5cm wavelength) dielectric thickness must be less than 6.25 cm. Moreover, antenna elements have to be at least half a wavelength from all edges. In any case, the antenna can not be mounted on curved surfaces.

Limitations on the NEC-BSC accuracy also stem from the high order term elimination. Eliminating higher order

diffracted rays improves computational efficiency, but it also makes the code unsuitable for certain types of EM calculations. For example, higher order diffracted rays are important for accurately predicting the radar cross section of a complex structure. Furthermore, flat plates and simple curved surface models are not always adequate for modeling complex environments found within buildings or shipboard compartments. Due to all these limitations, NEC-BSC program proved to give accurate results for approximately the first 25 dB of the results dynamic range.

As a whole, the present NEC-BSC execute module will accommodate models with the following parameter limits:

- Pattern points = 1801
- Defined pattern points = 181
- Defined frequencies = 181
- Plates = 200
- Plate edges = 30
- Curved entities = 200
- Curved sections = 10
- Material types = 25
- Material layers = 20
- Sources = 300

- Receivers = 300
- Antenna data points = 91
- Wires = 200

C. MODELING THE STRUCTURE

Most of the structures of practical interest can be successfully approximated by a combination of multi-sided flat plates and some finite elliptic surfaces. These can consist of either good conductors (even PECs) or dielectrics. A group of flat plates, each having a certain number of edges, can model most of the objects with slowly varying radii of curvature. In either case there is a certain procedure that one has to follow in order to construct an arbitrary object.

If a plate has to be modeled, one first has to specify the corners in a three dimensional Cartesian coordinate system. The only condition is that all these corners should form a flat plate. If the points are difficult to specify, the user can simply construct the plate in two dimensions and then rotate or translate it into its desired location in three dimensions using the appropriate commands provided by the software.

A plate can be attached to another plate in NEC-BSC in two different ways. First, two plates can share a pair of

corners, forming a wedge. The angle of the wedge is defined by the angle of the two plates, based on the direction of antenna's illumination. Alternately, one plate can be mounted slightly within the volume of the other. By piecing together a number of such isolated plates, a larger, more complex general structure can be approximated with sufficient accuracy.

NEC-BSC also has the capability to implement electrically thin dielectric layers in order to model structures like non-metallic doors, walls, glass windows, furniture, etc. For flat dielectric plates, the user has to specify the thickness (not exceeding one half of the operating wavelength), relative permittivity, relative permeability, and the loss tangents for the material.

If a surface with a non-trivial curvature has to be modeled, one can use elliptic cylinders, cone frustums and composite ellipsoids. In NEC-BSC all curved surfaces, are defined by their center coordinates and their major and minor axes. In case of an elliptic cylinder, the position of the first and the last cap is given with respect to the cylinder axis. The cone frustum is characterized by the position of its rim junctions. Finally, the ellipsoid is

constructed by setting different values of radii curvature along its maximum and minimum z-axis positions.

D. MAJOR COMPONENTS OF NEC-BSC MAIN PROGRAM

The NEC-BSC code is constructed in a systematic manner, meaning that all procedures are categorized and executed in modular sections. Figure 5 shows the major components of the NEC-BSC program.

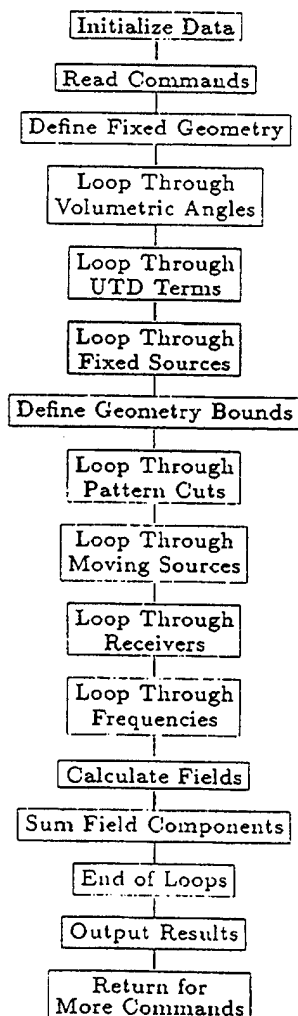


Figure 5. Block Diagram of NEC-BSC Main Program (from [34]).

In the input part the problem geometry is specified. The second section prepares all necessary parameters for later use. In the following section the fields resulting from individual propagation mechanisms are calculated and added to form the solution. Finally, all the outputs are provided to the user, either in the form of numerical results or as ray path visualization.

E. TABLE OF COMMANDS

A listing of NEC-BSC commands is provided in the preliminary draft of the NEC-BSC user's manual. (The listing of commands is still incomplete at the time of this writing). The commands can be grouped into six broad categories: the geometry control commands, the structure definition commands, the antenna definition commands, the pattern control commands, the output control commands, and the program control commands. In creating a NEC-BSC input file the order of groups should be as given above, but there is no required order for the commands within the same group. The default unit is meters for all lengths and the default frequency is 299.9 MHz. All angles are specified in degrees. The following examples illustrate most of these points and validate a sample NEC-BSC solution.

IV. DEVELOPMENT OF BASIC EXAMPLES

In this chapter, NEC-BSC results for several sample problems are presented. All pertinent Matlab, NEC-BSC, and Mathcad files are included in Appendices A through C, respectively.

The sample problems have been selected to illustrate various features of NEC-BSC. Each problem has been selected in order to show specific code capabilities and convenient options, as well as some unresolved problems still present in the most recent version of the code. The collection of results provides an insight into the tradeoffs of the NEC-BSC use for indoor propagation prediction.

A. COMPARISON OF NEC-BSC AND "PATCH" CODE RCS PREDICTIONS

The problem of EM scattering by a smooth, perfectly conducting convex surface, is investigated in this section. The scattered field results obtained from the "PATCH" code [9] will be compared to the scattered field calculated by the NEC-BSC for the same geometry. The first example involves an infinitely thin electric dipole, shown as a red dot in Figure 6, located parallel and relatively close to a metallic circular cylinder. The cylinder axis coincides with the z-axis of the coordinate system. The operating

frequency is 2.54 GHz, which corresponds to the operating wavelength of 11.81 cm. The obstacle is a metallic cylinder 1 meter in length and having a 17.5 cm radius. The antenna is 1 meter from the surface of the cylinder. The observation points of interest form a horizontal circle of 360 points, 5 meters away from the cylinder axis, as shown in the Figure 6.

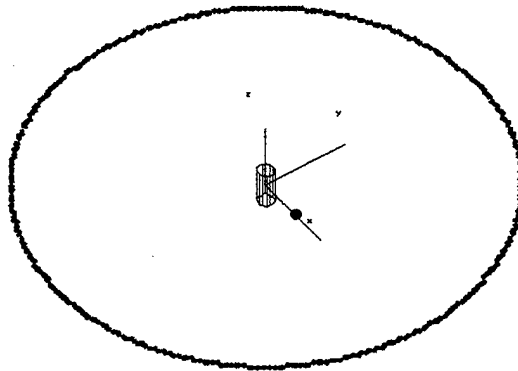


Figure 6. Geometry of the PEC Convex Surface and the Dipole.

The validity of NEC-BSC results is shown by comparing the NEC-BSC results with the solution obtained for the same problem by using the "PATCH" code. The results from the

two codes are shown combined in a single graph in Figure 7.

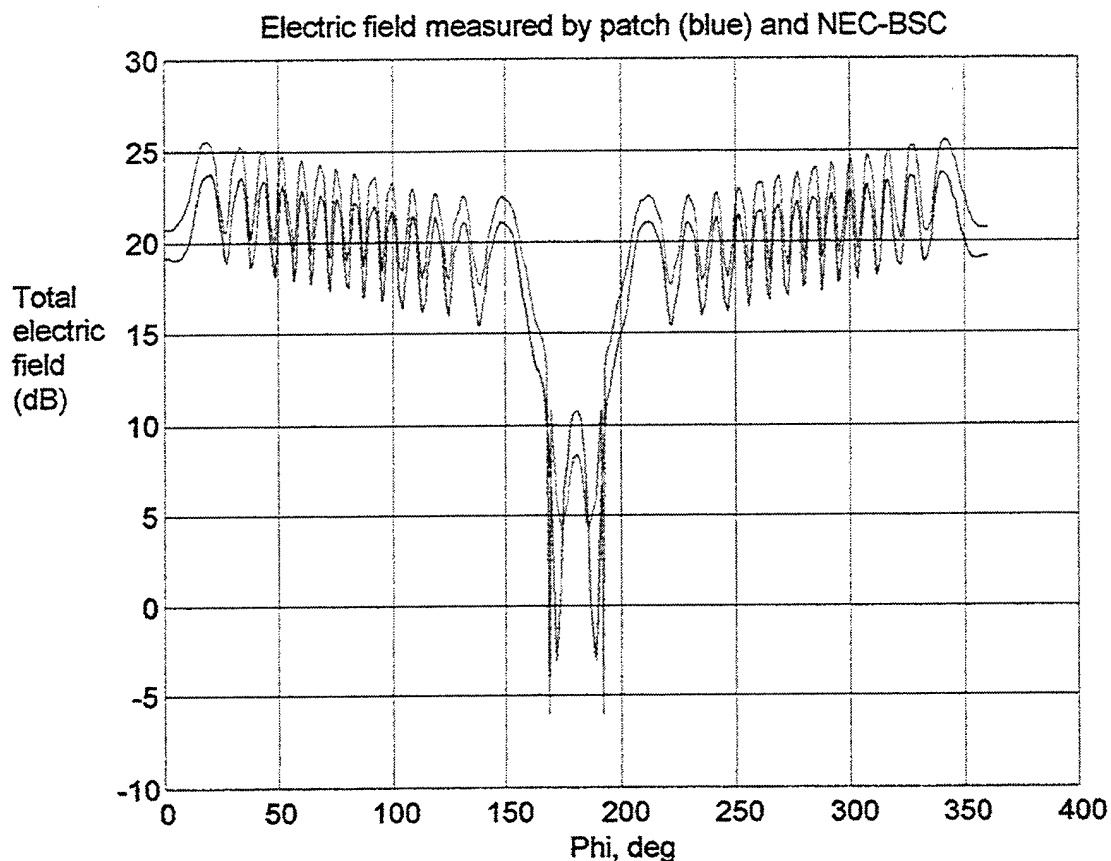


Figure 7. Comparison of Electric Fields Calculated by NEC-BSC and PATCH Codes.

It can be clearly stated that the match is not perfect. Although the number of minima and maxima are the same and the "shape" of the field variation with angle is almost identical, there is approximately 1.7 dB difference between the values at each point of the graph. Moreover, in the very deep shadow area exactly behind the cylinder, there seems to be some differences as well, although at a

relatively low level. Despite the small differences, there is good enough agreement between the two to validate the NEC-BSC code results.

NEC-BSC has been also extensively validated by its author. User's manual [34] contains several examples involving metallic cylinders, where patterns were taken in many different cuts, for many source positions and for different polarization. For these examples, comparison of NEC-BSC predictions with the measured results shows a very good agreement.

B. SIMPLE ROOM WITH METALLIC WALLS

This example considers a simple room with PEC walls and the following dimensions:

- Length of six meters
- Width of twelve meters
- Height of twelve meters.

The room walls are modeled using six PEC plates. Inside, there is a half-wavelength antenna located at (3,1,11) with respect to the origin, as shown in Figure 8 (the antenna is depicted as a red dot). The operating frequency is 2.4 GHz, which corresponds to a wavelength of 12.5 cm. A large metallic cylinder, representative of a missile tube, is positioned in the room such that the

antenna illuminates only about half of the surface of the cylinder. Our objective, in this specific example, is to visualize the propagation paths, especially the non-LOS ones. The observation points are thus positioned in a semicircle and appear as gray dots in the figure below.

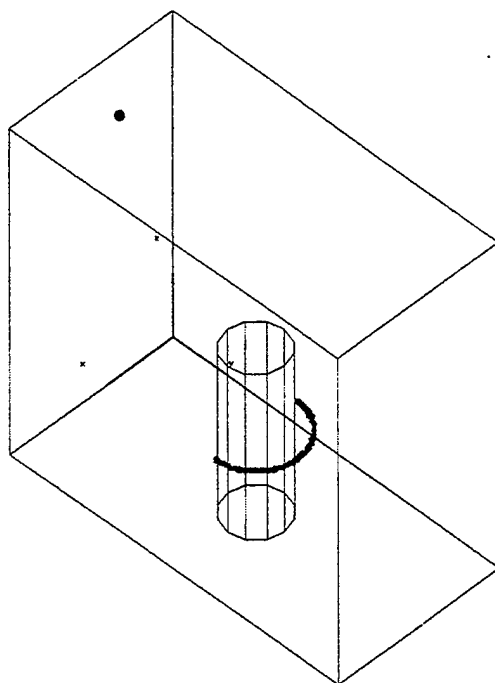


Figure 8. Room With PEC Walls and a Single PEC Cylinder.

Running the NEC-BSC program for even this relatively simple geometry results in a plethora of rays. Hence, even if we rotate or zoom into the figure, we will not get a clear picture of the individual propagation mechanisms involved.

NEC-BSC, however, provides the user with two very convenient options. The first is that the user can adjust the dynamic range of the results (in the ray menu) such that only the strongest rays are displayed (e.g., for LOS paths and single reflections only). For instance, in Figure 9 only the rays within 1 dB of the strongest ray are shown. Second, we can select a specific ray and transfer it to a figure, which only shows the geometry of the room (the "drag and drop" method). Therefore a "hand-picked" number of rays can be superimposed to the room geometry. To illustrate this for the room with the single cylinder example, only the diffracted rays to some certain observation points are shown in Figure 10.

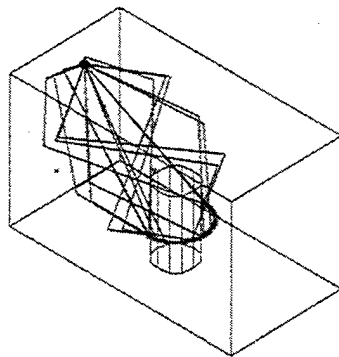


Figure 9. Propagation Paths for Signals Within 1 dB of the Strongest Signal Path.

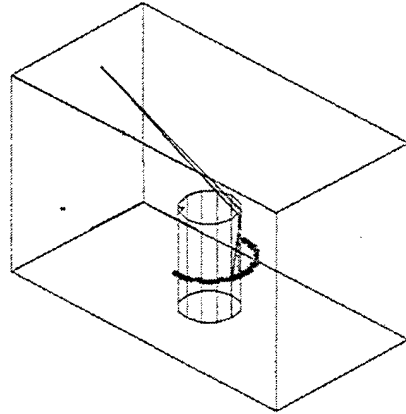


Figure 10. Sample Diffracted Rays, "Isolated" from Figure 7.

C. COMPLEX ROOM WITH METALLIC WALLS

Let us now consider a more complex room with PEC walls and the same dimensions as the room from the preceding section:

- Length of six meters
- Width of twelve meters
- Height of twelve meters.

Six PEC plates form the room. Inside, there is a half-wavelength antenna located at (3,3,1) with respect to the origin, depicted as the red dot. The operating frequency is 2.45 GHz, which corresponds to the wavelength

of 12.245 cm. Two large, vertical metallic cylinders, representing missile tubes, are placed in the center of the room. In addition, two large metallic tanks are located along the front and the rear wall of the room, as shown in Figure 11. The objective, in this specific example, is to obtain relative signal strength "map" of the room, revealing the areas where the received signal is strong, weak or virtually non-existent.

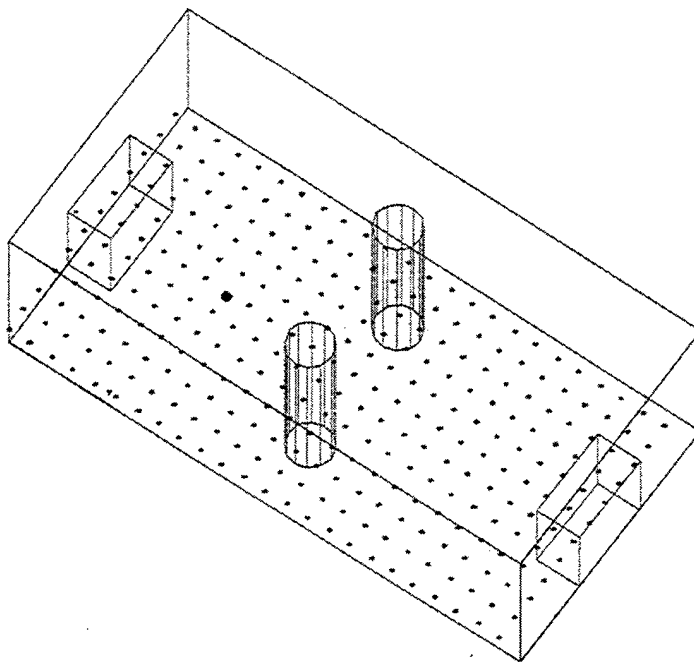


Figure 11. Room With PEC Wall, Two PEC Cylinders and Two PEC Storage Tanks

NEC-BSC does not have the 3D "relief map" plot capability to represent the calculated fields. A program has been written in Mathcad to create the relative signal strength "relief" (3D) map. More specifically, using the Notepad application, we convert the data file that NEC-BSC creates for the electric field at the observation points to an ASCII text file (*.txt extension). The ASCII data file is next imported into a Mathcad script, and the electric field magnitude is plotted in dB, as shown in the next Figure.

The observation points are all in the same plane so that the two horizontal axes are the coordinates in the observation plane and the color-coded vertical axis (the "height") indicates the electric field strength.

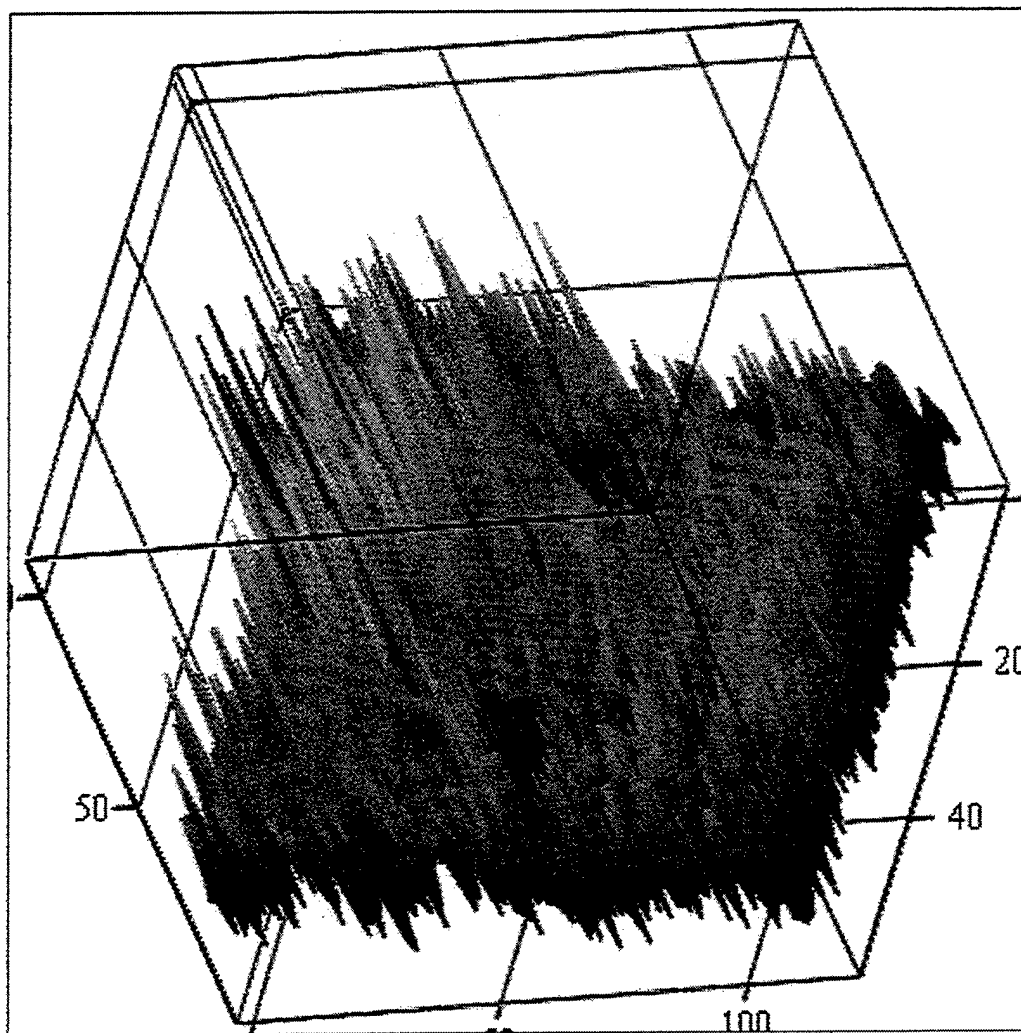


Figure 12. Signal Coverage of the Room, in Which Red Corresponds to 0 dB and Blue to -25 dB.

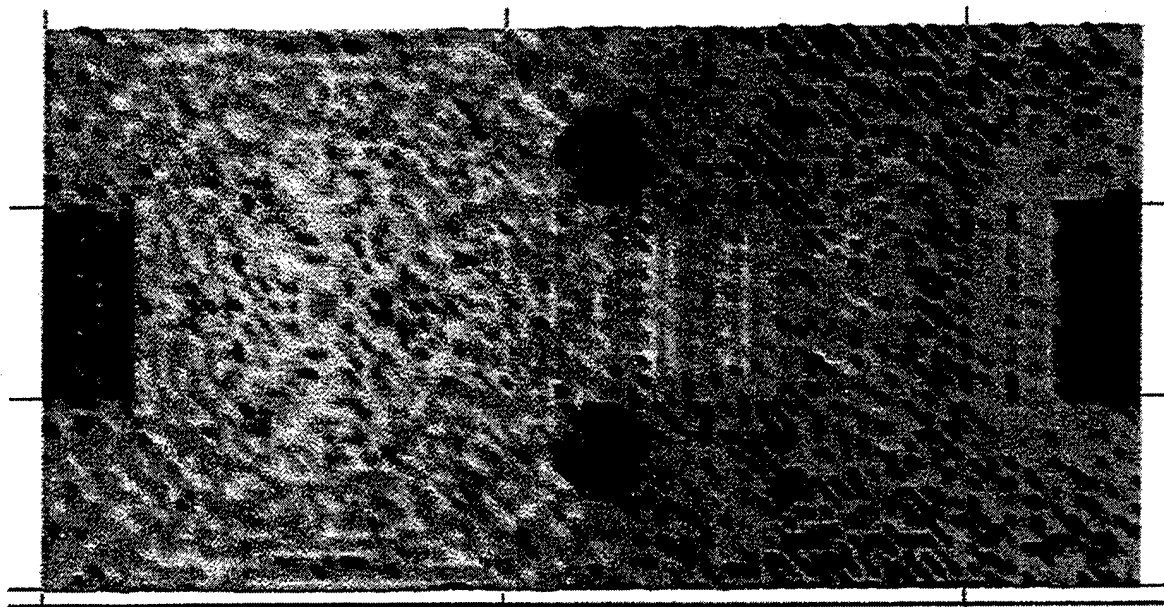


Figure 13. Top View of the Signal Coverage of the Room, in Which Red Corresponds to 0 dB and Blue to -25 dB.

The red color identifies the areas of the highest signal strength while blue identifies the areas of weakest signal. It is important to remember that although the NEC-BSC will report signal strengths with very high dynamic ranges, the NEC-BSC user's manual [34] cautions that only about 30 dB of the dynamic range (30 dB down from the highest signal level) should be considered reliable. Therefore, one can opt to place a threshold at 30 dB below the largest signal strength and thus establish a scale with red color indicating the largest signal strength and blue color indicating signal strengths at 30 dB lower (than the maximum).

As expected, the signal strength for observation points within PEC objects (the two cylinders and the tanks) are represented by blue color, while the area close to the antenna has a large number of red "spikes" corresponding to the standing wave peaks. The pronounced standing waves are a consequence of strong reflection off the PEC walls, cylinders and tanks. The field strength maps also reveal the presence of the signal in the "shadow" zones area behind the cylinders, due to diffracted and "creeping" waves.

D. OPENINGS

In this section the performance of NEC-BSC is evaluated for openings such as doors, hatches, and windows. The opening will be constructed according to the method recommended in the NEC-BSC user's manual. An electrically large opening, showing in Figure 14, will be constructed using a number PEC plates attached together (by the virtue of shared corner pairs). These individual plates form a larger flat plate with the opening in the middle. A half-wavelength antenna is positioned on one side of the opening and a set of observation points is defined on the opposite side as shown in Figure 15. In addition to the direct rays passing through the opening we expect to see the rays

diffracted from the edges of the opening, but no rays diffracted from the "seams" of the individual plates forming the large plate with the opening. The operating frequency is 2.4 GHz.

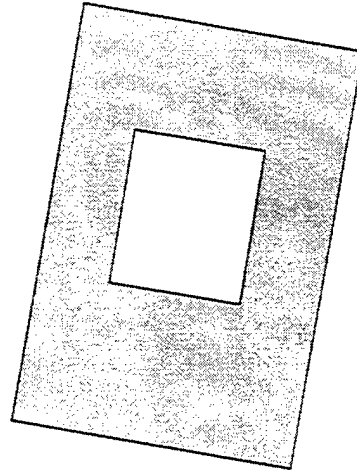


Figure 14. The Electrically Large Opening (White Area) Which Must be Simulated.

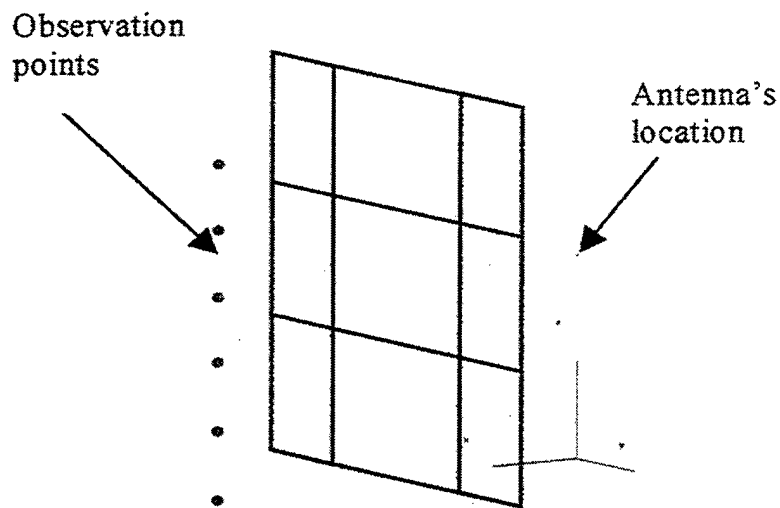


Figure 15. The Flat PEC Plate With the Opening in the Middle, as Constructed by NEC-BSC.

The NEC-BSC results for the PEC plate with the opening show that, in addition to the rays diffracted from the edges of the opening, there are non-physical rays diffracted by the seams of the individual plates, as shown in Figures 16 and 17.

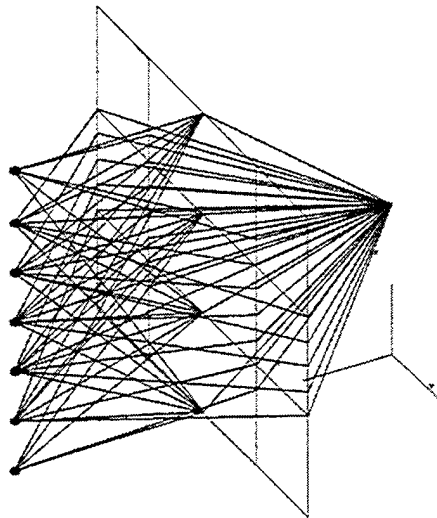


Figure 16. Sample Propagation Paths for the PEC Plate With the Opening.

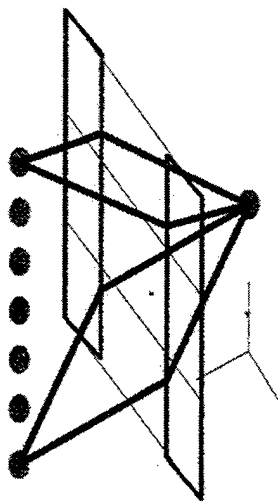


Figure 17. Non-Physical Rays "Diffracted" by the Plate "Seams."

Unfortunately, this problem was not resolved either by constructing the large plate using overlapping (by 0.1 of the wavelength) individual plates, or by using the multiple plate (PM) command. We have therefore concluded

that the most likely cause is an unreported (and perhaps an undetected) "bug" in the code that could affect the accuracy of the code in certain cases (for example for room-to-room propagation simulation). A way to circumvent the "leakage through the seams" problem has been discovered by trial and error.

In this approach one starts with a single, solid PEC plate. Next, a second plate is defined such that it coincides with the desired opening in the PEC plate. This second plate is assigned electrical properties (permittivity and permeability) of free space. The NEC-BSC apparently treats the second plate as an "opening," with direct and diffracted rays, but without the non-physical rays diffracted from the "seams" (because there are no seams). Figure 18 shows the LOS and the diffracted paths for the "seamless" PEC plate with the opening. The diffractions from the edges of the opening are evident.

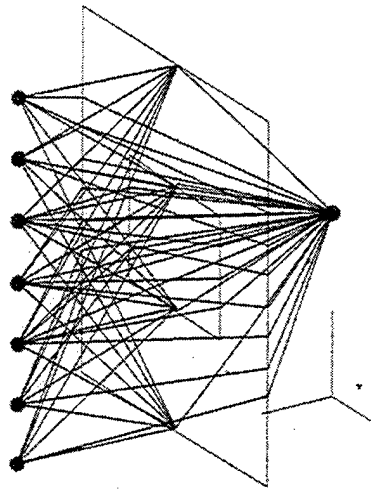


Figure 18. Propagation Paths for the "Seamless" Plate With the "Opening" Formed by a "Free Space Plate".

V. TYPICAL MISSILE ROOM

A. GENERAL DERSCRIPTION

As mentioned, providing good signal coverage for wireless communications on a military ship can be a very challenging task. One of the objectives is to provide the best coverage with the smallest number of "access point" stations ("base" stations). To accomplish this, computer simulations may be used for the particular shipboard compartments to determine the signal coverage for various combinations of the numbers and locations of antennas (with multiple antennas it is assumed that they transmit identical signals; that is, the "multicast" operation is assumed). The requirement to minimize the computational time must be balanced against the desired accuracy of the solution. Therefore, the optimum level of geometric detail in the compartment models results from a tradeoff between the desired accuracy and the computational resources available (CPU time and memory).

Simulation of a "typical" shipboard missile room is presented in this chapter. Although the geometry of missile room does not represent the missile compartment of any particular ship, it is typical of missile compartments for submarines.

The following software versions were used for the simulations:

- NEC-BSC graphical user interface (GUI) called Workbench, version 4.1.37 and
- NEC-BSC executable version 4.2-06.

These were the most recent releases by Prof. Ron Marhefka, Ohio State University, at the time of completion of this thesis.

In shipboard environments the majority of materials involved are metallic. Therefore, although lossy dielectric materials are also present in shipboard compartments (people for example), propagation within shipboard compartments will be dominated by reflections and diffraction of metallic surfaces. Furthermore, the metals involved may be approximated as PEC.

The large, parallelogram-shaped compartment shown in Figure 9 has the following dimensions:

- Length of twenty meters
- Width of ten meters
- Height of ten meters.

Six PEC plates form the compartment. Located at the first floor is a half-wavelength antenna, depicted as the red dot in the figures. The operating frequency is 2.4 GHz, which

corresponds to the wavelength of 12.5 cm. Six large, vertical metallic cylinders, representing missile tubes, are placed in the room. Each tube is 2 meters in diameter and 10 meters high.

Furthermore, there are three large tanks, which cover the walls parallel to the x-axis. The front and the rear tanks' height are 2.5 and 0.5 meters respectively, while the middle one's width is 1 meter and the height is 5 meters (same as the height of the first floor's ceiling). In addition to these six tanks, there is one large tank of 2.5 meters height along the wall parallel to y-axis on the rear side of the room.

One hatch is located in the middle of the front bulkhead. Since, hatches do not start at the floor level for the safety reasons (water containment), the hatch is positioned 30 centimeters from the floor and its height is 1.5 meters. Two similar hatches are located on the first and the second overheads.

The hatches can be modeled as either closed or opened. Therefore, propagation from one compartment section to the others through open hatches can be simulated. Finally, a nine-step stairway, complete with metallic handrails, connects the first and the second floor. The geometry of

the NEC-BSC missile compartment model is shown in Figure 19. The top view of the geometry of the compartment is provided in Figure 20.

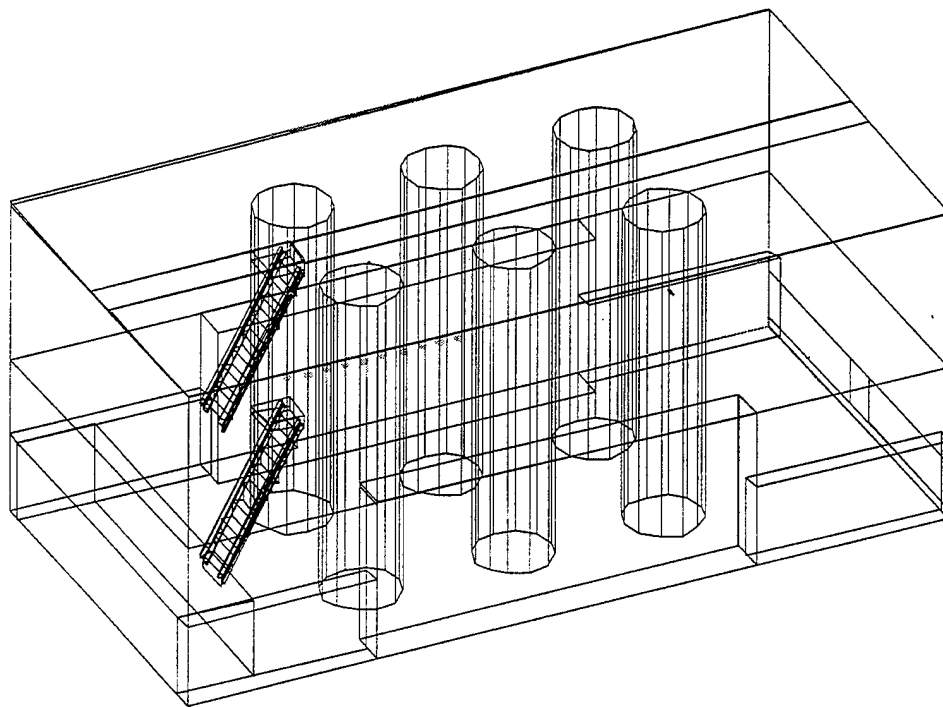


Figure 19. General View of a Typical Missile Shipboard Compartment.

B. NEC-BSC MODEL SPECIFICS

The NEC-BSC model described in the preceding section met all the requirements with respect to the limitations of the code, stated in Chapter III. In addition, all plates were modeled in a way that the code could infer which side of the plate was illuminated by the antenna. This was accomplished by defining all plates according to the right-hand rule described in Chapter V of the NEC-BSC manual. To eliminate NEC-BSC run-time "warnings" concerning the wall-attached plates of the rear tank, we had to define them as having corners not exactly identical, but positioned a small amount (0.5λ) through the surfaces to which there were being attached.

In the cases where we had to place identical objects in different locations, the NEC-BSC "Relative Rotate-Translate" (RR) command was used. This command enables the user to translate and/or rotate the coordinate system used to define the input data in order to simplify the specification of the set of missile tubes and the numerous stairs. Unlike the RT command, which always referred back to the reference coordinate system, the RR command accumulated the translations and/or rotations necessary for the desired positions. Therefore, at the end of the

procedure it was necessary to refer to the global coordinates again, by placing and then commenting out a test object at the origin that verified the accuracy of the procedure.

Finally, this NEC-BSC model did not account for the presence of the people. Although presence and/or motion of people can cause up to 10 dB attenuation of the average signal strength [35], the trend towards reduced ship manning [36] through increased automation and sensor monitoring via ship-wide networks, means that the presence of a large number of personnel in a missile compartment is unlikely.

C. SIMULATION RESULTS

1. Antenna Located in the Middle of the Room

In this case, both antenna and observation area are located on the first floor. The source is located in the middle of the compartment, 2 meters above the floor level, while the field observation points form a horizontal rectangle of 400 by 200 points (for a total of 80,000 observation points) at the same height as the antenna. Recall that the operating wavelength is 12.5 cm, while the x and y dimensions of the compartment are 20 by 10 meters respectively. Therefore, the minimum spatial sampling that

allows us to capture wave minima and maxima requires a sampling step of one half of the operating wavelength, which corresponds to at least $320 \times 160 = 51,200$ observation points. Increasing the density of the observation points results in a more accurate "map" of the field, but at the expense of increased computational time. It was decided that 80,000 points represent a good compromise between the detail level and the computational time required for the solution.

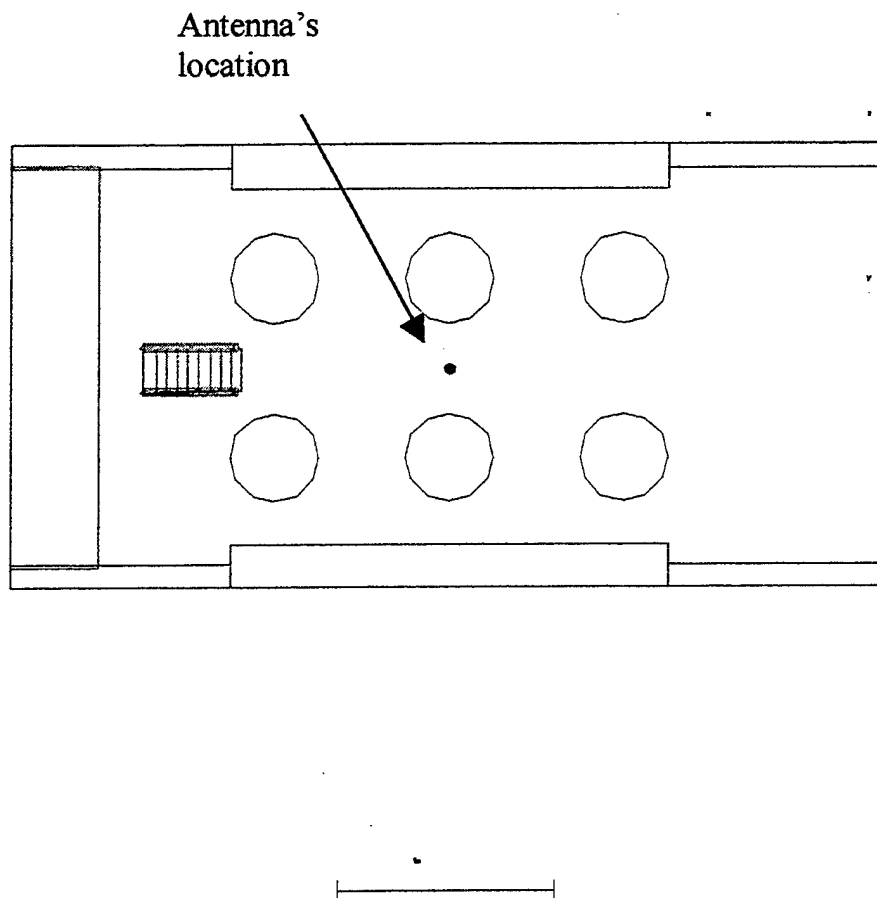


Figure 20. Top View of the Compartment.

Despite the reasonable computing resources used (a PC with a single Pentium III 600 MHz processor and 768 Megabytes of RAM), the simulation run time was still approximately seven hours for the 80,000 observation points.

By extracting the numerical results from NEC-BSC and importing them to Mathcad, a "map" of the signal strength within the compartment was obtained, shown in Figure 21. It should also be noted that the threshold for the signal strength at the observation points was set at 40 dB below the peak observed signal strength. As stated before, the dynamic range for which the NEC-BSC has good accuracy is approximately 25 dB. Nevertheless, a larger dynamic range has been selected, in order for the shadow areas and the obstacles to be clearly visible in the signal strength "map."

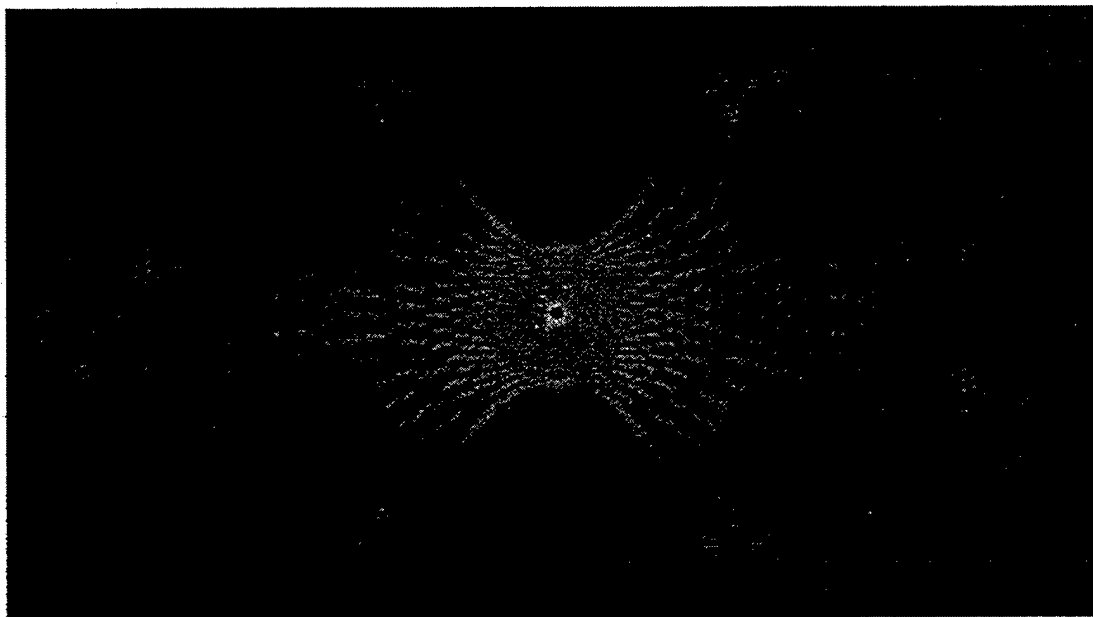


Figure 21. RF Energy Propagation Inside the Room (2 Meters Above the Floor).

2. Results for the Antenna in an Arbitrary Location

Again, both antenna and observation points are located on the first floor. The antenna, however, is now placed at an "arbitrary" location (no longer in the middle of the compartment) 1 meter above the floor, while the observation points form a horizontal rectangle of 400 by 200 points (for a total of 80,000 observation points) and 1.5 meters above the floor. The top view of the compartment is provided in Figure 22. The arrow indicates the antenna location.

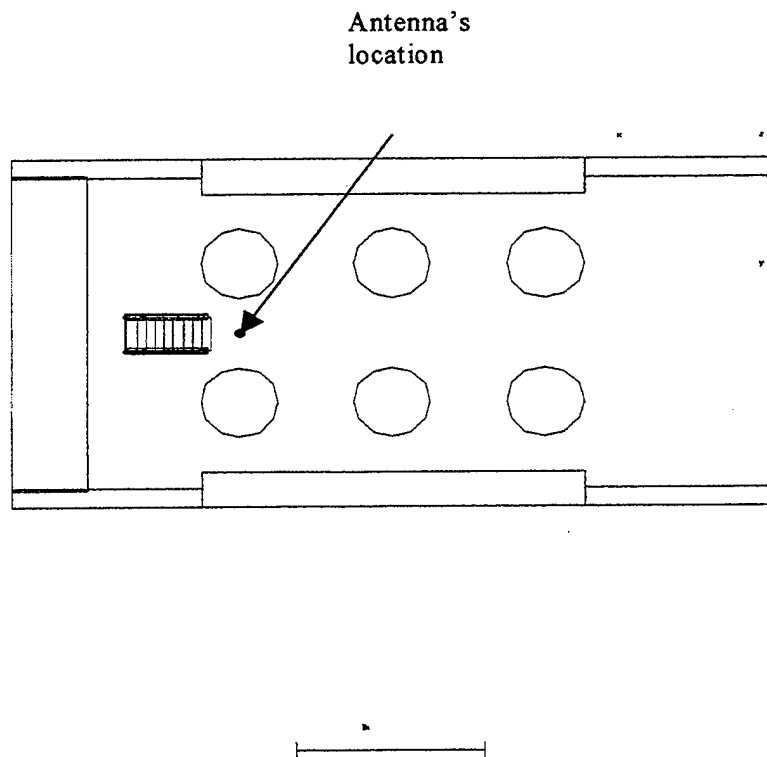


Figure 22. Top View of the Missile Compartment With the Antenna in an Arbitrary Location.

The "maps" of the signal strength are shown in Figures 23 and 24, for the dynamic ranges of 33 and 22 dB respectively. In the 33-dB dynamic range "map" we notice the apparent signal "leakage" into the missile tubes and the tanks. Since the tubes and the tanks are non-penetrable (modeled as PEC) these are clearly consequence of the code's limited dynamic range. Reducing the dynamic

range to 22 dB eliminates most of the "non-physical" rays,
as evident in Figure 24.

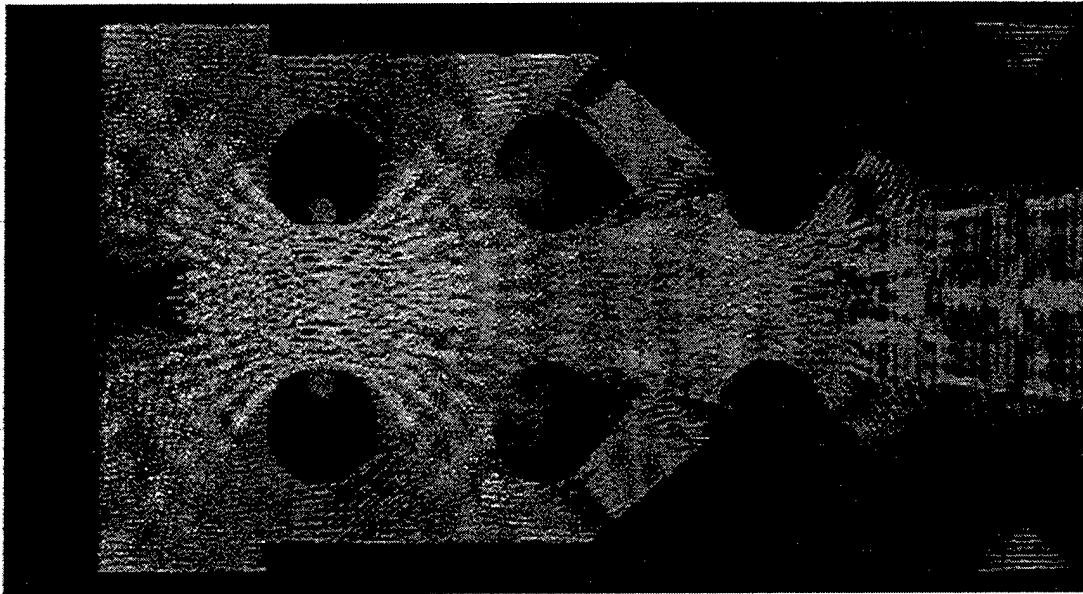


Figure 23. Signal Strength "Map" for the Missile Room Using
a Dynamic Range of 33 dB.

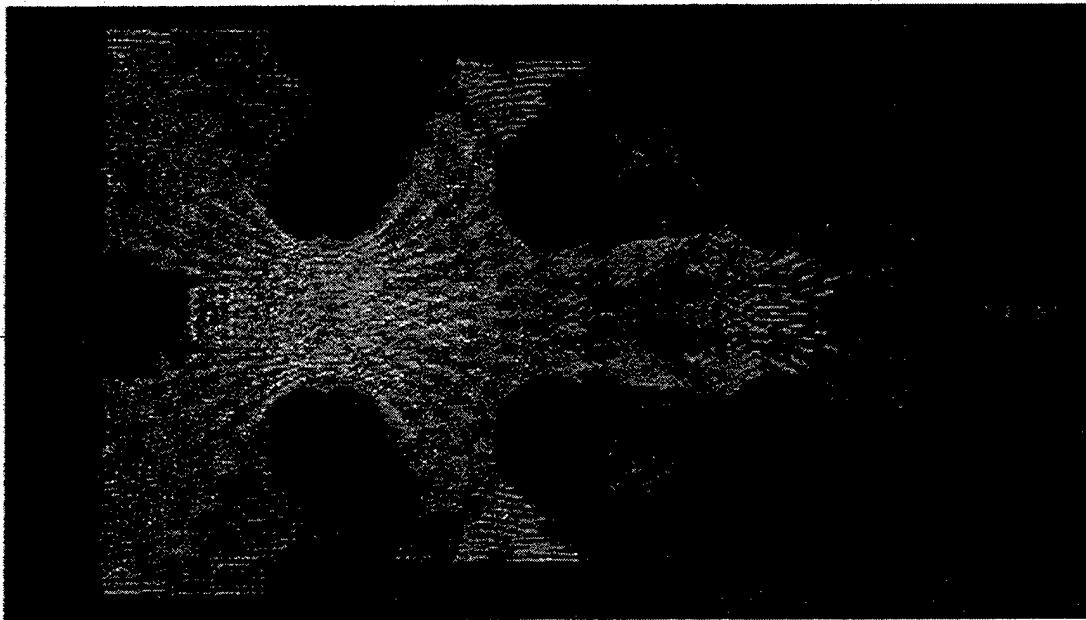


Figure 24. Signal Strength "Map" for the Missile Room Using
a Dynamic Range of 22 dB.

3. Results for two Antennas in the Missile Room

Next, the results are next presented for a "typical" wireless LAN installation where a number of antennas may be used to increase the uniformity of the signal coverage within the user space. In particular, it is assumed that the two antennas transmit identical signals, a situation commonly referred to as "multicasting." The two antennas are centrally located, close to the ceiling, at the height of 4 m above the floor, and 8 m apart from each other, as shown in Figure 25. The 80,000 observation points again form a horizontal rectangle (400 by 200 points) at 1 meter above the floor (approximately waist level).

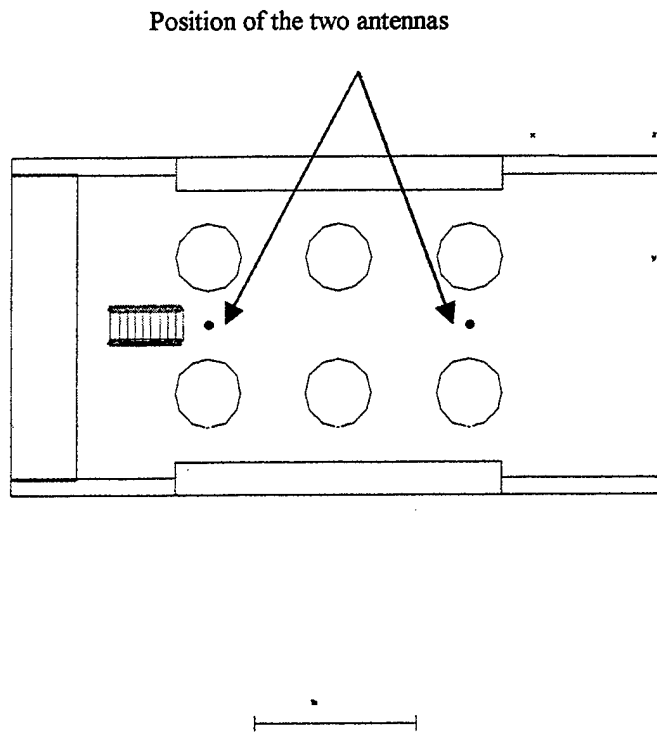


Figure 25. Top View of the Compartment With the Two Antennas.

By extracting the NEC-BSC solution (numerical results for the field strength) and importing it into Mathcad, we obtained the "map" of the signal strength within the compartment, shown in Figure 26. The dynamic range for this "map" was limited to 25 dB. As expected, the "map" shows that a much more uniform coverage is obtained with two antennas. There is even coverage behind the cylinders, due to reflected and "creeping" wave

contributions. The computer running time for this simulation was approximately 12 hours.

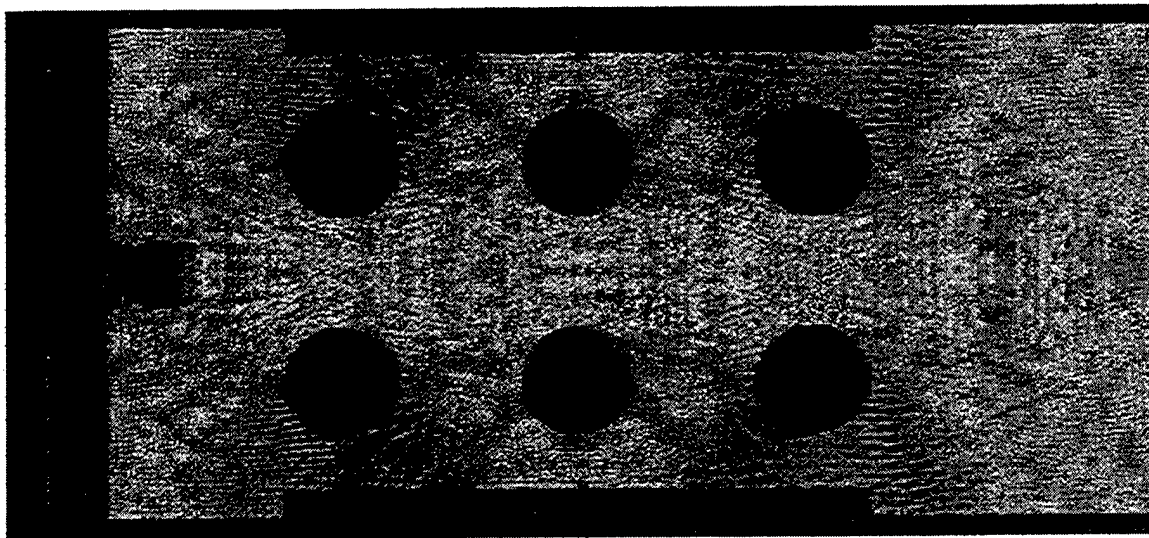


Figure 26. Signal Propagation Inside the Missile Room, 4 Meters Above the Floor and Using a Dynamic Range of 25 dB.

4. Floor-to-Floor Propagation

The simulations have confirmed the 20 to 30 dB dynamic range limitation of for NEC-BSC stated in the NEC-BSC User's Manual. The limited dynamic range suggests that NEC-BSC will not be well suited for applications where the desired signal levels could be very low, such as in the case of floor-to-floor propagation. Nevertheless, simulations were performed to test the NEC-BSC performance for room-to-room and floor-to-floor propagation. Presented here are the NEC-BSC results for floor-to-floor propagation

for the missile compartment. The transmitting antenna is located on the first floor, while the observation points are on the second floor. The antenna is in the same location as in Figure 22, 1 meter above the floor. The observation points are on the second floor, again forming a horizontal rectangle of 400 by 200 points 1.5 meters above the floor level. The side view of the missile compartment, with the observation points visible as a line, is shown in Figure 27.

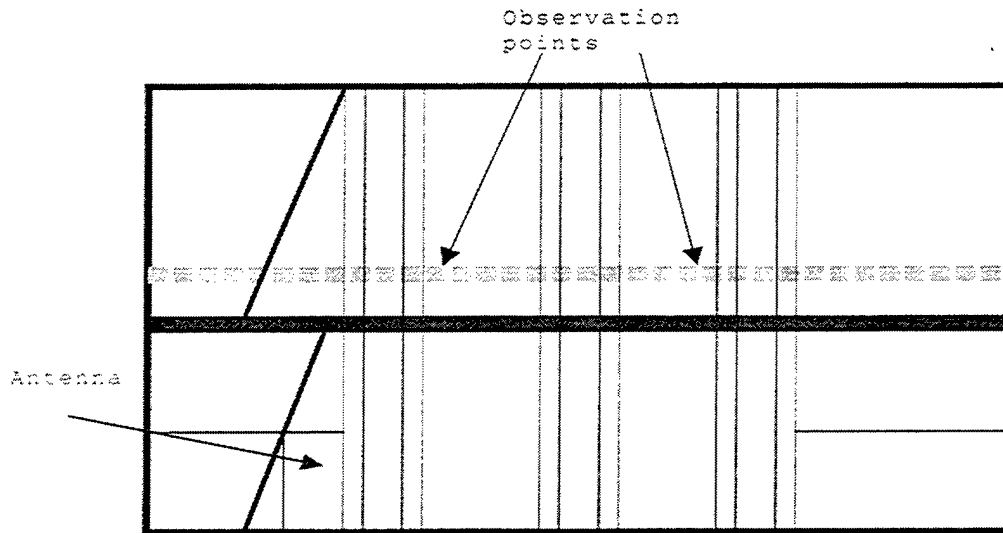


Figure 27. Side View of the Compartment and the Observation Area, Forming a Line.

By extracting the NEC-BSC numerical results and importing them to Mathcad, we obtain the "map" of the

signal strength for the floor-to-floor propagation, shown in Figure 27. Since floor-to-floor propagation incurs a considerable loss (no LOS path) we had to use 75-dB dynamic range for the "map." This is clearly beyond the stated reliable dynamic range of the NEC-BSC and is manifested by what appears to be the signal "leakage" at the "seams" between the plates forming the floor/ceiling and the "seams" between the tubes and the floor/ceiling, evident in Figure 28. Nevertheless, the code properly predicts the highest signal strength for the vicinity of the stairwell opening. The computer run time for this simulation was approximately 12 hours.

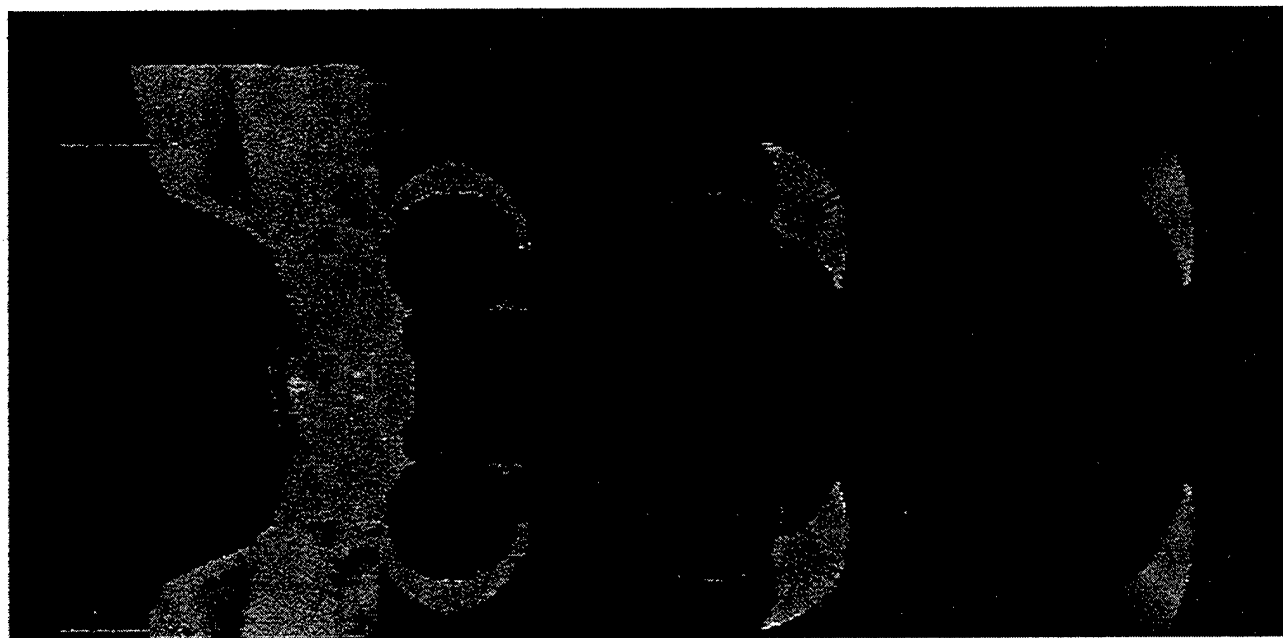


Figure 28. Signal Propagation Inside the Second Floor, Caused by an Antenna Located in the First one and Using a Dynamic Range of 75 dB.

However, this simulation does give us some insight about the diffraction and reflection mechanisms that take place in communication between floors. These phenomena, which dominate in room-to-room cases, can be generally seen in Figure 28. The run time for this program was approximately 12 hours.

D. PROPAGATION STATISTICS FOR THE MISSILE COMPARTMENT

1. Theoretical Background

Thus far, we have presented the signal strength "maps" for particular compartments using the numerical output results of the NEC-BSC and Mathcad. In this section the objective is to extract the statistics of the excess path gain/loss (relative to free space path loss) for the entire floor of a particular compartment and for different antenna placements. The result will be a random variable with a certain probability density function (pdf) expressing the likelihood of a particular excess path gain/loss.

The path loss for free space can be easily calculated for any distance between the transmitter and an observation point. Adding a random variable with a known pdf to the deterministic free space loss allows us to calculate the mean value, dispersion, etc. for the compartment path loss random variable. This applies, in statistical sense, to

any two points (the transmitter and the observation point) inside the particular compartment, regardless of their exact location as long as the distance between them is the same.

For each transmit antenna location, two NEC-BSC input files were created: one for the compartment and the other for the free space of exactly the same shape and volume as the compartment. All other parameters (antenna type and position, radiated frequency, observation points placement) were kept identical. The two output ASCII files, resulting from the execution of the input files, were formatted using the Windows WordPad editor and imported into Mathcad. Two column matrices were created in Mathcad for each input file, with the first column containing the relative distance between the transmit antenna and the observation point and the second column containing the corresponding E-field strength.

The matrices are then rearranged in the following manner. First, the distances (from minimum to maximum) are discretized into distance "bins," each bin 50 cm (4 wavelengths) wide. Next, all values within the same distance bins are placed on the same row of a new "matrix" (this "matrix" has a variable number of columns). The

distance "bins" geometrically correspond to concentric spherical shells of 50 cm thickness, all centered at the transmit antenna location. The number of observation points within each "shell" varies with the shell distance from the "origin" (the transmit antenna location).

The next step is to form the ratios of the compartment and "free space" fields at the same observation points. Expressing this ratio in dB creates a new variable that is referred to as the "excess compartment gain" R . Positive values of the excess compartment gain indicate that the signal in the compartment exceeds the free space signal at the same location, while the negative values of the excess compartment gain indicate that the signal in the compartment is weaker than the free space signal at the same location.

$$R = 20 \log \frac{|E_{ROOM}|}{|E_{free}|} \quad (5.1)$$

In Equation 5.1, R denotes the "excess room gain" with respect to free space. Since for a given distance bin there is a large number of values (because of a typically very large number of observation points) the values of R

from any given bin form a random variable. The random variables for the individual distance bins can be further combined to form a single random variable that now incorporates the excess gain statistics for the entire compartment, regardless of the distance.

The probability density function (pdf) and the cumulative distribution function (cdf) for the excess gain random variable are compared to the Gaussian pdf and cdf with the same mean and variance. The pdf's and the cdf's are plotted versus the excess gain in dB. The distributions obtained via simulation are plotted on the same graphs with the Gaussian distributions, to illustrate the "match" between the two. In addition, the histograms for the distance groups are also presented.

In order to obtain the aforementioned plots, we first had to resolve an important issue. Invoking the volumetric plot command (VN) results in a number of observation points. The observation points are uniformly spaced and thus would be positioned inside as well as outside non-penetrable objects like the cylinders, the tanks, even the steps of the stairways. Since the interiors of non-penetrable objects are not considered as "legitimate"

transceiver locations, the observation points within non-penetrable objects had to be eliminated.

A simple attempt to circumvent this problem by the multiple selective use of the same command failed since the code executed only the last of the commands. Therefore, we had to apply a rather time consuming procedure: we truncated the missile room and the free space area into a number of obstacle-free observation regions. We ran the program once for each of the observation regions, and then "stacked" (using Mathcad) the data resulting from each run to form a single "output" file.

The results of the simulations presented in this chapter indicate that the Gaussian distribution best describes the missile compartment excess gain (in dB) random variable. It has been reported [1] that the lognormal distribution also applies to indoor propagation between observation points that have different distances from the RF transmitter.

Furthermore, it has been reported recently [38] that the lognormal distribution applies to the "same distance points" that form concentric cycles around an arbitrarily placed source for indoor propagation within a building. The same approach has been applied in this, thesis to

metallic compartments, with similar results, that is the lognormal distribution for the excess gain random variable. Recall that the missile compartment is composed of PEC materials, hence it can be characterized as highly reflecting/diffracting environment.

Due to the absence of absorption and refraction, reflected, diffracted, and "creeping" waves dominate in the propagation mechanisms. Each of the multiple reflections that a single "ray" experiences within the compartment contributes a factor (the reflection coefficient to the magnitude of the ray at the particular observation point). Therefore the observed ray magnitude is a product of a number of factors. The logarithm of the product (that is the path gain/loss in dB) is equal to the sum of the logarithms of each term in the product. Since each reflection is by and large independent from the others (involving different locations, objects, and incident angles) the sum of logarithms tends to be a normally distributed random variable, hence the lognormal distributions.

2. Results

Let us now examine the results for several transmitting antenna locations. The observation points are

always located on a horizontal plane, but the observation plane height (above the floor level) may differ for each individual case.

2.1 First Location

The transmitting antenna is located at (14,5,1) and the observation points lay in a horizontal plane at $Z = 1.5\text{m}$, as show in Figure 29. The various cells are shown in Figures 30 through 40.

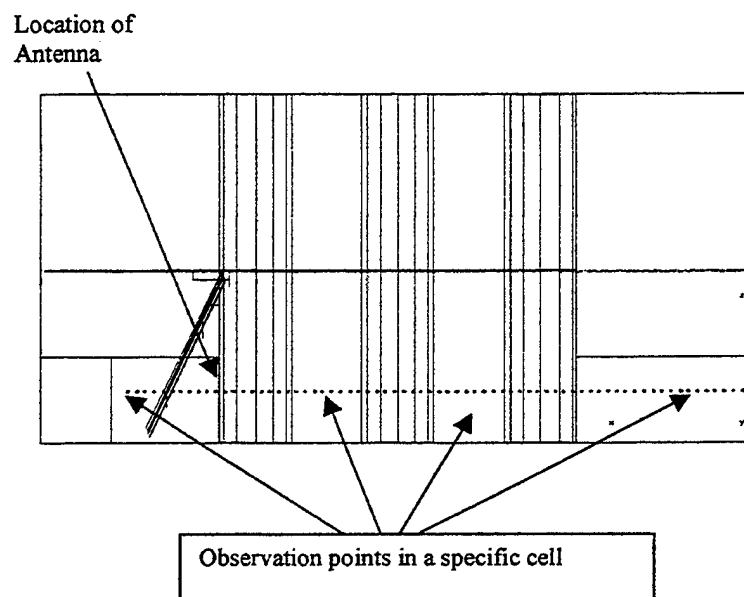


Figure 29. Side View of the Compartment, the Observation Area, Forming a Line, and the antenna at location 1.

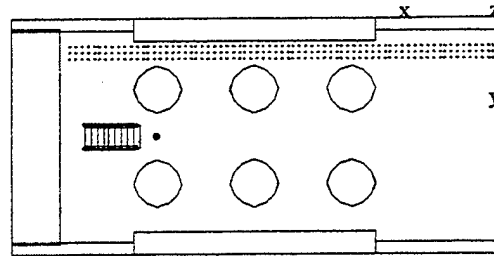


Figure 30. Top View of the Compartment, the First Observation cell, and the antenna at location 1.

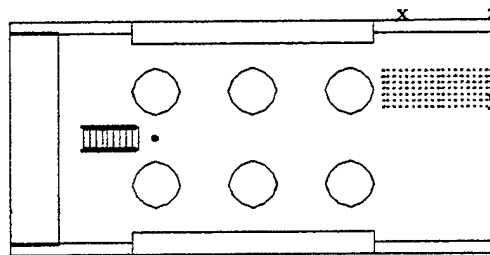


Figure 31. Top View of the Compartment, the Second Observation cell, and the antenna at location 1.

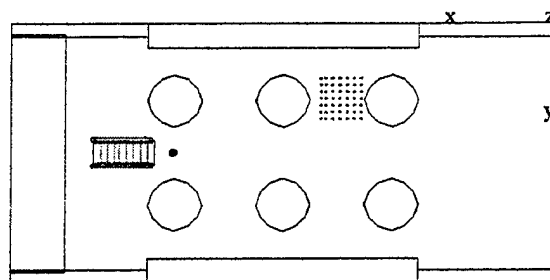


Figure 32. Top View of the Compartment, the Third Observation cell, and the antenna at location 1.

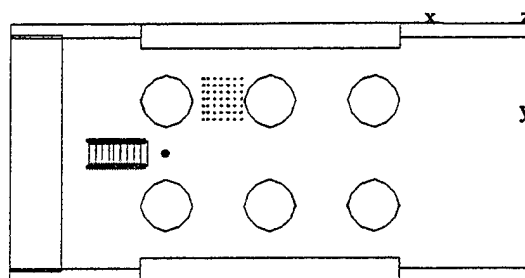
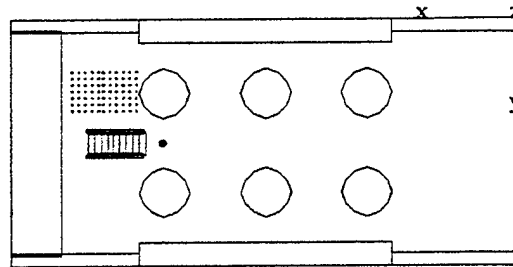
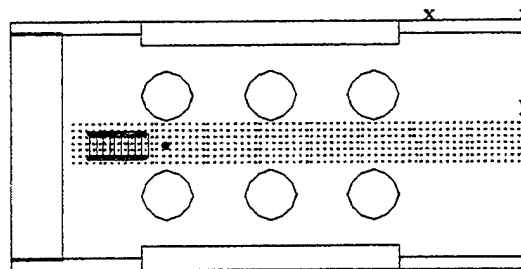


Figure 33. Top View of the Compartment, the Fourth Observation cell, and the antenna at location 1.



5 m

Figure 34. Top View of the Compartment, the Fifth Observation cell, and the antenna at location 1.



5 m

Figure 35. Top View of the Compartment, the Sixth Observation cell, and the antenna at location 1.

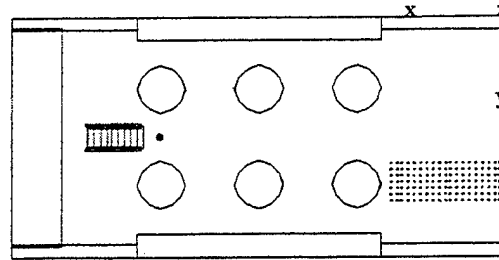


Figure 36. Top View of the Compartment, the Seventh Observation cell, and the antenna at location 1.

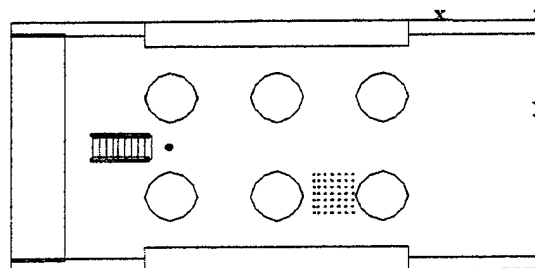
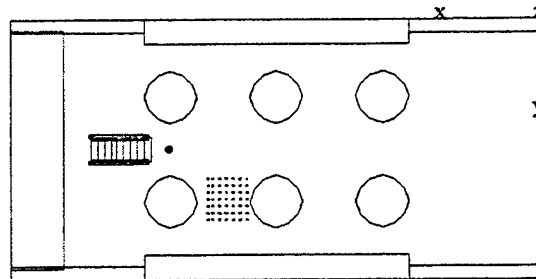
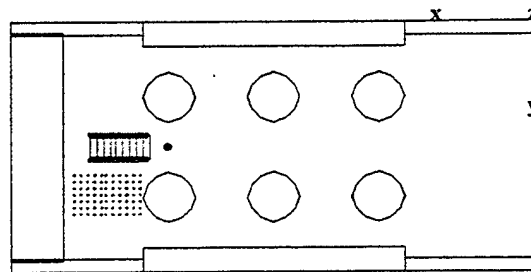


Figure 37. Top View of the Compartment, the Eighth Observation cell, and the antenna at location 1.



5 m

Figure 38. Top View of the Compartment, the Ninth Observation cell, and the antenna at location 1.



5 m

Figure 39. Top View of the Compartment, the Tenth Observation cell, and the antenna at location 1.

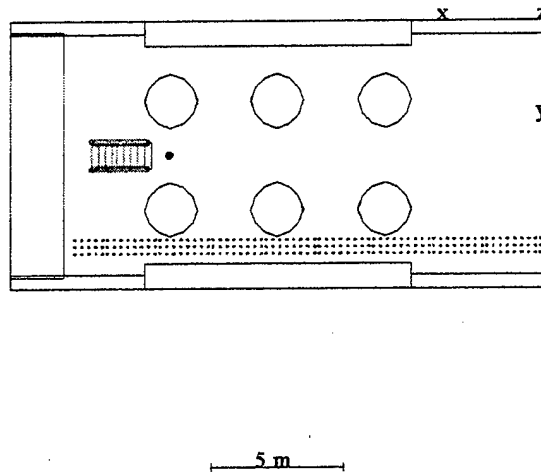


Figure 40. Top View of the Compartment, the Eleventh Observation cell, and the antenna at location 1.

The excess gain (in dB) pdf and cdf, obtained by averaging over all distance groups, are shown in Figures 41 and 42, respectively. Plotted on the same graphs are the lognormal (Gaussian) pdf and cdf, to visualize the agreement between the lognormal distribution model and the data obtained by simulation.

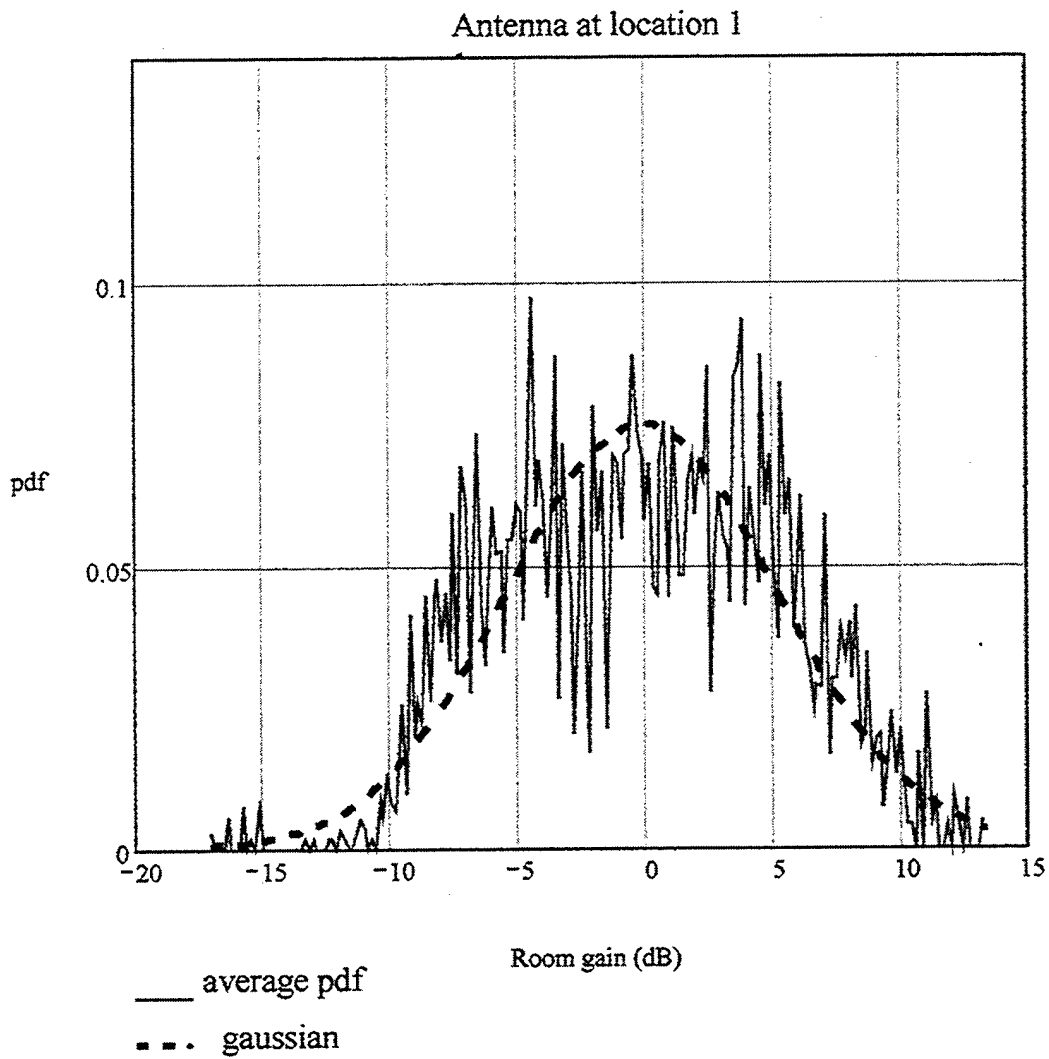


Figure 41. Pdf of the Excess Gain and the Lognormal (Gaussian) Pdf, Transmitting Antenna at Location 1

cdf's, which could have been expected as the integration "averages out" the statistical dispersion of the pdf. Note that the pdf oscillations are, on the average, equally likely to be either above or below the lognormal pdf, hence they tend to cancel out when the pdf is integrated to obtain the cdf. From the cdf we note that the compartment (for this particular antenna location) has a 0.5 probability of behaving exactly like free space; that is, it experiences neither gain nor loss relative to free space propagation.

2.2 Second Location

In this case the transmitting antenna is located at (2,2,2) and the observation points are in a horizontal plane at $Z = 2\text{m}$. The results are illustrated in the Figures 43 and 44.

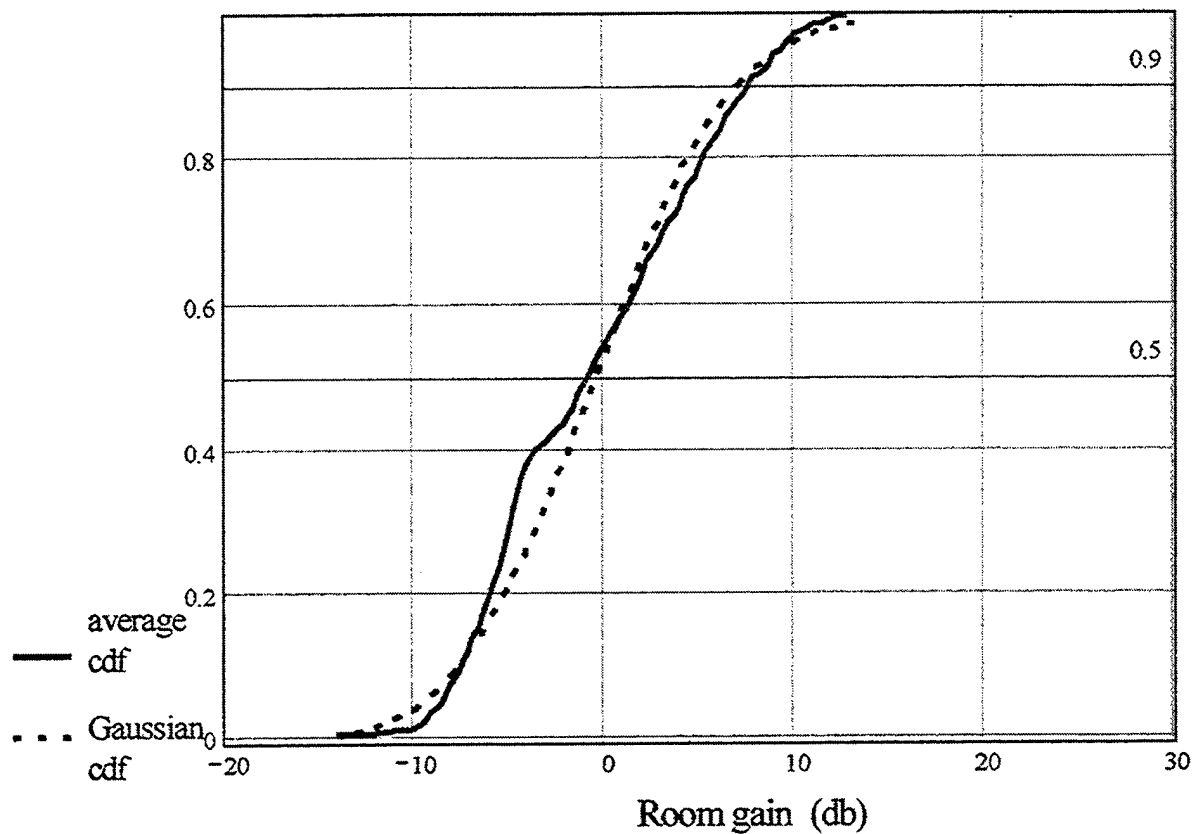


Figure 44. Cdf of the Excess Gain and Lognormal (Gaussian) Cdf, Antenna at Location 2.

The results show a discrepancy between the simulation results and the lognormal distribution. The cause of the discrepancy is the dynamic range restriction we implemented to eliminate the non-physical ray "leakage" into non-penetrable compartments. Recall that, according to NEC-BSC limitations stated in the manual [41], reliable results can be expected for only about the first 30 dB of the dynamic range. Therefore, all values below that number are filtered and set to 30 dB below the maximum. Inevitably

this "thresholding" causes a distinct peak to appear in the pdf, distorting the pdf's shape relative to the expected lognormal distribution. To illustrate the effects of the dynamic range limiting on the pdf obtained via simulation, the pdf for the 40-dB dynamic range is shown in Figure 45. Compared with the 30-dB dynamic range pdf, the 40-dB dynamic range pdf shows a more prominent peak, shifted further to the left (larger values of excess path loss).

In order to mitigate the effects of the dynamic range limitation inherent to the NEC-BSC (as a matter of fact all simulation codes have a finite dynamic range, due to the "numerical noise") a "fix" has been implemented in Mathcad. The essence of the "fix" was to replace the value of the "offending" peak with the value that corresponds to the lognormal distribution and then scale the resulting distribution such that its integral is equal to 1 (as it has to be for any pdf). Shown in Figure 45 are the pdf's for the 30 and 40 dB dynamic ranges and the "corrected" (in the manner described above) pdf for the 30-dB dynamic range. It is evident that the outlined procedure results in a pdf that is again close to the lognormal pdf.

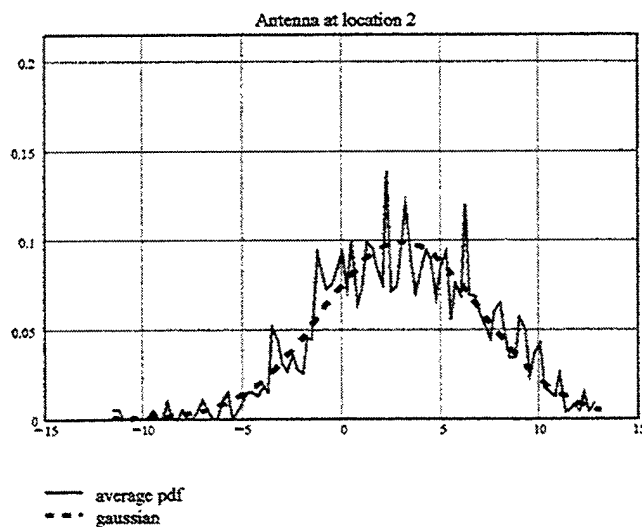
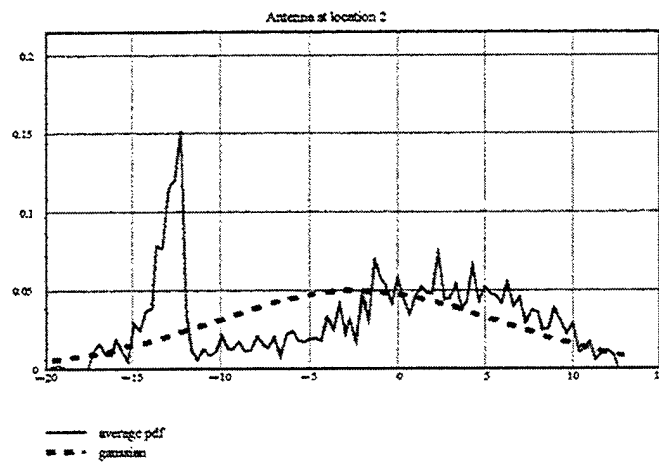
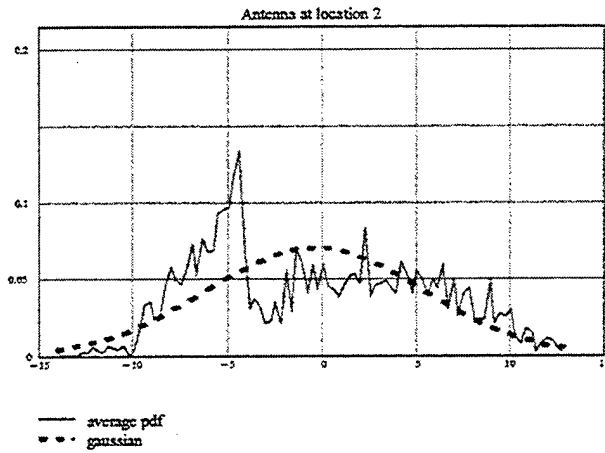


Figure 45. Original (30 dB Dynamic Range), "Shifted" (40 dB Dynamic Range) and "Corrected" 30 dB Dynamic Range Pdf for the Second Location.

2.3 Third Location

In this case the transmitting antenna is located at (2,2,2.2) and the observation points are in a horizontal plane at $Z = 2.2\text{m}$ (at the same height as the transmitting antenna). Note that the difference between this and the preceding case is that the antenna and the observation points have been translated upward by 20 cm. The reason to do this is to examine the consequences of a translation by a relatively small distance, commensurate with the operating wavelength (approximately 1.5 wavelengths in this case). In addition, the observation points do not fall on the wide horizontal steps of the stairway. The results are shown in Figures 46 and 47.

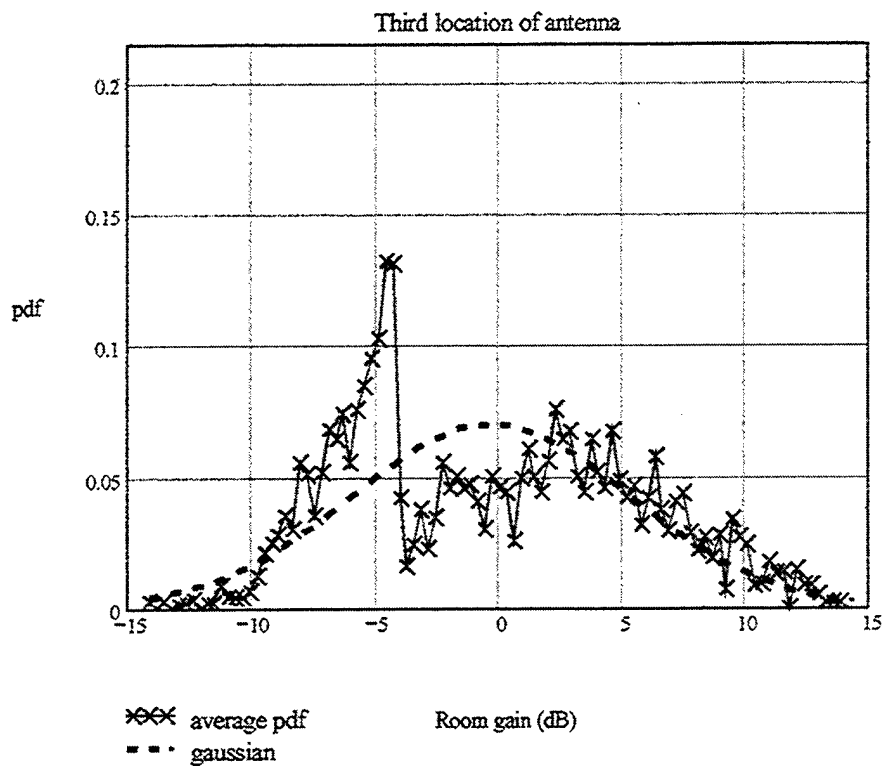


Figure 46. Pdf of the Excess Gain and the Lognormal (Gaussian) Pdf, Transmitting Antenna at Location 3.

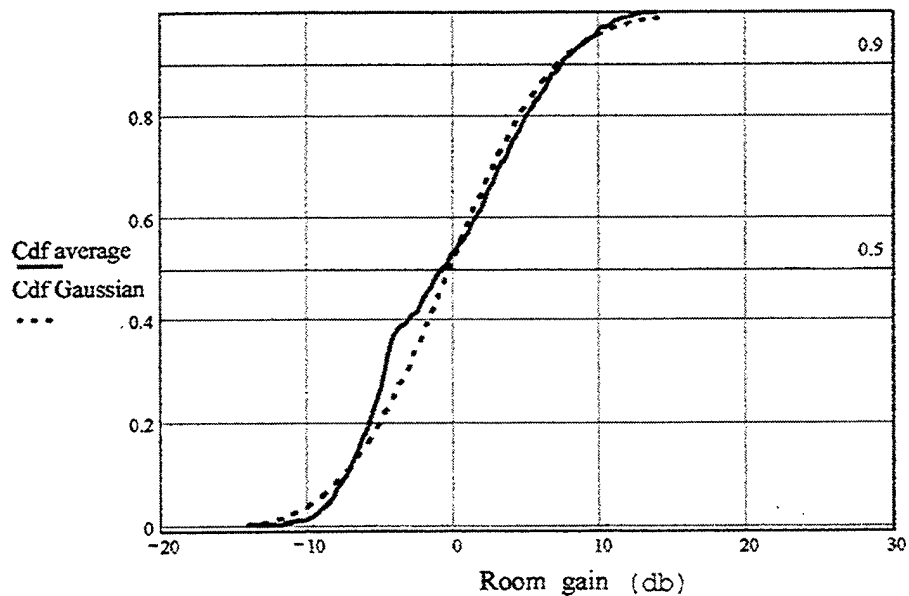


Figure 47. Cdf of the Excess Gain and the Lognormal (Gaussian) Cdf, Antenna at Location 3.

Again, we encountered the same problem as before, caused by the dynamic range limitation. However, by applying the aforementioned "fix," we resolved the issue. Figures 48 and 49 show the pdf's before and after the mitigation of the effects of the limited dynamic range.

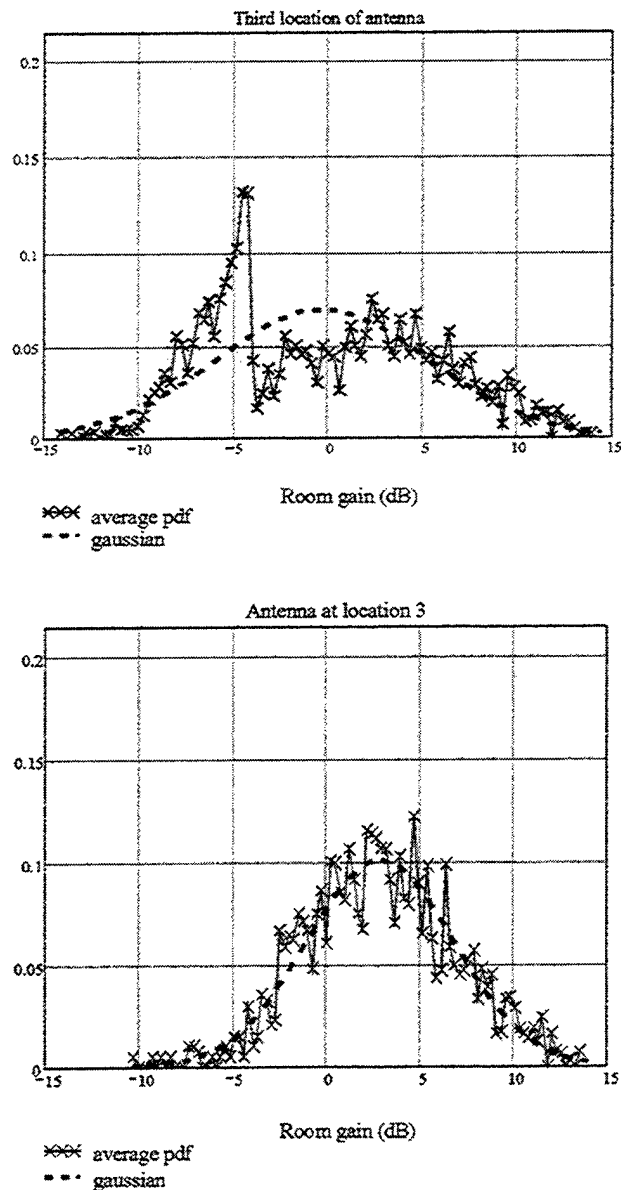


Figure 48. Original and "Corrected" Pdfs for the Third Location, 30 dB Dynamic Range.

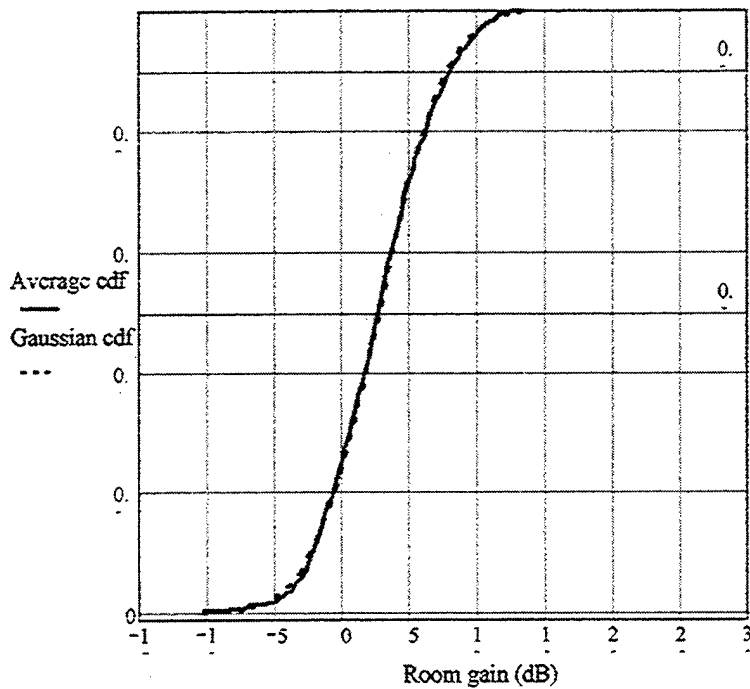
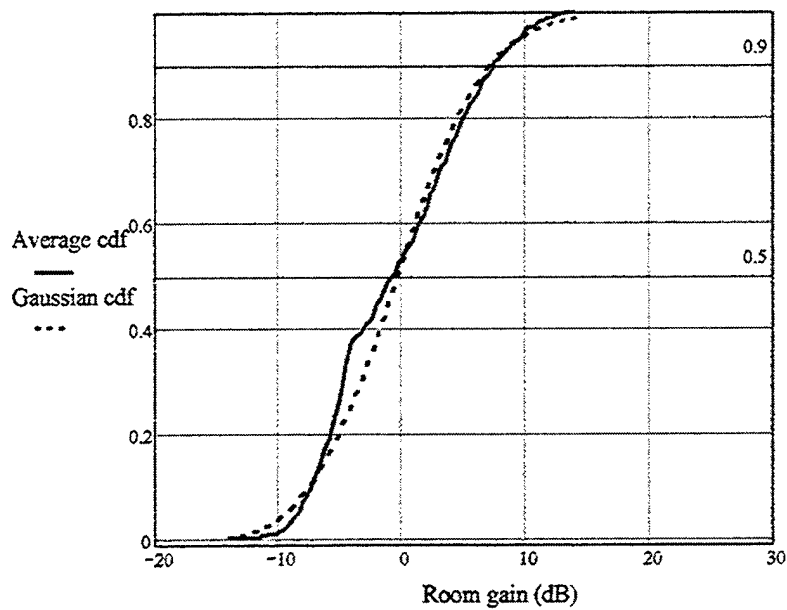


Figure 49. Original and Corrected Cdf for the Excess Gain and Lognormal (Gaussian) Cdf, Antenna at Location 3.

2.4 Fourth Location

In this case the transmitting antenna is located at $(4,3,1)$ and the observation points are in a horizontal plane at $Z = 1$ m (at the same height as the transmitting antenna). This is the last case considered, for which the transmitting antenna is placed at an "arbitrary" location (not in a plane of symmetry, or the like). However, the observation points are still in a horizontal plane, at the same height as the transmitting antenna. Following the same procedure as for the preceding three locations, we obtain the results shown in Figures 50 and 51.

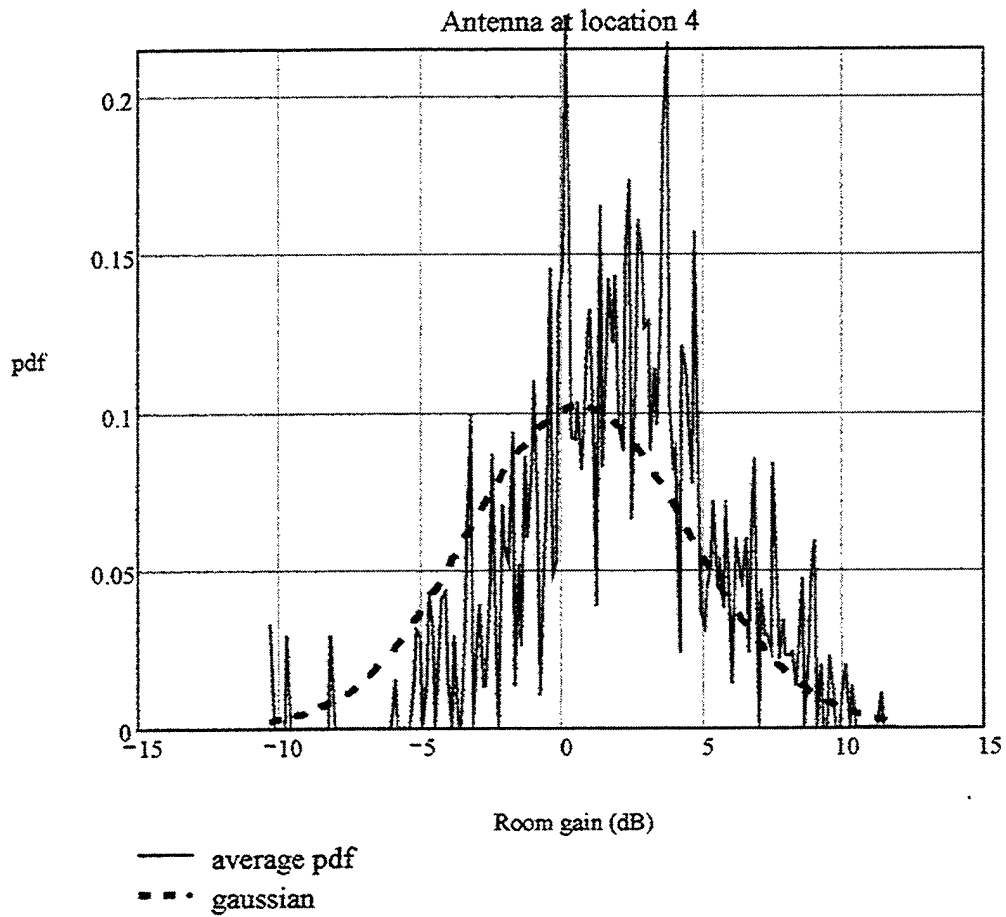


Figure 50. Pdf of the Excess Gain and the Lognormal (Gaussian) Pdf, Transmitting Antenna at Location 4.

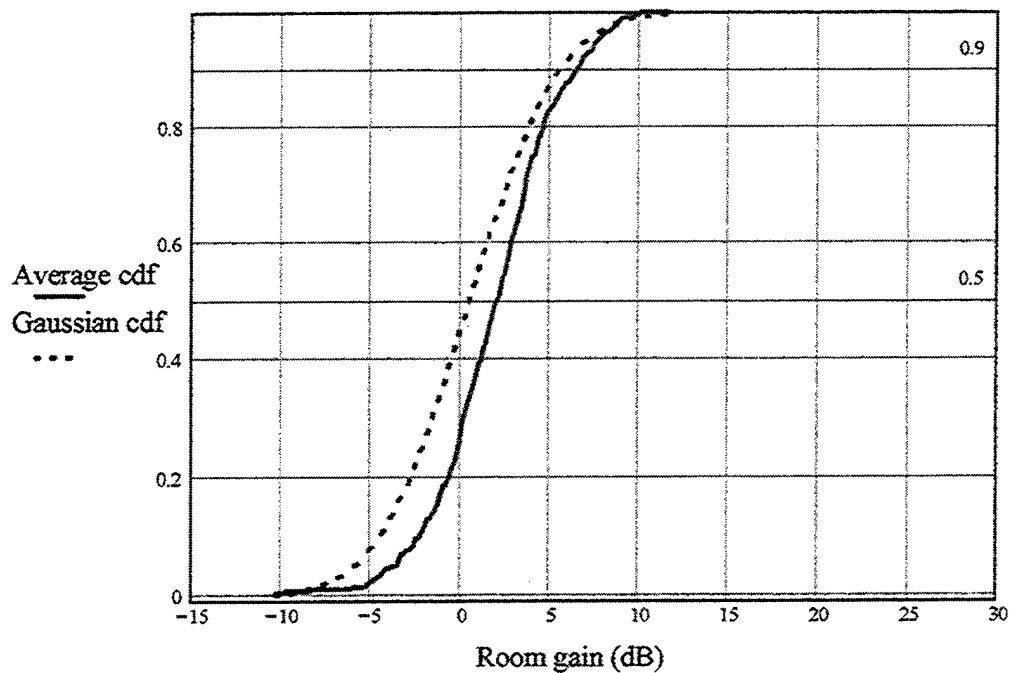


Figure 51. Cdf of the Excess Gain and the Lognormal (Gaussian) Cdf, Antenna at Location 4.

The data for the four antenna locations used in the simulations are presented in Table 5.1.

Antenna location	Antenna Coordinates	Observation points height	Excess gain Mean (dB)	Excess gain St. Deviation (dB)
First	(14,5,1)	Z=1.5	-0.10	5.31
Second	(2,2,2)	Z=2	1.43	4.85
Third	(2,2,2.2)	Z=2.2	2.91	3.95
Forth	(4,3,1)	Z=1	0.58	3.9

Table 5.1. Data for the Four Propagation Simulations.

VI. UNRESOLVED ISSUES, RECOMMENDATIONS, AND CONCLUSIONS

A. UNRESOLVED PROBLEMS

1. Floor-to-Floor Propagation

The case in which the antenna was located inside the first floor of the missile room, and the observation points in the second (and vice versa), could not be thoroughly examined due to the problems caused by the "ray leakage," as reported in Chapter IV. Therefore the compartment-to-compartment propagation statistics were not addressed. Note that the limited dynamic range is also an issue with regard to compartment-to-compartment coupling that "by definition" involves large attenuation.

2. Problematic PN Command

The Near Zone Pattern (PN) command enabled us to define the near zone pattern coordinate system, the volumetric pattern cut, and the spatial range of desired observation points. However, as reported in Chapter V, the multiple and selective use of the PN command to exclude the undesired observation points (inside non-penetrable objects) was unsuccessful, because the code executed only the last of the multiple PN commands. The truncation of

the room into several regions, exclusive of non-penetrable objects, did work but at the expense of excluding some points located near the non-penetrable obstacles and it increased time requirements for processing of multiple data files.

3. Running Time

All simulation programs executed in Chapter V were time consuming and had run times, ranging from seven to twelve hours. As expected, time requirements depended on the complexity of the compartment, the number of the observation points and the number of antennas used.

B. RECOMMENDATIONS

All recommendations for further study are made in the light of existing information, based on NEC-BSC Workbench version 4.1.37 and executable NEC-BSC FORTRAN program versions 4.2-06.

Some commands, namely BF, FT, LY, NC, NG, NM, NP, NR, NS, NX, PT, RI, SI, TA, TD, TW, TY, VM, were not supported by the Command Wizard window of the code's Graphical User Interface (GUI). Moreover, the function of the command ZC, provided by Workbench, remains mysterious, since there is no description for it, either "on-line" or in the User's manual.

In addition, the Zoom In command in the main toolbar was inconvenient, because the user was not able to specify the desired scale, which by default was inadequately large. The accuracy of the Zoom was also questionable, since it altered the location of certain objects, presented the cylinder caps as polygons, and showed some rays diffracted from cylinders as if the rays penetrated the cylinders and then diffracted from the inside of the cylinders.

It should also be stated that the very useful and convenient "drag and drop" option couldn't be used in all cases; the user could not always distinguish and select an individual ray among a plethora of others. Finally, the coordinate system of the code, which by default placed the origin in the left upper corner of the display, used unknown units and was difficult to work with.

A recent, extensive study [38] includes a number of recommendations that would significantly improve the applicability of the NEC-BSC for indoor propagation simulation. In addition to these, parallel execution option [37] would also decrease the run-times, especially in complex cases that approach the limitations of the code, as reported in Chapter III.

Moreover, a considerable improvement in the calculation speed and memory requirements could be made if the near-field computation by NEC-BSC did not include both the Electric and the Magnetic field components simultaneously. In situations where the computation of the signal strength was the goal, the calculation of the H-field could not be skipped. The user should be able to choose the particular quantity that the code should calculate in order to reduce the computational time.

Another factor that would improve code performance is the support of all commands in the Workbench. In addition, the Users Manual should be completed and should include all the figures omitted in the previous versions, along with more examples that illustrate the workflow.

Finally, the creation of the problem geometry will be greatly simplified if future versions of NEC-BSC would support data import in a standard CAD file format (.dxf, .dwg, etc.).

C. CONCLUSIONS

The primary objective of this research was to provide simple statistical models for indoor propagation in complex environments, such as shipboard compartments. The emphasis in this research was on the basic principles and a simple

statistical description for a representative shipboard environment rather than on encyclopedic compilation for indoor propagation data for vastly diverse complex environments. Previous work using NEC-BSC for indoor propagation simulation, involving environments with no material uniformity [38] showed satisfactory agreement with both the results reported in [40], and with the measurements conducted in the Bullard Hall at the Naval Postgraduate School in Monterey, California [38].

In our case, as well as for the Bullard Hall case [38], the "room excess gain" random variable was defined to describe how the propagation in the indoor environment differs from the deterministic (formula-predictable) free space propagation. The simulation results in both cases show that the excess gain (in dB) random variable could be approximated as lognormal (Gaussian) distributed [39]. Note that this random variable is representative for all distance combinations and locations of the source and observation points within a single compartment. Although the shape of the probability density function for the excess gain (in dB) random variable does not depend on the particular choice of the source location or the compartment details, the parameters defining the pdf, such as the mean

value and the variance, do depend on the position of the source and the observation points relative to the obstacles present in the compartment.

It appears that the key parameter in defining the mean value of the excess gain is the relative number of observation points that are shadowed by the obstacles and thus experience non-line-of-sight propagation attenuation. If there is a large number of observation points in deep shadows, which depends primarily on the location of the source relative to the obstacles in the compartment, the mean value of the excess gain is negative, indicating a loss (on the average) relative to the free space propagation. If on the other case most of the observation points are either direct line-of-sight or are obstructed by low-loss penetrable obstacles, the mean value of the excess gain (in dB) becomes positive, indicating that the signal strength in that compartment exceeds, on average, signal strength in free space.

The later can be physically understood by observing that the signal energy in free space propagates outward, with the corresponding decrease in the power density, while in an indoor environment some of the energy is reflected back by the walls, window panes, etc., thus increasing the

average power density within the compartment. The particular compartment analyzed in this research and for the several transmitting antenna locations is by and large "free space" neutral, with the excess gain mean value between -0.1 and +2.9 dB, depending on the source location. The restrictions of time and computer resources limited this research to only one complex compartment. Furthermore, the computer resources available would not allow the placement of observation points at separations below "two per operating wavelength" to allow very fine sampling of the fields inside the compartments.

These facts, as well as the code limitation with respect to the dynamic range, should be taken into account, and offer plenty of opportunities for further research. Nonetheless, the results definitely confirmed the applicability of the excess gain random variable approach in general and the lognormal distribution model in particular. NEC-BSC is generally accepted as a very useful tool for modeling a variety of radiation and scattering phenomena. Over the years it was reported to provide reliable results especially when used for outdoor environments. Recently, other studies ([38] and the present one) showed quite promising results in using NEC-BSC for modeling indoor

propagation as well. However, definite conclusions require extensive further investigation and modeling of a multitude of diverse indoor environments.

APPENDIX A. MATLAB FILES

This is the Matlab file used to read the data, resulted from "PATCH" software and create the plots necessary for the comparison between that and NEC-BSC (Case: cylinder and dipole)

```
% plot near field data
clear
rad=pi/180;
iff=1;
if iff==0
load amptff1.m
load amppff1.m
amptff=amptff1; amppff=amppff1;
P=[0:180];
figure(1),clf
plot(P,amptff(1:181),P,amppff(1:181),'--'),grid
xlabel('Phi, deg')
ylabel('Total electric field (dB)')
title('Far field, a=0.175m, L=1m, theta=90, dip @ phi=0')
axis([0,180,-30,0])
end

% currents (get from outnear files)
Js=0.17859E+01+j*0.20941E+01; iplt=0; % 2.54 GHz outnear
2
% Js=0.0041847+j*0.40483E+00; iplt=0; % 1 GHz outnear 3
% Js=0.18605E+01-j*0.83378; iplt=1; % 1 GHz dipole
outnear 6 (20 segs)
% Js=0.96774E+01-j*0.48566E+01; iplt=1; % 1 GHz skinny
dipole 20 segs outnear 7
% Js=2.4268-j*0.62429; iplt=0; % outnear 9 (longer dip
for 1 GHz)

I=Js*.005; % I=Js*(width of dipole)
V=1;
Z=V/I;
% D=20*log10(abs(I)*.19); % for outnear 3 L is not wavl/2
but 0.19

D=20*log10(abs(I));% factor of nonunit amplitudecurrent
load nearpts2.m
nearpts=nearpts2;
[nrow,ncol]=size(nearpts);
npts=nrow/2;
```

```

Ez(1:npts)=nearpts(1:2:nrow,7)+j*nearpts(1:2:nrow,8);
Ey(1:npts)=nearpts(1:2:nrow,5)+j*nearpts(1:2:nrow,6);
Ex(1:npts)=nearpts(1:2:nrow,3)+j*nearpts(1:2:nrow,4);

if iplt==0,
load nearfldpts180.m; nearfldpts=nearfldpts180;
end

if iplt==1, load nearfldptsz.m; nearfldpts=nearfldptsz;
end
x=nearfldpts(:,1); y=nearfldpts(:,2); z=nearfldpts(:,3); %
set for 180 points
R=sqrt(x.^2+y.^2+z.^2);
T=acos(z./R);
P=atan2(y,x);
U=cos(T).*cos(P);
V=cos(T).*sin(P);
W=-sin(T);
Y=cos(P);
Z=sin(P);
Et=U.*transpose(Ex)+V.*transpose(Ey)+W.*transpose(Ez);
Ep=-Z.*transpose(Ex)+Y.*transpose(Ey);
Emax=sqrt(Et.*conj(Et)); % +Ep.*conj(Ep));
% Emax=sqrt(Ex.*conj(Ex)+Ey.*conj(Ey)+Ez.*conj(Ez));
Edb=20*log10(Emax)-D;
load gtddat.m
E=gtddat(:,6); E(361)=E(1);

if iplt==0 % plot cylinder and dipole
E2=[Edb fliplr(Edb)]; % mirror image of pattern
P2=[P/rad 360-fliplr(P/rad)];
figure(2),clf
plot(P2,E2,'b',[0:360],E,'r--'),grid
xlabel('Phi, deg')
ylabel('Total electric field (dB)')
title('Electric field by patch (blue) and NEC-BSC (red)')
end

if iplt==1 % just plot dipole data
for i=1:length(T)
TT(i)=T(i);
if P(i)==pi, TT(i)=2*pi-T(i);
end
end
end

```



```

plot(TT/rad,Edb,'-'),hold on
xlabel('Theta, deg')
ylabel('|E|, dB')
title('half-wave dipole field at R=5m (f=1 GHz)')
axis([0,360,-20,30])
figure(3),clf
polar2d((TT/rad).',Edb,'-')
title('short dipole field at R=5m (f=1 GHz)')
% analytical dipole field (current is I from above)
Et=377/2/pi/5*abs(cos(pi/2.*cos(TT))./sin(TT+1e-3));
Etdb=20*log10(Et);
figure(2)
plot(TT/rad,Etdb,'--')
axis([0,360,-20,30])
hold off
end

```

End of all Matlab files

THIS PAGE INTENTIONALLY LEFT BLANK

APPENDIX B. NEC-BSC INPUT FILES

CE: This is the input file used in the comparison between
CE: NEC-BSC and PATCH software in the case of the cylinder
CE: and the dipole

ZD:
0

UN:
1

FR: 2.54
2.54000

US: wavelengths
0

SG:
1.00000, 0.000000, 0.000000
0.000000, 0.000000, 90.0000, 0.000000
-2, 0.500000, 0.000000
1.00000, 0.000000

CG:
0.000000, 0.000000, 0.000000
0.000000, 0.000000, 90.0000, 0.000000
0.175000, 0.175000
-0.500000, 90.0000, 0.500000, 90.0000

PN:
0.000000, 0.000000, 0.000000
0.000000, 0.000000, 90.0000, 0.000000
F
5.00000, 90.0000, 0.000000
0.000000, 0.000000, 1.00000
360

PL:
T
LY
T
XQ: Execute the program
EN: End

CE: This is the input file used in the simple metallic room

CE: Six box room with a cylindrical obstacle inside it

ZD: type of material: PEC

0

FR: we will use a frequency of 2.4 GH
2.40000

US:

0

SG: Source geometry (3,1,11).

3.00000, 1.00000, 11.0000
0.000000, 0.000000, 90.0000, 0.000000
-2, 0.500000, 0.000000
1.00000, 0.000000

PG: First plate

4, 0
0.000000, 0.000000, 0.000000
0.000000, 12.0000, 0.000000
6.00000, 12.0000, 0.000000
6.00000, 0.000000, 0.000000

PG: second plate

4, 0
0.000000, 0.000000, 0.000000
6.00000, 0.000000, 0.000000
6.00000, 0.000000, 12.0000
0.000000, 0.000000, 12.0000

PG: Third plate

4, 0
6.00000, 0.000000, 12.0000
6.00000, 0.000000, 0.000000
6.00000, 12.0000, 0.000000
6.00000, 12.0000, 12.0000

PG: Forth plate ==front

4, 0
6.00000, 12.0000, 12.0000

6.00000, 12.0000, 0.000000
0.000000, 12.0000, 0.000000
0.000000, 12.0000, 12.0000

PG: Fifth plate

4, 0
6.00000, 0.000000, 12.0000
6.00000, 12.0000, 12.0000
0.000000, 12.0000, 12.0000
0.000000, 0.000000, 12.0000

PG: Sixth plate

4, 0
0.000000, 0.000000, 12.0000
0.000000, 12.0000, 12.0000
0.000000, 12.0000, 0.000000
0.000000, 0.000000, 0.000000

CG: Put a cylinder as an obstacle inside the room

3.00000, 6.00000, 0.000000
0.000000, 0.000000, 90.0000, 0.000000
1.00000, 1.00000
0.000000, 90.0000, 6.00000, 90.0000

PN: Near zone cut

3.00000, 6.00000, 3.00000
0.000000, 0.000000, 90.0000, 0.000000
F
1.50000, 90.0000, 0.000000
0.000000, 0.000000, 1.00000
180

PL:

T

LY

T

XQ: Execute the program

EN: End

CE: This is the input file used in the complex metallic
room

CM: Six box room (6,12,12) with two cylindrical obstacles
CE: and two tanks inside

ZD: type of material: PEC

0

FR: we will use a frequency of 2.45 GH
2.45000

US:

0

SG: Source geometry (3,3,1).

3.00000, 3.00000, 1.00000

0.000000, 0.000000, 90.0000, 0.000000

-2, 0.500000, 0.000000

1.00000, 0.000000

VN: VOLUMETRIC PLOT at Z=1.5 m.

0.000000, 0.000000, 0.000000

0.000000, 0.000000, 90.0000, 0.000000

T

0.000000, 0.000000, 1.50000

0.100000, 0.100000, 0.000000

1, 60, 120

PG: First plate

4, 0

0.000000, 0.000000, 0.000000

0.000000, 12.0000, 0.000000

6.00000, 12.0000, 0.000000

6.00000, 0.000000, 0.000000

PG: second plate

4, 0

0.000000, 0.000000, 0.000000

6.00000, 0.000000, 0.000000

6.00000, 0.000000, 12.0000

0.000000, 0.000000, 12.0000

PG: Third plate

4, 0

6.00000, 0.000000, 12.0000

6.00000, 0.000000, 0.000000

6.00000, 12.0000, 0.000000

6.00000, 12.0000, 12.0000

PG: Forth plate ==front

4, 0

6.00000, 12.0000, 12.0000
6.00000, 12.0000, 0.000000
0.000000, 12.0000, 0.000000
0.000000, 12.0000, 12.0000

PG: Fifth plate

4, 0
6.00000, 0.000000, 12.0000
6.00000, 12.0000, 12.0000
0.000000, 12.0000, 12.0000
0.000000, 0.000000, 12.0000

PG: Sixth plate

4, 0
0.000000, 0.000000, 12.0000
0.000000, 12.0000, 12.0000
0.000000, 12.0000, 0.000000
0.000000, 0.000000, 0.000000

CG: Put a cylinder as an obstacle inside the room

1.50000, 6.00000, 0.000000
0.000000, 0.000000, 90.0000, 0.000000
0.500000, 0.500000
0.000000, 90.0000, 12.0000, 90.0000

CG: Put a second cylinder as an obstacle inside the room

4.50000, 6.00000, 0.000000
0.000000, 0.000000, 90.0000, 0.000000
0.500000, 0.500000
0.000000, 90.0000, 12.0000, 90.0000

PG: first tank front

4, 0
2.00000, 1.00000, 0.000000
2.00000, 1.00000, 6.00000
4.00000, 1.00000, 6.00000
4.00000, 1.00000, 0.000000

PG: first tank side

4, 0
4.00000, 0.000000, 6.00000
4.00000, 0.000000, 0.000000
4.00000, 1.00000, 0.000000
4.00000, 1.00000, 6.00000

PG: first tank side

4, 0
2.00000, 0.000000, 6.00000
2.00000, 1.00000, 6.00000
2.00000, 1.00000, 0.000000
2.00000, 0.000000, 0.000000

PG: first tank up

4, 0
2.00000, 0.000000, 6.00000
4.00000, 0.000000, 6.00000
4.00000, 1.00000, 6.00000
2.00000, 1.00000, 6.00000

PG: second tank front

4, 0
2.00000, 11.0000, 0.000000
4.00000, 11.0000, 0.000000
4.00000, 11.0000, 6.00000
2.00000, 11.0000, 6.00000

PG: second tank side

4, 0
4.00000, 11.0000, 6.00000
4.00000, 11.0000, 0.000000
4.00000, 12.0000, 0.000000
4.00000, 12.0000, 6.00000

PG: second tank side

4, 0
2.00000, 11.0000, 6.00000
2.00000, 12.0000, 6.00000
2.00000, 12.0000, 0.000000
2.00000, 11.0000, 0.000000

PG: second tank up

4, 0
2.00000, 11.0000, 6.00000
4.00000, 11.0000, 6.00000
4.00000, 12.0000, 6.00000
2.00000, 12.0000, 6.00000

PL:

T

XQ:

EN: End

CE: This is the input file used for openings

CE: right hand ok, commands ok problem with penetration

FR: We will use a frequency of 2.4 GHz (ISM band)
2.40000

US:
0

PG: platel up

4, 0
6.00000, -6.00000, 12.0000
6.00000, -6.00000, 8.00000
6.00000, 6.00000, 8.0000
6.00000, 6.00000, 12.00000

PG: plate 2

4, 0
6.00000, 6.00000, 12.0000
6.00000, 3.00000, 12.0000
6.00000, 3.00000, 0.000000
6.00000, 6.00000, 0.000000

PG: plate 3

4, 0
6.00000, 6.00000, 0.000000
6.00000, 6.00000, 4.00000
6.00000, -6.00000, 4.00000
6.00000, -6.00000, 0.000000

PG: plate 4

4, 0
6.00000, -6.00000, 0.000000
6.00000, -3.00000, 0.000000
6.00000, -3.00000, 12.0000
6.00000, -6.00000, 12.0000

SG: Source in height 6

0.000000, 0.000000, 6.000000
0.000000, 0.000000, 90.0000, 0.000000
-1, 1.00000, 0.000000
1.00000, 0.000000

PN: Near zone cut

9.000000, 0.000000, 0.000000
0.000000, 0.000000, 90.0000, 0.000000

T

3.00000, 0.000000, 0.000000
0.000000, 0.000000, 2.00000

7

PL:

T

LY

T

XQ: Execute the program

EN: End

CE: This is the input file used for pseudo-openings

CE: right hand ok

FR: We will use a frequency of 2.4 GHz (ISM band)
2.40000

US:

0

PG: wall

4, 0

6.00000, -6.000000, 12.0000
6.00000, -6.000000, 0.000000
6.00000, 6.0000, 0.000000
6.00000, 6.0000, 12.0000

ZD: opening-thin material slab

1

1

0.0500000, 1.01000, 0.000000, 1.00000, 0.000000

PG: door

4, 0

6.00000, -3.000000, 8.0000
6.00000, -3.000000, 4.000000
6.00000, 3.00000, 4.000000
6.00000, 3.0000, 8.0000

SG: Source in height 6

0.000000, 0.000000, 6.00000

0.000000, 0.000000, 90.0000, 0.000000
-1, 0.500000, 0.000000
1.00000, 0.000000

PN: Near zone cut
9.00000, 0.000000, 0.000000
0.000000, 0.000000, 90.0000, 0.000000
T
3.00000, 0.000000, 0.000000
0.000000, 0.000000, 2.00000
7

PL:
T

LY
T

XQ: Execute the program

EN: End

CE: This is the input file used for one Antenna located in
CE: the middle of the room

CE: Rear tank plates overlap to avoid diffraction
CE: inside them

CM: Dimensions of the missile room: Dim(20,10,10) Origin at
CE: the most FORWARD and PORT point of the default view

CM: All materials would be Perfect Electric Conductors,
CE: unless otherwise defined.

ZD: P.E.C.
0

FR: We will use a frequency of 2.4 GHz (ISM band)
2.40000

US: (Necessary) in Wavelengths
0

SG: Put the source at (10,5,2) position
10.0000, 5.00000, 2.00000
0.000000, 0.000000, 90.0000, 0.000000

-1, 0.500000, 0.000000
1.00000, 0.000000

VN: VOLUMETRIC PLOT at Z=2 m.
0.000000, 0.000000, 0.000000
0.000000, 0.000000, 90.0000, 0.000000
T
0.000000, 0.000000, 2.00000
0.0500000, 0.0500000, 0.000000
1, 400, 200

CE: Construct the room, according to the RIGHT-HAND RULE

CM: Since we can not simulate the opening with an adequate
CM: material, we define five different plates for the
CE: Forward Level.

CM: PG: room: (20,10,10) FORWARD level
CM: 4, 0
CM: 0.000000, 10.0000, 0.000000
CM: 0.000000, 10.0000, 10.0000
CM: 0.000000, 0.000000, 10.0000
CE: 0.000000, 0.000000, 0.000000

CE: Construct all the plates, but the opening itself

PM:
12
0.000000, 0.000000, 0.000000
0.000000, 10.0000, 0.000000
0.000000, 10.0000, 0.300000
0.000000, 0.000000, 0.300000
0.000000, 5.50000, 1.80000
0.000000, 10.0000, 1.80000
0.000000, 10.0000, 10.0000
0.000000, 0.000000, 10.0000
0.000000, 5.50000, 0.300000
0.000000, 0.000000, 1.80000
0.000000, 4.50000, 0.300000
0.000000, 4.50000, 1.80000
0
1
2
3
4
0

9
3
6
5
0
4
11
12
10
0
10
6
7
8
0
0

CM: In case we want the wall without the opening (solid),
CE: we uncomment the following command:

CM: PG: This is the opening in the forward bulkhead

CM: 4, 0

CM: 0.000000, 4.50000, 0.300000

CM: 0.000000, 4.50000, 1.80000

CM: 0.000000, 5.50000, 1.80000

CE: 0.000000, 5.50000, 0.300000

PG: room:(20,10,10) GROUND level

4, 0

0.000000, 0.000000, 0.000000

20.0000, 0.000000, 0.000000

20.0000, 10.0000, 0.000000

0.000000, 10.0000, 0.000000

PG: room:(20,10,10) UPPER level

4, 0

0.000000, 10.0000, 10.0000

20.0000, 10.0000, 10.0000

20.0000, 0.000000, 10.0000

0.000000, 0.000000, 10.0000

PG: room:(20,10,10) AFT level

4, 0

20.0000, 0.000000, 0.000000

20.0000, 0.000000, 10.0000

20.0000, 10.0000, 10.0000

20.0000, 10.0000, 0.000000

PG: PORT BULKHEAD

4, 0

0.000000, 0.000000, 0.000000

0.000000, 0.000000, 10.0000

20.0000, 0.000000, 10.0000

20.0000, 0.000000, 0.000000

PG: STARBOARD BULKHEAD

4, 0

0.000000, 10.0000, 0.000000

20.0000, 10.0000, 0.000000

20.0000, 10.0000, 10.0000

0.000000, 10.0000, 10.0000

CE: First OVERHEAD: This is an intermediate floor at z=5

CE:level

PG: level:(0,0,5) first walking floor

4, 0

0.000000, 0.000000, 5.00000

0.000000, 10.0000, 5.00000

20.0000, 10.0000, 5.00000

20.0000, 0.000000, 5.00000

CE: Construct all the plates, but the opening itself

CM: PG: RIGHT

CM: 4, 0

CM: 0.000000, 5.50000, 5.00000

CM: 0.000000, 10.0000, 5.00000

CM: 20.0000, 10.0000, 5.00000

CM: 20.0000, 5.50000, 5.00000

CM:

CM: PG: MIDDLE

CM: 4, 0

CM: 15.7500, 5.51000, 5.00000

CM: 20.0000, 5.51000, 5.00000

CM: 20.0000, 4.49000, 5.00000

CM: 15.7500, 4.49000, 5.00000

CM:

CM: PG: MIDDLE

CM: 4, 0

CM: 0.000000, 5.51000, 5.00000

CM: 14.7500, 5.51000, 5.00000

CM: 14.7500, 4.49000, 5.00000
CM: 0.000000, 4.49000, 5.00000
CM:
CM: PG: LEFT
CM: 4, 0
CM: 0.000000, 0.000000, 5.00000
CM: 0.000000, 4.50000, 5.00000
CM: 20.0000, 4.50000, 5.00000
CE: 20.0000, 0.000000, 5.00000

CM: In case we want the overhead without the opening
CM: (solid),
CE: we uncomment the following command:

CM: PG: This is an opening in the overhead
CM: 4, 0
CM: 15.7500, 4.50000, 5.00000
CM: 14.7500, 4.50000, 5.00000
CM: 14.7500, 5.50000, 5.00000
CE: 15.7500, 5.50000, 5.00000

CE: These are the 6 missile tubes

CG: First (FORWARD PORT) missile tube
6.00000, 3.00000, 0.000000
0.000000, 0.000000, 90.0000, 0.000000
1.00000, 1.00000
0.000000, 90.0000, 10.0000, 90.0000

CG: Second (FORWARD STARBOARD) missile tube
6.00000, 7.00000, 0.000000
0.000000, 0.000000, 90.0000, 0.000000
1.00000, 1.00000
0.000000, 90.0000, 10.0000, 90.0000

RR: Make the remaining symmetric tubes. First shift
4.00000, 0.000000, 0.000000
0.000000, 0.000000, 90.0000, 0.000000

CG: Third (PORT) missile tube
6.00000, 3.00000, 0.000000
0.000000, 0.000000, 90.0000, 0.000000
1.00000, 1.00000
0.000000, 90.0000, 10.0000, 90.0000

CG: Forth (STARBOARD) missile tube
6.00000, 7.00000, 0.000000
0.000000, 0.000000, 90.0000, 0.000000
1.00000, 1.00000
0.000000, 90.0000, 10.0000, 90.0000

RR: Make the remaining symmetric tubes. Second shift
4.00000, 0.000000, 0.000000
0.000000, 0.000000, 90.0000, 0.000000

CG: Fifth (PORT) missile tube
6.00000, 3.00000, 0.000000
0.000000, 0.000000, 90.0000, 0.000000
1.00000, 1.00000
0.000000, 90.0000, 10.0000, 90.0000

CG: Sixth (STARBOARD) missile tube
6.00000, 7.00000, 0.000000
0.000000, 0.000000, 90.0000, 0.000000
1.00000, 1.00000
0.000000, 90.0000, 10.0000, 90.0000

CE: We have to revert to global coordinates. AGAIN

RR: Back to global coordinates
-8.00000, 0.000000, 0.000000
0.000000, 0.000000, 90.0000, 0.000000

CM: CG: Test tube at new(0,0,0). Should be placed at origin. CM: OK!

CM: 0.000000, 0.000000, 0.000000
CM: 0.000000, 0.000000, 90.0000, 0.000000
CM: 1.00000, 1.00000
CE: 0.000000, 90.0000, 10.0000, 90.0000

CE: FIRST FLOOR INTERIOR, TANKS, STAIRS, OPENING

CM: Construct the TANKS inside the first floor. There will
CM: be three tanks along the PORT side of the room. The
CM: FORWARD and
CM: AFT one will have half the height of the room (2.5m)
and
CM: the middle one will go up to the OVERHEAD (5m).
CM: Similarly
CM: and symmetrically, will be the STARBOARD side of the

CM: room.

CM: In addition, one big tank will be placed in the AFT part

CE: with a height of 2.5m.

CM: We CAN NOT consider PORT tanks, as if there was only one CM: large,

CM: along the PORT side and an additional one in the center

CM: because

CM: of the warnings we get. For the first,

CM: length 20m, width 0.5m and height 2.5m (half the way

CM: up).

CM: We only need to put the STARBOARD and UPPER plate of it,

CE: since the rest are already put as walls in the room.

PG: PORT large tank, STARBOARD+ forward plate only

4, 0

0.000000, 0.500000, 0.000000

0.000000, 0.500000, 2.50000

5.00000, 0.500000, 2.50000

5.00000, 0.500000, 0.000000

PG: PORT large tank, UPPER +forward plate only

4, 0

0.000000, 0.500000, 2.50000

0.000000, 0.000000, 2.50000

5.00000, 0.000000, 2.50000

5.00000, 0.500000, 2.50000

PG: PORT large tank, STARBOARD+ aft plate only

4, 0

15.0000, 0.500000, 0.000000

15.0000, 0.500000, 2.50000

20.0000, 0.500000, 2.50000

20.0000, 0.500000, 0.000000

PG: PORT large tank, UPPER +aft plate only

4, 0

15.0000, 0.500000, 2.50000

15.0000, 0.000000, 2.50000

20.0000, 0.000000, 2.50000

20.0000, 0.500000, 2.50000

PG: PORT additional tank, FORWARD plate only

4, 0

5.00000, 0.000000, 0.000000
5.00000, 0.000000, 5.00000
5.00000, 1.00000, 5.00000
5.00000, 1.00000, 0.000000

PG: PORT additional tank, AFT plate only

4, 0
15.0000, 0.000000, 0.000000
15.0000, 1.00000, 0.000000
15.0000, 1.00000, 5.00000
15.0000, 0.000000, 5.00000

PG: PORT additional tank, STARBOARD plate only

4, 0
5.00000, 1.00000, 0.000000
5.00000, 1.00000, 5.00000
15.0000, 1.00000, 5.00000
15.0000, 1.00000, 0.000000

PG: PORT additional tank, UPPER plate only

4, 0
5.00000, 0.000000, 5.00000
15.0000, 0.000000, 5.00000
15.0000, 1.00000, 5.00000
5.00000, 1.00000, 5.00000

PG: STARBOARD large tank, PORT+ forward plate only

4, 0
0.000000, 9.50000, 0.000000
5.00000, 9.50000, 0.000000
5.00000, 9.50000, 2.50000
0.000000, 9.50000, 2.50000

PG: STARBOARD large tank, UPPER and forward plate only

4, 0
0.000000, 9.50000, 2.50000
5.00000, 9.50000, 2.50000
5.00000, 10.0000, 2.50000
0.000000, 10.0000, 2.50000

PG: STARBOARD large tank, PORT and aft plate only

4, 0
15.0000, 9.50000, 0.000000
20.0000, 9.50000, 0.000000
20.0000, 9.50000, 2.50000
15.0000, 9.50000, 2.50000

PG: STARBOARD large tank, UPPER+ aft plate only

4, 0

15.0000, 9.50000, 2.50000

20.0000, 9.50000, 2.50000

20.0000, 10.0000, 2.50000

15.0000, 10.0000, 2.50000

PG: STARBOARD additional tank, FORWARD plate only

4, 0

5.00000, 9.00000, 0.000000

5.00000, 10.0000, 0.000000

5.00000, 10.0000, 5.00000

5.00000, 9.00000, 5.00000

PG: STARBOARD additional tank, AFT plate only

4, 0

15.0000, 9.00000, 0.000000

15.0000, 10.0000, 0.000000

15.0000, 10.0000, 4.99000

15.0000, 9.00000, 4.99000

PG: STARBOARD additional tank, PORT plate only

4, 0

5.00000, 9.00000, 0.000000

15.0000, 9.00000, 0.000000

15.0000, 9.00000, 5.00000

5.00000, 9.00000, 5.00000

PG: STARBOARD additional tank, UPPER plate only

4, 0

5.00000, 9.00000, 5.00000

15.0000, 9.00000, 5.00000

15.0000, 10.0000, 5.00000

5.00000, 10.0000, 5.00000

CM: We now construct the AFT tank, whose height is 2.5m. We only

CE: need the FORWARD and the UPPER part

PG: AFT tank FORWARD plate

4, 0

18.0000, 0.4500000, 0.000000

18.0000, 0.4500000, 2.50000

18.0000, 9.550000, 2.50000

18.0000, 9.550000, 0.000000

PG: AFT tank UPPER plate

4, 0

18.0000, 0.4500000, 2.50000

20.0000, 0.4500000, 2.50000

20.0000, 9.550000, 2.50000

18.0000, 9.550000, 2.50000

CM: The Offset Multi-level(up and down) Ladderway will be put in

CM: the center of the room. First we put a vertical plate at x=17

CE: and z=0.5. This does not count as a stair

PG: Initial vertical plate, before first stair

4, 0

17.0000, 4.50000, 0.000000

17.0000, 4.50000, 0.500000

17.0000, 5.50000, 0.500000

17.0000, 5.50000, 0.000000

PG: First Stair (two plates vertical each other).

Horizontal

4, 0

17.0000, 4.50000, 0.500000

17.0000, 5.50000, 0.500000

16.7500, 5.50000, 0.500000

16.7500, 4.50000, 0.500000

PG: First Stair (two vertical plates). Vertical

4, 0

16.7500, 5.50000, 0.500000

16.7500, 4.50000, 0.500000

16.7500, 4.50000, 1.00000

16.7500, 5.50000, 1.00000

RR: Make the remaining symmetric stairs. First shift

-0.250000, 0.000000, 0.500000

0.000000, 0.000000, 90.0000, 0.000000

PG: Second Stair (two vertical plates). Horizontal

4, 0

17.0000, 4.50000, 0.500000

17.0000, 5.50000, 0.500000

16.7500, 5.50000, 0.500000

16.7500, 4.50000, 0.500000

PG: Second Stair (two vertical plates). Vertical
4, 0

16.7500, 5.50000, 0.500000
16.7500, 4.50000, 0.500000
16.7500, 4.50000, 1.00000
16.7500, 5.50000, 1.00000

RR: Make the remaining symmetric stairs. Second shift
-0.250000, 0.000000, 0.500000
0.000000, 0.000000, 90.0000, 0.000000

PG: Third Stair (two vertical plates). Horizontal
4, 0

17.0000, 4.50000, 0.500000
17.0000, 5.50000, 0.500000
16.7500, 5.50000, 0.500000
16.7500, 4.50000, 0.500000

PG: Third Stair (two vertical plates). Vertical
4, 0

16.7500, 5.50000, 0.500000
16.7500, 4.50000, 0.500000
16.7500, 4.50000, 1.00000
16.7500, 5.50000, 1.00000

RR: Make the remaining symmetric stairs. Third shift
-0.250000, 0.000000, 0.500000
0.000000, 0.000000, 90.0000, 0.000000

PG: Forth Stair (two vertical plates). Horizontal
4, 0

17.0000, 4.50000, 0.500000
17.0000, 5.50000, 0.500000
16.7500, 5.50000, 0.500000
16.7500, 4.50000, 0.500000

PG: Forth Stair (two vertical plates). Vertical
4, 0

16.7500, 5.50000, 0.500000
16.7500, 4.50000, 0.500000
16.7500, 4.50000, 1.00000
16.7500, 5.50000, 1.00000

RR: Make the remaining symmetric stairs. Forth shift
-0.250000, 0.000000, 0.500000

0.000000, 0.000000, 90.0000, 0.000000

PG: Fifth Stair (two vertical plates). Horizontal
4, 0

17.0000, 4.50000, 0.500000
17.0000, 5.50000, 0.500000
16.7500, 5.50000, 0.500000
16.7500, 4.50000, 0.500000

PG: Fifth Stair (two vertical plates). Vertical
4, 0

16.7500, 5.50000, 0.500000
16.7500, 4.50000, 0.500000
16.7500, 4.50000, 1.00000
16.7500, 5.50000, 1.00000

RR: Make the remaining symmetric stairs. Fifth shift
-0.250000, 0.000000, 0.500000
0.000000, 0.000000, 90.0000, 0.000000

PG: Sixth Stair (two vertical plates). Horizontal
4, 0

17.0000, 4.50000, 0.500000
17.0000, 5.50000, 0.500000
16.7500, 5.50000, 0.500000
16.7500, 4.50000, 0.500000

PG: Sixth Stair (two vertical plates). Vertical
4, 0

16.7500, 5.50000, 0.500000
16.7500, 4.50000, 0.500000
16.7500, 4.50000, 1.00000
16.7500, 5.50000, 1.00000

RR: Make the remaining symmetric stairs. Sixth shift
-0.250000, 0.000000, 0.500000
0.000000, 0.000000, 90.0000, 0.000000

PG: Seventh Stair (two vertical plates). Horizontal
4, 0

17.0000, 4.50000, 0.500000
17.0000, 5.50000, 0.500000
16.7500, 5.50000, 0.500000
16.7500, 4.50000, 0.500000

PG: Seventh Stair (two vertical plates). Vertical

4, 0
16.7500, 5.50000, 0.500000
16.7500, 4.50000, 0.500000
16.7500, 4.50000, 1.00000
16.7500, 5.50000, 1.00000

RR: Make the remaining symmetric stairs. Seventh shift
-0.250000, 0.000000, 0.500000
0.000000, 0.000000, 90.0000, 0.000000

PG: Eighth Stair (two vertical plates). Horizontal
4, 0
17.0000, 4.50000, 0.500000
17.0000, 5.50000, 0.500000
16.7500, 5.50000, 0.500000
16.7500, 4.50000, 0.500000

PG: Eighth Stair (two vertical plates). Vertical
4, 0
16.7500, 5.50000, 0.500000
16.7500, 4.50000, 0.500000
16.7500, 4.50000, 1.00000
16.7500, 5.50000, 1.00000

RR: Make the remaining symmetric stairs. Eighth shift
-0.250000, 0.000000, 0.500000
0.000000, 0.000000, 90.0000, 0.000000

PG: Ninth Stair (two vertical plates). Horizontal
4, 0
17.0000, 4.50000, 0.500000
17.0000, 5.50000, 0.500000
16.7500, 5.50000, 0.500000
16.7500, 4.50000, 0.500000

PG: Ninth Stair, Vertical 0.1cm higher to avoid warning
(p.161)
4, 0
16.7500, 5.50000, 0.500000
16.7500, 4.50000, 0.500000
16.7500, 4.50000, 1.00100
16.7500, 5.50000, 1.00100

CE: We have to revert to global coordinates. AGAIN

RR: Back to global coordinates

2.000000, 0.000000, -4.000000
0.000000, 0.000000, 90.0000, 0.000000

CM: CG: Test tube at new(0,0,0). Should be placed at
origin. CM: OK!

CM: 0.000000, 0.000000, 0.000000
CM: 0.000000, 0.000000, 90.0000, 0.000000
CM: 1.000000, 1.000000
CE: 0.000000, 90.0000, 10.0000, 90.0000

CM: We have already put the forward vertical plate that
CM: surrounds
CM: the opening. We now put the remaining three, trying to
CE: eliminate the warnings (thus Zmax=5.001)

PG: REST of the frame that surrounds the opening: LEFT
4, 0
14.7500, 4.50000, 5.00100
15.7500, 4.50000, 5.00100
15.7500, 4.50000, 4.70000
14.7500, 4.50000, 4.70000

PG: REST of the frame that surrounds the opening: RIGHT
4, 0
14.7500, 5.50000, 5.00100
14.7500, 5.50000, 4.70000
15.7500, 5.50000, 4.70000
15.7500, 5.50000, 5.00100

PG: REST of the frame that surrounds the opening: AFT
4, 0
15.7500, 4.50000, 5.00100
15.7500, 5.50000, 5.00100
15.7500, 5.50000, 4.70000
15.7500, 4.50000, 4.70000

CM: We should now "attach" a specific material with certain
CM: characteristics in the overhead of the first floor in
CM: order to simulate the opening where the stairs end!
CM: Center
CM: of the opening: 15 5 5 From x=14->15 y=4.5->5.5 z=5.
CM: THIS UNORTHODOX METHOD DOES NOT WORK PROPERLY, SO WE
CM: CHOOSE
CM: TO WORK ANALYTICALLY, BY CONSTRUCTING EACH OTHER PART
OF CM: THE

CE: OVERHEAD BUT THE OPENING ITSELF AND THEN "GLUE" THEM
TOGETHER!

CM: ZD: Simulated opening. Permittivity 1.01CM: 1
CM: 1
CM: 0.0500000, 1.01000, 0.000000, 1.00000, 0.000000
CM:
CM: PG: This is an opening in the overhead
CM: 4, 0
CM: 15.7500, 4.50000, 5.00000
CM: 14.7500, 4.50000, 5.00000
CM: 14.7500, 5.50000, 5.00000
CM: 15.7500, 5.50000, 5.00000
CM:
CM: ZD: Back again to P.E.C.
CE: 0

CM: We now try to construct the HANDRAILS as cylinders with
CM: small radius and adequate angle. USE THE Z AXIS
CE: POSITION- ROTATE

CG: LEFT HANDRAIL
17.0000, 4.50000, 0.250000
335.000, 0.000000, 0.000000, -999.000
0.100000, 0.100000
0.000000, 45.0000, 5.00000, 45.0000

CG: RIGHT HANDRAIL
17.0000, 5.50000, 0.250000
335.000, 0.000000, 0.000000, -999.000
0.100000, 0.100000
0.000000, 45.0000, 5.00000, 45.0000

CM: -----
-
CM: -----END OF FIRST FLOOR-----
-
CE: -----
-

PL:
T

XQ:

EN: End

CE: This is the input file when Antenna is located in a
CE: random place. We will present only the commands
different from the previous file.

CE: Put one antenna in (14,5,1).

SG: Put the source at (14,5,1) position
14.0000, 5.00000, 1.00000
0.000000, 0.000000, 90.0000, 0.000000
-1, 0.500000, 0.000000
1.00000, 0.000000

VN: VOLUMETRIC PLOT at Z=1.5 m.
0.000000, 0.000000, 0.000000
0.000000, 0.000000, 90.0000, 0.000000
T
0.000000, 0.000000, 1.50000
0.0500000, 0.0500000, 0.000000
1, 400, 200

EN: End

CE: This is the input file when two Antennas are located in
CE: the room. We will present only the commands different
from the previous file

CM: Put 2 sources in Z=4m level and observation
CM: area at Z=1m. Rear tank plates overlap to avoid
CE: diffraction inside the tank

SG: Put the source at (14,5,4) position
14.0000, 5.00000, 4.00000
0.000000, 0.000000, 90.0000, 0.000000
-1, 0.500000, 0.000000
1.00000, 0.000000

SG: Put ANOTHER source at (6,5,4) position
6.0000, 5.00000, 4.00000
0.000000, 0.000000, 90.0000, 0.000000
-1, 0.500000, 0.000000
1.00000, 0.000000

VN: VOLUMETRIC PLOT at Z=1.0 m.
0.000000, 0.000000, 0.000000
0.000000, 0.000000, 90.0000, 0.000000
T
0.000000, 0.000000, 1.00000
0.0500000, 0.0500000, 0.000000
1, 400, 200

EN: End

CE: This is the input file for room to room case. This is
a different file. We will present only the commands
different from the previous file.

ZD: P.E.C.
0

FR: We will use a frequency of 2.4 GHz (ISM band)
2.40000

US: (Necessary) in Wavelengths
0

SG: Put the source at (14,5,1) position
14.0000, 5.00000, 1.00000
0.000000, 0.000000, 90.0000, 0.000000
-1, 0.500000, 0.000000
1.00000, 0.000000

CM: Antenna is located in the first floor, but
CM: observation
CM: points are in the second floor (1.5m above the floor).
CM: Recall that the problem with the plate edges
diffraction
CE: still exists

VN: VOLUMETRIC PLOT at Z=6.5 m
0.000000, 0.000000, 0.000000
0.000000, 0.000000, 90.0000, 0.000000
T
1.00000, 1.00000, 6.50000
0.0500000, 0.0500000, 0.000000

1, 400, 200

CE: Construct the ROOM, according to the RIGHT-HAND RULE
(SAME AS BEFORE)

CM: -----

-

CM: -----END OF FIRST FLOOR-----

-

CE: -----

-

CE: SECOND FLOOR (MISSILES AND FRAME ALREADY PUT)

CM: SECOND OVERHEAD: This is an Overhead at z=10 level. We

CM: will

CE: use the first construction, shifted by 5m along Z axis

CM: PG: level: (0,0,10) ----SECOND OVERHEAD----

CM: Theoretically----

CM: 4, 0

CM: 0.000000, 0.000000, 10.00000

CM: 0.000000, 10.0000, 10.00000

CM: 20.0000, 10.0000, 10.00000

CE: 20.0000, 0.000000, 10.00000

CE: Construct all the plates, but the opening itself

PG: RIGHT

4, 0

0.000000, 5.50000, 10.00000

0.000000, 10.0000, 10.00000

20.0000, 10.0000, 10.00000

20.0000, 5.50000, 10.00000

PG: MIDDLE

4, 0

15.7500, 5.51000, 10.00000

20.0000, 5.51000, 10.00000

20.0000, 4.49000, 10.00000

15.7500, 4.49000, 10.00000

PG: MIDDLE

4, 0

0.000000, 5.51000, 10.00000

14.7500, 5.51000, 10.00000

14.7500, 4.49000, 10.00000
0.000000, 4.49000, 10.00000

PG: LEFT

4, 0

0.000000, 0.000000, 10.00000
0.000000, 4.50000, 10.00000
20.0000, 4.50000, 10.00000
20.0000, 0.000000, 10.00000

CM: In case we want the overhead without the
OPENING(solid),

CE: we uncomment the following command:

CM: PG: This is an OPENING in the second overhead

CM: 4, 0

CM: 15.7500, 4.50000, 10.00000

CM: 14.7500, 4.50000, 10.00000

CM: 14.7500, 5.50000, 10.00000

CE: 15.7500, 5.50000, 10.00000

CM: The SECOND Offset Multi-level(up and down) Ladderway

CM: will be put in

CM: the aft part of the room. First we put a vertical plate

CM: at x=17

CE: and z=0.5. This does not count as a stair

RR: Use the first construction for the SECOND LADDERWAY

0.000000, 0.000000, 5.00000

0.000000, 0.000000, 90.0000, 0.000000

CM: PG: Initial vertical plate, before first stair Warnings

CM: 4, 0

CM: 17.0000, 4.50000, 0.000000

CM: 17.0000, 4.50000, 0.500000

CM: 17.0000, 5.50000, 0.500000

CE: 17.0000, 5.50000, 0.000000

PG: First Stair (two plates vertical each other).Horizontal

4, 0

17.0000, 4.50000, 0.500000

17.0000, 5.50000, 0.500000

16.7500, 5.50000, 0.500000

16.7500, 4.50000, 0.500000

PG: First Stair (two vertical plates). Vertical

4, 0

16.7500, 5.50000, 0.500000

16.7500, 4.50000, 0.500000

16.7500, 4.50000, 1.00000

16.7500, 5.50000, 1.00000

RR: Make the remaining symmetric stairs. First shift

-0.250000, 0.000000, 0.500000

0.000000, 0.000000, 90.0000, 0.000000

PG: Second Stair (two vertical plates). Horizontal

4, 0

17.0000, 4.50000, 0.500000

17.0000, 5.50000, 0.500000

16.7500, 5.50000, 0.500000

16.7500, 4.50000, 0.500000

PG: Second Stair (two vertical plates). Vertical

4, 0

16.7500, 5.50000, 0.500000

16.7500, 4.50000, 0.500000

16.7500, 4.50000, 1.00000

16.7500, 5.50000, 1.00000

RR: Make the remaining symmetric stairs. Second shift

-0.250000, 0.000000, 0.500000

0.000000, 0.000000, 90.0000, 0.000000

PG: Third Stair (two vertical plates). Horizontal

4, 0

17.0000, 4.50000, 0.500000

17.0000, 5.50000, 0.500000

16.7500, 5.50000, 0.500000

16.7500, 4.50000, 0.500000

PG: Third Stair (two vertical plates). Vertical

4, 0

16.7500, 5.50000, 0.500000

16.7500, 4.50000, 0.500000

16.7500, 4.50000, 1.00000

16.7500, 5.50000, 1.00000

RR: Make the remaining symmetric stairs. Third shift

-0.250000, 0.000000, 0.500000

0.000000, 0.000000, 90.0000, 0.000000

PG: Forth Stair (two vertical plates). Horizontal
4, 0

17.0000, 4.50000, 0.500000
17.0000, 5.50000, 0.500000
16.7500, 5.50000, 0.500000
16.7500, 4.50000, 0.500000

PG: Forth Stair (two vertical plates). Vertical
4, 0

16.7500, 5.50000, 0.500000
16.7500, 4.50000, 0.500000
16.7500, 4.50000, 1.00000
16.7500, 5.50000, 1.00000

RR: Make the remaining symmetric stairs. Forth shift
-0.250000, 0.000000, 0.500000
0.000000, 0.000000, 90.0000, 0.000000

PG: Fifth Stair (two vertical plates). Horizontal
4, 0

17.0000, 4.50000, 0.500000
17.0000, 5.50000, 0.500000
16.7500, 5.50000, 0.500000
16.7500, 4.50000, 0.500000

PG: Fifth Stair (two vertical plates). Vertical
4, 0

16.7500, 5.50000, 0.500000
16.7500, 4.50000, 0.500000
16.7500, 4.50000, 1.00000
16.7500, 5.50000, 1.00000

RR: Make the remaining symmetric stairs. Fifth shift
-0.250000, 0.000000, 0.500000
0.000000, 0.000000, 90.0000, 0.000000

PG: Sixth Stair (two vertical plates). Horizontal
4, 0

17.0000, 4.50000, 0.500000
17.0000, 5.50000, 0.500000
16.7500, 5.50000, 0.500000
16.7500, 4.50000, 0.500000

PG: Sixth Stair (two vertical plates). Vertical
4, 0

16.7500, 5.50000, 0.500000
16.7500, 4.50000, 0.500000
16.7500, 4.50000, 1.00000
16.7500, 5.50000, 1.00000

RR: Make the remaining symmetric stairs. Sixth shift
-0.250000, 0.000000, 0.500000
0.000000, 0.000000, 90.0000, 0.000000

PG: Seventh Stair (two vertical plates). Horizontal
4, 0
17.0000, 4.50000, 0.500000
17.0000, 5.50000, 0.500000
16.7500, 5.50000, 0.500000
16.7500, 4.50000, 0.500000

PG: Seventh Stair (two vertical plates). Vertical
4, 0
16.7500, 5.50000, 0.500000
16.7500, 4.50000, 0.500000
16.7500, 4.50000, 1.00000
16.7500, 5.50000, 1.00000

RR: Make the remaining symmetric stairs. Seventh shift
-0.250000, 0.000000, 0.500000
0.000000, 0.000000, 90.0000, 0.000000

PG: Eighth Stair (two vertical plates). Horizontal
4, 0
17.0000, 4.50000, 0.500000
17.0000, 5.50000, 0.500000
16.7500, 5.50000, 0.500000
16.7500, 4.50000, 0.500000

PG: Eighth Stair (two vertical plates). Vertical
4, 0
16.7500, 5.50000, 0.500000
16.7500, 4.50000, 0.500000
16.7500, 4.50000, 1.00000
16.7500, 5.50000, 1.00000

RR: Make the remaining symmetric stairs. Eighth shift
-0.250000, 0.000000, 0.500000
0.000000, 0.000000, 90.0000, 0.000000

PG: Ninth Stair (two vertical plates). Horizontal

4, 0
17.0000, 4.50000, 0.500000
17.0000, 5.50000, 0.500000
16.7500, 5.50000, 0.500000
16.7500, 4.50000, 0.500000

PG: Ninth Stair, Vertical. 0.1cm higher to avoid warnings
(p.161)

4, 0
16.7500, 5.50000, 0.500000
16.7500, 4.50000, 0.500000
16.7500, 4.50000, 1.00100
16.7500, 5.50000, 1.00100

CE: We have to revert to global coordinates. AGAIN

RR: Back to global coordinates. Z TRANSLATIONS HAS CHANGED
2.00000, 0.000000, -9.00000
0.000000, 0.000000, 90.0000, 0.000000

CM: CG: Test tube at new(0,0,0). Should be placed at .
origin. CM: OK!

CM: 0.000000, 0.000000, 0.000000
CM: 0.000000, 0.000000, 90.0000, 0.000000
CM: 1.00000, 1.00000
CE: 0.000000, 90.0000, 10.0000, 90.0000

CM: We have already put the forward vertical plate that
surrounds

CM: the opening. We now put the remaining three, trying to

CE: eliminate the warnings (thus Zmax=5.001)

PG: REST of the frame that surrounds the opening: LEFT

4, 0
14.7500, 4.50000, 10.00100
15.7500, 4.50000, 10.00100
15.7500, 4.50000, 9.70000
14.7500, 4.50000, 9.70000

PG: REST of the frame that surrounds the opening: RIGHT

4, 0
14.7500, 5.50000, 10.00100
14.7500, 5.50000, 9.70000
15.7500, 5.50000, 9.70000
15.7500, 5.50000, 10.00100

PG: REST of the frame that surrounds the opening: AFT
4, 0

15.7500, 4.50000, 10.00100
15.7500, 5.50000, 10.00100
15.7500, 5.50000, 9.70000
15.7500, 4.50000, 9.70000

CM: ZD: Simulated opening. Permittivity 1.01

CM: 1

CM: 1

CM: 0.0500000, 1.01000, 0.000000, 1.00000, 0.000000

CM:

CM: PG: This is an opening in the overhead

CM: 4, 0

CM: 15.7500, 4.50000, 5.00000

CM: 14.7500, 4.50000, 5.00000

CM: 14.7500, 5.50000, 5.00000

CM: 15.7500, 5.50000, 5.00000

CM:

CM: ZD: Back again to P.E.C.

CE: 0

CM: We now try to construct the HANDRAILS as cylinders with

CM: small radius and adequate angle. USE THE Z AXIS

CE: POSITION- ROTATE

RR: Use the first construction for the SECOND LADDERWAY

0.000000, 0.000000, 5.00000

0.000000, 0.000000, 90.0000, 0.000000

CG: LEFT HANDRAIL

17.0000, 4.50000, 0.250000

335.000, 0.000000, 0.000000, -999.000

0.100000, 0.100000

0.000000, 45.0000, 5.00000, 45.0000

CG: RIGHT HANDRAIL

17.0000, 5.50000, 0.250000

335.000, 0.000000, 0.000000, -999.000

0.100000, 0.100000

0.000000, 45.0000, 5.00000, 45.0000

CE: We have to revert to global coordinates. AGAIN

RR: Back to global coordinates. Z GOES 5m DOWN:

0.00000, 0.000000, -5.00000

0.000000, 0.000000, 90.0000, 0.000000

CM: CG: Test tube at (0,0,0). Should be placed at origin.

CM: OK!

CM: 0.000000, 0.000000, 0.000000

CM: 0.000000, 0.000000, 90.0000, 0.000000

CM: 1.00000, 1.00000

CE: 0.000000, 90.0000, 10.0000, 90.0000

LY:

T

CM: LP: See data in the out file the same with PL command

CE: T

PL:

T

XQ:

EN: End

The following, are the input sub-files for the truncation of the CE: room. Each room, as well as the free space volume, is truncated into several CELLS, in order to avoid observation points inside the numerous obstacles. For the shake of simplicity, (we would need at least 700 pages for all the files), we will only present the different commands for antenna and observation points placements.

ROOM DECOMPOSITION INTO CELLS (FIRST LOCATION)

CELL 1

SG: Put the source at (14,5,1) position

14.0000, 5.00000, 1.00000

0.000000, 0.000000, 90.0000, 0.000000

-1, 0.500000, 0.000000

1.00000, 0.000000

VN: VOLUMETRIC PLOT 1 at Z=1.5 m.

0.000000, 0.000000, 0.000000

0.000000, 0.000000, 90.0000, 0.000000

T

0.100000, 1.20000, 1.50000

0.250000, 0.250000, 0.000000
1, 71, 3

CELL 2

SG: Put the source at (14,5,1) position
14.0000, 5.00000, 1.00000
0.000000, 0.000000, 90.0000, 0.000000
-1, 0.500000, 0.000000
1.00000, 0.000000

VN: VOLUMETRIC PLOT 1 at Z=1.5 m.
0.000000, 0.000000, 0.000000
0.000000, 0.000000, 90.0000, 0.000000
T
0.100000, 2.20000, 1.50000
0.250000, 0.250000, 0.000000
1, 19, 7

CELL 3

SG: Put the source at (14,5,1) position
14.0000, 5.00000, 1.00000
0.000000, 0.000000, 90.0000, 0.000000
-1, 0.500000, 0.000000
1.00000, 0.000000

VN: VOLUMETRIC PLOT 1 at Z=1.5 m.
0.000000, 0.000000, 0.000000
0.000000, 0.000000, 90.0000, 0.000000
T
7.10000, 2.20000, 1.50000
0.250000, 0.250000, 0.000000
1, 7, 7

CELL 4

SG: Put the source at (14,5,1) position
14.0000, 5.00000, 1.00000
0.000000, 0.000000, 90.0000, 0.000000
-1, 0.500000, 0.000000
1.00000, 0.000000

VN: VOLUMETRIC PLOT 1 at Z=1.5 m.
0.000000, 0.000000, 0.000000
0.000000, 0.000000, 90.0000, 0.000000
T
11.1000, 2.20000, 1.50000
0.250000, 0.250000, 0.000000

1, 7, 7

CELL 5

SG: Put the source at (14,5,1) position

14.0000, 5.00000, 1.00000
0.000000, 0.000000, 90.0000, 0.000000
-1, 0.500000, 0.000000
1.00000, 0.000000

VN: VOLUMETRIC PLOT 1 at Z=1.5 m.

0.000000, 0.000000, 0.000000
0.000000, 0.000000, 90.0000, 0.000000
T
15.1000, 2.20000, 1.50000
0.250000, 0.250000, 0.000000
1, 11, 7

CELL 6

SG: Put the source at (14,5,1) position

14.0000, 5.00000, 1.00000
0.000000, 0.000000, 90.0000, 0.000000
-1, 0.500000, 0.000000
1.00000, 0.000000

VN: VOLUMETRIC PLOT 1 at Z=1.5 m.

0.000000, 0.000000, 0.000000
0.000000, 0.000000, 90.0000, 0.000000
T
0.100000, 4.20000, 1.50000
0.250000, 0.250000, 0.000000
1, 71, 7

CELL 7

SG: Put the source at (14,5,1) position

14.0000, 5.00000, 1.00000
0.000000, 0.000000, 90.0000, 0.000000
-1, 0.500000, 0.000000
1.00000, 0.000000

VN: VOLUMETRIC PLOT 1 at Z=1.5 m.

0.000000, 0.000000, 0.000000
0.000000, 0.000000, 90.0000, 0.000000
T
0.100000, 6.20000, 1.50000
0.250000, 0.250000, 0.000000
1, 19, 7

CELL 8

SG: Put the source at (14,5,1) position

14.0000, 5.00000, 1.00000
0.000000, 0.000000, 90.0000, 0.000000
-1, 0.500000, 0.000000
1.00000, 0.000000

VN: VOLUMETRIC PLOT 1 at Z=1.5 m.

0.000000, 0.000000, 0.000000
0.000000, 0.000000, 90.0000, 0.000000
T
7.10000, 6.20000, 1.50000
0.250000, 0.250000, 0.000000
1, 7, 7

CELL 9

SG: Put the source at (14,5,1) position

14.0000, 5.00000, 1.00000
0.000000, 0.000000, 90.0000, 0.000000
-1, 0.500000, 0.000000
1.00000, 0.000000

VN: VOLUMETRIC PLOT 1 at Z=1.5 m.

0.000000, 0.000000, 0.000000
0.000000, 0.000000, 90.0000, 0.000000
T
11.1000, 6.20000, 1.50000
0.250000, 0.250000, 0.000000
1, 7, 7

CELL 10

SG: Put the source at (14,5,1) position

14.0000, 5.00000, 1.00000
0.000000, 0.000000, 90.0000, 0.000000
-1, 0.500000, 0.000000
1.00000, 0.000000

VN: VOLUMETRIC PLOT 1 at Z=1.5 m.

0.000000, 0.000000, 0.000000
0.000000, 0.000000, 90.0000, 0.000000
T
15.1000, 6.20000, 1.50000
0.250000, 0.250000, 0.000000
1, 11, 7

CELL 11

SG: Put the source at (14,5,1) position
14.0000, 5.0000, 1.0000
0.000000, 0.000000, 90.0000, 0.000000
-1, 0.500000, 0.000000
1.00000, 0.000000

VN: VOLUMETRIC PLOT 1 at Z=1.5 m.
0.000000, 0.000000, 0.000000
0.000000, 0.000000, 90.0000, 0.000000
T
0.100000, 8.20000, 1.50000
0.250000, 0.250000, 0.000000
1, 71, 3

**FREE SPACE
CELL 1**

SG: Put the source at (14,5,1) position
14.0000, 5.0000, 1.0000
0.000000, 0.000000, 90.0000, 0.000000
-1, 0.500000, 0.000000
1.00000, 0.000000

VN: VOLUMETRIC PLOT 1 at Z=1.5 m.
0.000000, 0.000000, 0.000000
0.000000, 0.000000, 90.0000, 0.000000
T
0.100000, 1.20000, 1.50000
0.250000, 0.250000, 0.000000
1, 71, 3

CELL 2

SG: Put the source at (14,5,1) position
14.0000, 5.0000, 1.0000
0.000000, 0.000000, 90.0000, 0.000000
-1, 0.500000, 0.000000
1.00000, 0.000000

VN: VOLUMETRIC PLOT 1 at Z=1.5 m.
0.000000, 0.000000, 0.000000
0.000000, 0.000000, 90.0000, 0.000000
T
0.100000, 2.20000, 1.50000

0.250000, 0.250000, 0.000000
1, 19, 7

LY:

CELL 3

SG: Put the source at (14,5,1) position
14.0000, 5.00000, 1.00000
0.000000, 0.000000, 90.0000, 0.000000
-1, 0.500000, 0.000000
1.00000, 0.000000

VN: VOLUMETRIC PLOT 1 at Z=1.5 m.
0.000000, 0.000000, 0.000000
0.000000, 0.000000, 90.0000, 0.000000
T
7.10000, 2.20000, 1.50000
0.250000, 0.250000, 0.000000
1, 7, 7

CELL 4

SG: Put the source at (14,5,1) position
14.0000, 5.00000, 1.00000
0.000000, 0.000000, 90.0000, 0.000000
-1, 0.500000, 0.000000
1.00000, 0.000000

VN: VOLUMETRIC PLOT 1 at Z=1.5 m.
0.000000, 0.000000, 0.000000
0.000000, 0.000000, 90.0000, 0.000000
T
11.1000, 2.20000, 1.50000
0.250000, 0.250000, 0.000000
1, 7, 7

CELL 5

SG: Put the source at (14,5,1) position
14.0000, 5.00000, 1.00000
0.000000, 0.000000, 90.0000, 0.000000

-1, 0.500000, 0.000000
1.00000, 0.000000

VN: VOLUMETRIC PLOT 1 at Z=1.5 m.
0.000000, 0.000000, 0.000000
0.000000, 0.000000, 90.0000, 0.000000
T
15.1000, 2.20000, 1.50000
0.250000, 0.250000, 0.000000
1, 11, 7

CELL 6

SG: Put the source at (14,5,1) position
14.0000, 5.00000, 1.00000
0.000000, 0.000000, 90.0000, 0.000000
-1, 0.500000, 0.000000
1.00000, 0.000000

VN: VOLUMETRIC PLOT 1 at Z=1.5 m.
0.000000, 0.000000, 0.000000
0.000000, 0.000000, 90.0000, 0.000000
T
0.100000, 4.20000, 1.50000
0.250000, 0.250000, 0.000000
1, 71, 7

EN

CELL 7

SG: Put the source at (14,5,1) position
14.0000, 5.00000, 1.00000
0.000000, 0.000000, 90.0000, 0.000000
-1, 0.500000, 0.000000
1.00000, 0.000000

VN: VOLUMETRIC PLOT 1 at Z=1.5 m.
0.000000, 0.000000, 0.000000
0.000000, 0.000000, 90.0000, 0.000000
T
0.100000, 6.20000, 1.50000
0.250000, 0.250000, 0.000000

1, 19, 7

CELL 8

SG: Put the source at (14,5,1) position
14.0000, 5.00000, 1.00000
0.000000, 0.000000, 90.0000, 0.000000
-1, 0.500000, 0.000000
1.00000, 0.000000

VN: VOLUMETRIC PLOT 1 at Z=1.5 m.
0.000000, 0.000000, 0.000000
0.000000, 0.000000, 90.0000, 0.000000
T
7.10000, 6.20000, 1.50000
0.250000, 0.250000, 0.000000
1, 7, 7

CELL 9

SG: Put the source at (14,5,1) position
14.0000, 5.00000, 1.00000
0.000000, 0.000000, 90.0000, 0.000000
-1, 0.500000, 0.000000
1.00000, 0.000000

VN: VOLUMETRIC PLOT 1 at Z=1.5 m.
0.000000, 0.000000, 0.000000
0.000000, 0.000000, 90.0000, 0.000000
T
11.1000, 6.20000, 1.50000
0.250000, 0.250000, 0.000000
1, 7, 7

CELL 10

SG: Put the source at (14,5,1) position
14.0000, 5.00000, 1.00000
0.000000, 0.000000, 90.0000, 0.000000
-1, 0.500000, 0.000000
1.00000, 0.000000

VN: VOLUMETRIC PLOT 1 at Z=1.5 m.

0.000000, 0.000000, 0.000000
0.000000, 0.000000, 90.0000, 0.000000
T
15.1000, 6.20000, 1.50000
0.250000, 0.250000, 0.000000
1, 11, 7

CELL 11

SG: Put the source at (14,5,1) position
14.0000, 5.00000, 1.00000
0.000000, 0.000000, 90.0000, 0.000000
-1, 0.500000, 0.000000
1.00000, 0.000000

VN: VOLUMETRIC PLOT 1 at Z=1.5 m.
0.000000, 0.000000, 0.000000
0.000000, 0.000000, 90.0000, 0.000000
T
0.100000, 8.20000, 1.50000
0.250000, 0.250000, 0.000000
1, 71, 3

ROOM DECOMPOSITION INTO CELLS (SECOND LOCATION)

CELL 1

SG: Put the source at (2,2,2) position
2.00000, 2.00000, 2.00000
0.000000, 0.000000, 90.0000, 0.000000
-1, 0.500000, 0.000000
1.00000, 0.000000

VN: VOLUMETRIC PLOT 1 at Z=2 m.
0.000000, 0.000000, 0.000000
0.000000, 0.000000, 90.0000, 0.000000
T
0.100000, 1.20000, 2.00000
0.250000, 0.250000, 0.000000
1, 71, 3

CELL 2

SG: Put the source at (2,2,2) position
2.00000, 2.00000, 2.00000
0.000000, 0.000000, 90.0000, 0.000000

-1, 0.500000, 0.000000
1.00000, 0.000000

VN: VOLUMETRIC PLOT 1 at Z=2 m.
0.000000, 0.000000, 0.000000
0.000000, 0.000000, 90.0000, 0.000000
T
0.100000, 2.20000, 2.00000
0.250000, 0.250000, 0.000000
1, 19, 7

CELL 3

SG: Put the source at (2,2,2) position
2.00000, 2.00000, 2.00000
0.000000, 0.000000, 90.0000, 0.000000
-1, 0.500000, 0.000000
1.00000, 0.000000

VN: VOLUMETRIC PLOT 1 at Z=2m
0.000000, 0.000000, 0.000000
0.000000, 0.000000, 90.0000, 0.000000
T
7.10000, 2.20000, 2.00000
0.250000, 0.250000, 0.000000
1, 7, 7

CELL 4

SG: Put the source at (2,2,2) position
2.00000, 2.00000, 2.00000
0.000000, 0.000000, 90.0000, 0.000000
-1, 0.500000, 0.000000
1.00000, 0.000000

VN: VOLUMETRIC PLOT 1 at Z=2m.
0.000000, 0.000000, 0.000000
0.000000, 0.000000, 90.0000, 0.000000
T
11.1000, 2.20000, 2.00000
0.250000, 0.250000, 0.000000
1, 7, 7

CELL 5

SG: Put the source at (2,2,2) position
2.00000, 2.00000, 2.00000

0.000000, 0.000000, 90.0000, 0.000000
-1, 0.500000, 0.000000
1.00000, 0.000000

VN: VOLUMETRIC PLOT 1 at Z=2 m.

0.000000, 0.000000, 0.000000
0.000000, 0.000000, 90.0000, 0.000000
T
15.1000, 2.20000, 2.00000
0.250000, 0.250000, 0.000000
1, 11, 7

CELL 6

SG: Put the source at (2,2,2) position
2.00000, 2.00000, 2.00000
0.000000, 0.000000, 90.0000, 0.000000
-1, 0.500000, 0.000000
1.00000, 0.000000

VN: VOLUMETRIC PLOT 1 at Z=2m.

0.000000, 0.000000, 0.000000
0.000000, 0.000000, 90.0000, 0.000000
T
0.100000, 4.20000, 2.00000
0.250000, 0.250000, 0.000000
1, 71, 7

CELL 7

SG: Put the source at (2,2,2) position
2.00000, 2.00000, 2.00000
0.000000, 0.000000, 90.0000, 0.000000
-1, 0.500000, 0.000000
1.00000, 0.000000

VN: VOLUMETRIC PLOT 1 at Z=2m.

0.000000, 0.000000, 0.000000
0.000000, 0.000000, 90.0000, 0.000000
T
0.100000, 6.20000, 2.00000
0.250000, 0.250000, 0.000000
1, 19, 7

CELL 8

SG: Put the source at (2,2,2) position
2.00000, 2.00000, 2.00000
0.000000, 0.000000, 90.0000, 0.000000

-1, 0.500000, 0.000000
1.00000, 0.000000

VN: VOLUMETRIC PLOT 1 at Z=2 m.
0.000000, 0.000000, 0.000000
0.000000, 0.000000, 90.0000, 0.000000
T
7.10000, 6.20000, 2.00000
0.250000, 0.250000, 0.000000
1, 7, 7

CELL 9

SG: Put the source at (2,2,2) position
2.00000, 2.00000, 2.00000
0.000000, 0.000000, 90.0000, 0.000000
-1, 0.500000, 0.000000
1.00000, 0.000000

VN: VOLUMETRIC PLOT 1 at Z=2m.
0.000000, 0.000000, 0.000000
0.000000, 0.000000, 90.0000, 0.000000
T
11.1000, 6.20000, 2.00000
0.250000, 0.250000, 0.000000
1, 7, 7

CELL 10

SG: Put the source at (2,2,2) position
2.00000, 2.00000, 2.00000
0.000000, 0.000000, 90.0000, 0.000000
-1, 0.500000, 0.000000
1.00000, 0.000000

VN: VOLUMETRIC PLOT 1 at Z=2 m.
0.000000, 0.000000, 0.000000
0.000000, 0.000000, 90.0000, 0.000000
T
15.1000, 6.20000, 2.00000
0.250000, 0.250000, 0.000000
1, 11, 7

CELL 11

SG: Put the source at (2,2,2) position
2.00000, 2.00000, 2.00000
0.000000, 0.000000, 90.0000, 0.000000
-1, 0.500000, 0.000000

1.00000, 0.000000

VN: VOLUMETRIC PLOT 1 at Z=2m.

0.000000, 0.000000, 0.000000

0.000000, 0.000000, 90.0000, 0.000000

T

0.100000, 8.20000, 2.00000

0.250000, 0.250000, 0.000000

1, 71, 3

FREE SPACE

CELL 1

SG: Put the source at (2,2,2) position

2.00000, 2.00000, 2.00000

0.000000, 0.000000, 90.0000, 0.000000

-1, 0.500000, 0.000000

1.00000, 0.000000

VN: VOLUMETRIC PLOT 1 at Z=2m.

0.000000, 0.000000, 0.000000

0.000000, 0.000000, 90.0000, 0.000000

T

0.100000, 1.20000, 2.00000

0.250000, 0.250000, 0.000000

1, 71, 3

CELL 2

SG: Put the source at (2,2,2) position

2.00000, 2.00000, 2.00000

0.000000, 0.000000, 90.0000, 0.000000

-1, 0.500000, 0.000000

1.00000, 0.000000

VN: VOLUMETRIC PLOT 1 at Z=2m.

0.000000, 0.000000, 0.000000

0.000000, 0.000000, 90.0000, 0.000000

T

0.100000, 2.20000, 2.00000

0.250000, 0.250000, 0.000000

1, 19, 7

CELL 3

SG: Put the source at (2,2,2) position
2.00000, 2.00000, 2.00000
0.000000, 0.000000, 90.0000, 0.000000
-1, 0.500000, 0.000000
1.00000, 0.000000

VN: VOLUMETRIC PLOT 1 at Z=2m.
0.000000, 0.000000, 0.000000
0.000000, 0.000000, 90.0000, 0.000000
T
7.10000, 2.20000, 2.00000
0.250000, 0.250000, 0.000000
1, 7, 7

CELL 4

SG: Put the source at (2,2,2) position
2.00000, 2.00000, 2.00000
0.000000, 0.000000, 90.0000, 0.000000
-1, 0.500000, 0.000000
1.00000, 0.000000

VN: VOLUMETRIC PLOT 1 at Z=2 m.
0.000000, 0.000000, 0.000000
0.000000, 0.000000, 90.0000, 0.000000
T
11.1000, 2.20000, 2.00000
0.250000, 0.250000, 0.000000
1, 7, 7

CELL 5

SG: Put the source at (2,2,2) position
2.00000, 2.00000, 2.00000
0.000000, 0.000000, 90.0000, 0.000000
-1, 0.500000, 0.000000
1.00000, 0.000000

VN: VOLUMETRIC PLOT 1 at Z=2m.
0.000000, 0.000000, 0.000000
0.000000, 0.000000, 90.0000, 0.000000
T

15.1000, 2.20000, 2.00000
0.250000, 0.250000, 0.000000
1, 11, 7

CELL 6

SG: Put the source at (2,2,2) position
2.00000, 2.00000, 2.00000
0.000000, 0.000000, 90.0000, 0.000000
-1, 0.500000, 0.000000
1.00000, 0.000000

VN: VOLUMETRIC PLOT 1 at Z=2m.
0.000000, 0.000000, 0.000000
0.000000, 0.000000, 90.0000, 0.000000
T
0.100000, 4.20000, 2.00000
0.250000, 0.250000, 0.000000
1, 71, 7

CELL 7

SG: Put the source at (2,2,2) position
2.00000, 2.00000, 2.00000
0.000000, 0.000000, 90.0000, 0.000000
-1, 0.500000, 0.000000
1.00000, 0.000000

VN: VOLUMETRIC PLOT 1 at Z=2m.
0.000000, 0.000000, 0.000000
0.000000, 0.000000, 90.0000, 0.000000
T
0.100000, 6.20000, 2.00000
0.250000, 0.250000, 0.000000
1, 19, 7

CELL 8

SG: Put the source at (2,2,2) position
2.00000, 2.00000, 2.00000
0.000000, 0.000000, 90.0000, 0.000000
-1, 0.500000, 0.000000

1.00000, 0.000000

VN: VOLUMETRIC PLOT 1 at Z=2m.

0.000000, 0.000000, 0.000000

0.000000, 0.000000, 90.0000, 0.000000

T

7.10000, 6.20000, 2.00000

0.250000, 0.250000, 0.000000

1, 7, 7

CELL 9

SG: Put the source at (2,2,2) position

2.00000, 2.00000, 2.00000

0.000000, 0.000000, 90.0000, 0.000000

-1, 0.500000, 0.000000

1.00000, 0.000000

VN: VOLUMETRIC PLOT 1 at Z=2m.

0.000000, 0.000000, 0.000000

0.000000, 0.000000, 90.0000, 0.000000

T

11.1000, 6.20000, 2.00000

0.250000, 0.250000, 0.000000

1, 7, 7

CELL 10

SG: Put the source at (2,2,2) position

2.00000, 2.00000, 2.00000

0.000000, 0.000000, 90.0000, 0.000000

-1, 0.500000, 0.000000

1.00000, 0.000000

VN: VOLUMETRIC PLOT 1 at Z=2m.

0.000000, 0.000000, 0.000000

0.000000, 0.000000, 90.0000, 0.000000

T

15.1000, 6.20000, 2.00000

0.250000, 0.250000, 0.000000

1, 11, 7

CELL 11

SG: Put the source at (2,2,2) position
2.00000, 2.00000, 2.00000
0.000000, 0.000000, 90.0000, 0.000000
-1, 0.500000, 0.000000
1.00000, 0.000000

VN: VOLUMETRIC PLOT 1 at Z=2 m.
0.000000, 0.000000, 0.000000
0.000000, 0.000000, 90.0000, 0.000000
T
0.100000, 8.20000, 2.00000
0.250000, 0.250000, 0.000000
1, 71, 3

ROOM DECOMPOSITION INTO CELLS (THIRD LOCATION)

CELL 1

SG: Put the source at (2,2,2.2) position
2.00000, 2.00000, 2.20000
0.000000, 0.000000, 90.0000, 0.000000
-1, 0.500000, 0.000000
1.00000, 0.000000

VN: VOLUMETRIC PLOT 1 at Z=2.2 m.
0.000000, 0.000000, 0.000000
0.000000, 0.000000, 90.0000, 0.000000
T
0.100000, 1.20000, 2.20000
0.250000, 0.250000, 0.000000
1, 71, 3

CELL 2

SG: Put the source at (2,2,2.2) position
2.00000, 2.00000, 2.20000
0.000000, 0.000000, 90.0000, 0.000000
-1, 0.500000, 0.000000
1.00000, 0.000000

VN: VOLUMETRIC PLOT 1 at Z=2.2 m.
0.000000, 0.000000, 0.000000
0.000000, 0.000000, 90.0000, 0.000000
T
0.100000, 2.20000, 2.200000
0.250000, 0.250000, 0.000000
1, 19, 7

CELL 3

SG: Put the source at (2,2,2.2) position
2.00000, 2.00000, 2.20000
0.000000, 0.000000, 90.0000, 0.000000
-1, 0.500000, 0.000000
1.00000, 0.000000

VN: VOLUMETRIC PLOT 1 at Z=2.2m
0.000000, 0.000000, 0.000000
0.000000, 0.000000, 90.0000, 0.000000
T
7.10000, 2.20000, 2.200000
0.250000, 0.250000, 0.000000
1, 7, 7

CELL 4

SG: Put the source at (2,2,2.2) position
2.00000, 2.00000, 2.20000
0.000000, 0.000000, 90.0000, 0.000000
-1, 0.500000, 0.000000
1.00000, 0.000000

VN: VOLUMETRIC PLOT 1 at Z=2.2m.
0.000000, 0.000000, 0.000000
0.000000, 0.000000, 90.0000, 0.000000
T
11.1000, 2.20000, 2.200000
0.250000, 0.250000, 0.000000
1, 7, 7

CELL 5

SG: Put the source at (2,2,2.2) position
2.00000, 2.00000, 2.20000
0.000000, 0.000000, 90.0000, 0.000000
-1, 0.500000, 0.000000
1.00000, 0.000000

VN: VOLUMETRIC PLOT 1 at Z=2.2 m.
0.000000, 0.000000, 0.000000
0.000000, 0.000000, 90.0000, 0.000000
T
15.1000, 2.20000, 2.200000
0.250000, 0.250000, 0.000000
1, 11, 7

CELL 6

SG: Put the source at (2,2,2.2) position
2.00000, 2.00000, 2.20000
0.000000, 0.000000, 90.0000, 0.000000
-1, 0.500000, 0.000000
1.00000, 0.000000

VN: VOLUMETRIC PLOT 1 at Z=2.2m.
0.000000, 0.000000, 0.000000
0.000000, 0.000000, 90.0000, 0.000000
T
0.100000, 4.20000, 2.200000
0.250000, 0.250000, 0.000000
1, 71, 7

CELL 7

SG: Put the source at (2,2,2.2) position
2.00000, 2.00000, 2.20000
0.000000, 0.000000, 90.0000, 0.000000
-1, 0.500000, 0.000000
1.00000, 0.000000

VN: VOLUMETRIC PLOT 1 at Z=2.2m.
0.000000, 0.000000, 0.000000
0.000000, 0.000000, 90.0000, 0.000000
T
0.100000, 6.20000, 2.200000
0.250000, 0.250000, 0.000000
1, 19, 7

CELL 8

SG: Put the source at (2,2,2.2) position
2.00000, 2.00000, 2.20000
0.000000, 0.000000, 90.0000, 0.000000
-1, 0.500000, 0.000000

1.00000, 0.000000

VN: VOLUMETRIC PLOT 1 at Z=2.2 m.

0.000000, 0.000000, 0.000000

0.000000, 0.000000, 90.0000, 0.000000

T

7.10000, 6.20000, 2.200000

0.250000, 0.250000, 0.000000

1, 7, 7

CELL 9

SG: Put the source at (2,2,2.2) position

2.00000, 2.00000, 2.20000

0.000000, 0.000000, 90.0000, 0.000000

-1, 0.500000, 0.000000

1.00000, 0.000000

VN: VOLUMETRIC PLOT 1 at Z=2.2m.

0.000000, 0.000000, 0.000000

0.000000, 0.000000, 90.0000, 0.000000

T

11.1000, 6.20000, 2.20000

0.250000, 0.250000, 0.000000

1, 7, 7

CELL 10

SG: Put the source at (2,2,2.2) position

2.00000, 2.00000, 2.20000

0.000000, 0.000000, 90.0000, 0.000000

-1, 0.500000, 0.000000

1.00000, 0.000000

VN: VOLUMETRIC PLOT 1 at Z=2.2 m.

0.000000, 0.000000, 0.000000

0.000000, 0.000000, 90.0000, 0.000000

T

15.1000, 6.20000, 2.200000

0.250000, 0.250000, 0.000000

1, 11, 7

CELL 11

SG: Put the source at (2,2,2.2) position

2.00000, 2.00000, 2.20000

0.000000, 0.000000, 90.0000, 0.000000

-1, 0.500000, 0.000000

1.00000, 0.000000

VN: VOLUMETRIC PLOT 1 at Z=2.2m.
0.000000, 0.000000, 0.000000
0.000000, 0.000000, 90.0000, 0.000000
T
0.100000, 8.20000, 2.200000
0.250000, 0.250000, 0.000000
1, 71, 3

FREE SPACE
CELL 1

SG: Put the source at (2,2,2.2) position
2.00000, 2.00000, 2.20000
0.000000, 0.000000, 90.0000, 0.000000
-1, 0.500000, 0.000000
1.00000, 0.000000

VN: VOLUMETRIC PLOT 1 at Z=2.2m.
0.000000, 0.000000, 0.000000
0.000000, 0.000000, 90.0000, 0.000000
T
0.100000, 1.20000, 2.200000
0.250000, 0.250000, 0.000000
1, 71, 3

CELL 2

SG: Put the source at (2,2,2.2) position
2.00000, 2.00000, 2.20000
0.000000, 0.000000, 90.0000, 0.000000
-1, 0.500000, 0.000000
1.00000, 0.000000

VN: VOLUMETRIC PLOT 1 at Z=2.2m.
0.000000, 0.000000, 0.000000
0.000000, 0.000000, 90.0000, 0.000000
T
0.100000, 2.20000, 2.200000
0.250000, 0.250000, 0.000000
1, 19, 7

CELL 3

SG: Put the source at (2,2,2.2) position
2.00000, 2.00000, 2.20000
0.000000, 0.000000, 90.0000, 0.000000
-1, 0.500000, 0.000000
1.00000, 0.000000

VN: VOLUMETRIC PLOT 1 at Z=2.2m.
0.000000, 0.000000, 0.000000
0.000000, 0.000000, 90.0000, 0.000000
T
7.10000, 2.20000, 2.200000
0.250000, 0.250000, 0.000000
1, 7, 7

CELL 4

SG: Put the source at (2,2,2.2) position
2.00000, 2.00000, 2.20000
0.000000, 0.000000, 90.0000, 0.000000
-1, 0.500000, 0.000000
1.00000, 0.000000

VN: VOLUMETRIC PLOT 1 at Z=2.2 m.
0.000000, 0.000000, 0.000000
0.000000, 0.000000, 90.0000, 0.000000
T
11.1000, 2.20000, 2.200000
0.250000, 0.250000, 0.000000
1, 7, 7

CELL 5

SG: Put the source at (2,2,2.2) position
2.00000, 2.00000, 2.20000
0.000000, 0.000000, 90.0000, 0.000000
-1, 0.500000, 0.000000
1.00000, 0.000000

VN: VOLUMETRIC PLOT 1 at Z=2.2m.
0.000000, 0.000000, 0.000000
0.000000, 0.000000, 90.0000, 0.000000
T
15.1000, 2.20000, 2.200000

0.250000, 0.250000, 0.000000
1, 11, 7

CELL 6

SG: Put the source at (2,2,2.2) position
2.00000, 2.00000, 2.20000
0.000000, 0.000000, 90.0000, 0.000000
-1, 0.500000, 0.000000
1.00000, 0.000000

VN: VOLUMETRIC PLOT 1 at Z=2.2m.
0.000000, 0.000000, 0.000000
0.000000, 0.000000, 90.0000, 0.000000
T
0.100000, 4.20000, 2.200000
0.250000, 0.250000, 0.000000
1, 71, 7

CELL 7

SG: Put the source at (2,2,2.2) position
2.00000, 2.00000, 2.20000
0.000000, 0.000000, 90.0000, 0.000000
-1, 0.500000, 0.000000
1.00000, 0.000000

VN: VOLUMETRIC PLOT 1 at Z=2.2m.
0.000000, 0.000000, 0.000000
0.000000, 0.000000, 90.0000, 0.000000
T
0.100000, 6.20000, 2.00000
0.250000, 0.250000, 0.000000
1, 19, 7

CELL 8

SG: Put the source at (2,2,2.2) position
2.00000, 2.00000, 2.20000
0.000000, 0.000000, 90.0000, 0.000000
-1, 0.500000, 0.000000
1.00000, 0.000000

VN: VOLUMETRIC PLOT 1 at Z=2.2m.
0.000000, 0.000000, 0.000000
0.000000, 0.000000, 90.0000, 0.000000
T
7.10000, 6.20000, 2.200000
0.250000, 0.250000, 0.000000
1, 7, 7

CELL 9

SG: Put the source at (2,2,2.2) position
2.00000, 2.00000, 2.20000
0.000000, 0.000000, 90.0000, 0.000000
-1, 0.500000, 0.000000
1.00000, 0.000000

VN: VOLUMETRIC PLOT 1 at Z=2.2m.
0.000000, 0.000000, 0.000000
0.000000, 0.000000, 90.0000, 0.000000
T
11.1000, 6.20000, 2.200000
0.250000, 0.250000, 0.000000
1, 7, 7

CELL 10

SG: Put the source at (2,2,2.2) position
2.00000, 2.00000, 2.20000
0.000000, 0.000000, 90.0000, 0.000000
-1, 0.500000, 0.000000
1.00000, 0.000000

VN: VOLUMETRIC PLOT 1 at Z=2.2m.
0.000000, 0.000000, 0.000000
0.000000, 0.000000, 90.0000, 0.000000
T
15.1000, 6.20000, 2.200000
0.250000, 0.250000, 0.000000
1, 11, 7

CELL 11

SG: Put the source at (2,2,2.2) position
2.00000, 2.00000, 2.20000
0.000000, 0.000000, 90.0000, 0.000000
-1, 0.500000, 0.000000
1.00000, 0.000000

VN: VOLUMETRIC PLOT 1 at Z=2.2 m.
0.000000, 0.000000, 0.000000
0.000000, 0.000000, 90.0000, 0.000000
T
0.100000, 8.20000, 2.200000
0.250000, 0.250000, 0.000000
1, 71, 3

:

EN: END

ROOM DECOMPOSITION INTO CELLS (FORTH LOCATION)

CELL 1

SG: Put the source at (4,3,1) position
4.00000, 3.00000, 1.00000
0.000000, 0.000000, 90.0000, 0.000000
-1, 0.500000, 0.000000
1.00000, 0.000000

VN: VOLUMETRIC PLOT 1 at Z=1 m.
0.000000, 0.000000, 0.000000
0.000000, 0.000000, 90.0000, 0.000000
T
0.100000, 1.20000, 1.00000
0.250000, 0.250000, 0.000000
1, 71, 3

CELL 2

SG: Put the source at (4,3,1) position
4.00000, 3.00000, 1.00000
0.000000, 0.000000, 90.0000, 0.000000
-1, 0.500000, 0.000000
1.00000, 0.000000

VN: VOLUMETRIC PLOT 1 at Z=1 m.

0.000000, 0.000000, 0.000000
0.000000, 0.000000, 90.0000, 0.000000
T
0.100000, 2.20000, 1.00000
0.250000, 0.250000, 0.000000
1, 19, 7

CELL 3

SG: Put the source at (4,3,1) position
4.00000, 3.00000, 1.00000
0.000000, 0.000000, 90.0000, 0.000000
-1, 0.500000, 0.000000
1.00000, 0.000000
VN: VOLUMETRIC PLOT 1 at Z=1m
0.000000, 0.000000, 0.000000
0.000000, 0.000000, 90.0000, 0.000000
T
7.10000, 2.20000, 1.00000
0.250000, 0.250000, 0.000000
1, 7, 7

CELL 4

SG: Put the source at (4,3,1) position
4.00000, 3.00000, 1.00000
0.000000, 0.000000, 90.0000, 0.000000
-1, 0.500000, 0.000000
1.00000, 0.000000

VN: VOLUMETRIC PLOT 1 at Z=1m.
0.000000, 0.000000, 0.000000
0.000000, 0.000000, 90.0000, 0.000000
T
11.1000, 2.20000, 1.00000
0.250000, 0.250000, 0.000000
1, 7, 7

CELL 5

SG: Put the source at (4,3,1) position
4.00000, 3.00000, 1.00000
0.000000, 0.000000, 90.0000, 0.000000
-1, 0.500000, 0.000000
1.00000, 0.000000

VN: VOLUMETRIC PLOT 1 at Z=1 m.
0.000000, 0.000000, 0.000000
0.000000, 0.000000, 90.0000, 0.000000

T
15.1000, 2.20000, 1.00000
0.250000, 0.250000, 0.000000
1, 11, 7

CELL 6

SG: Put the source at (4,3,1) position
4.00000, 3.00000, 1.00000
0.000000, 0.000000, 90.0000, 0.000000
-1, 0.500000, 0.000000
1.00000, 0.000000

VN: VOLUMETRIC PLOT 1 at Z=1m.
0.000000, 0.000000, 0.000000
0.000000, 0.000000, 90.0000, 0.000000
T
0.100000, 4.20000, 1.00000
0.250000, 0.250000, 0.000000
1, 71, 7

CELL 7

SG: Put the source at (4,3,1) position
4.00000, 3.00000, 1.00000
0.000000, 0.000000, 90.0000, 0.000000
-1, 0.500000, 0.000000
1.00000, 0.000000

VN: VOLUMETRIC PLOT 1 at Z=1m.
0.000000, 0.000000, 0.000000
0.000000, 0.000000, 90.0000, 0.000000
T
0.100000, 6.20000, 1.00000
0.250000, 0.250000, 0.000000
1, 19, 7

CELL 8

SG: Put the source at (4,3,1) position
4.00000, 3.00000, 1.00000
0.000000, 0.000000, 90.0000, 0.000000
-1, 0.500000, 0.000000
1.00000, 0.000000

VN: VOLUMETRIC PLOT 1 at Z=1m.
0.000000, 0.000000, 0.000000
0.000000, 0.000000, 90.0000, 0.000000
T

7.10000, 6.20000, 1.00000
0.250000, 0.250000, 0.000000
1, 7, 7

CELL 9

SG: Put the source at (4,3,1) position
4.00000, 3.00000, 1.00000
0.000000, 0.000000, 90.0000, 0.000000
-1, 0.500000, 0.000000
1.00000, 0.000000

VN: VOLUMETRIC PLOT 1 at Z=1m.
0.000000, 0.000000, 0.000000
0.000000, 0.000000, 90.0000, 0.000000
T
11.1000, 6.20000, 1.0000
0.250000, 0.250000, 0.000000
1, 7, 7

CELL 10

SG: Put the source at (4,3,1) position
4.00000, 3.00000, 1.00000
0.000000, 0.000000, 90.0000, 0.000000
-1, 0.500000, 0.000000
1.00000, 0.000000

VN: VOLUMETRIC PLOT 1 at Z=1 m.
0.000000, 0.000000, 0.000000
0.000000, 0.000000, 90.0000, 0.000000
T
15.1000, 6.20000, 1.00000
0.250000, 0.250000, 0.000000
1, 11, 7

CELL 11

SG: Put the source at (4,3,1) position
4.00000, 3.00000, 1.00000
0.000000, 0.000000, 90.0000, 0.000000
-1, 0.500000, 0.000000
1.00000, 0.000000

VN: VOLUMETRIC PLOT 1 at Z=1m.
0.000000, 0.000000, 0.000000
0.000000, 0.000000, 90.0000, 0.000000
T
0.100000, 8.20000, 1.00000

0.250000, 0.250000, 0.000000
1, 71, 3

FREE SPACE
CELL 1

SG: Put the source at (4,3,1) position
4.00000, 3.00000, 1.00000
0.000000, 0.000000, 90.0000, 0.000000
-1, 0.500000, 0.000000
1.00000, 0.000000

VN: VOLUMETRIC PLOT 1 at Z=1m.
0.000000, 0.000000, 0.000000
0.000000, 0.000000, 90.0000, 0.000000
T
0.100000, 1.20000, 1.00000
0.250000, 0.250000, 0.000000
1, 71, 3

CELL 2

SG: Put the source at (4,3,1) position
4.00000, 3.00000, 1.00000
0.000000, 0.000000, 90.0000, 0.000000
-1, 0.500000, 0.000000
1.00000, 0.000000

VN: VOLUMETRIC PLOT 1 at Z=1m.
0.000000, 0.000000, 0.000000
0.000000, 0.000000, 90.0000, 0.000000
T
0.100000, 2.20000, 1.00000
0.250000, 0.250000, 0.000000
1, 19, 7

CELL 3

SG: Put the source at (4,3,1) position
4.00000, 3.00000, 1.00000
0.000000, 0.000000, 90.0000, 0.000000
-1, 0.500000, 0.000000

1.00000, 0.000000
VN: VOLUMETRIC PLOT 1 at Z=1m.
0.000000, 0.000000, 0.000000
0.000000, 0.000000, 90.0000, 0.000000
T
7.10000, 2.20000, 1.00000
0.250000, 0.250000, 0.000000
1, 7, 7

CELL 4

SG: Put the source at (4,3,1) position
4.00000, 3.00000, 1.00000
0.000000, 0.000000, 90.0000, 0.000000
-1, 0.500000, 0.000000
1.00000, 0.000000
VN: VOLUMETRIC PLOT 1 at Z=1 m.
0.000000, 0.000000, 0.000000
0.000000, 0.000000, 90.0000, 0.000000
T
11.1000, 2.20000, 1.00000
0.250000, 0.250000, 0.000000
1, 7, 7

CELL 5

SG: Put the source at (4,3,1) position
4.00000, 3.00000, 1.00000
0.000000, 0.000000, 90.0000, 0.000000
-1, 0.500000, 0.000000
1.00000, 0.000000
VN: VOLUMETRIC PLOT 1 at Z=1m.
0.000000, 0.000000, 0.000000
0.000000, 0.000000, 90.0000, 0.000000
T
15.1000, 2.20000, 1.00000
0.250000, 0.250000, 0.000000
1, 11, 7

CELL 6

SG: Put the source at (4,3,1) position
4.00000, 3.00000, 1.00000
0.000000, 0.000000, 90.0000, 0.000000
-1, 0.500000, 0.000000

1.00000, 0.000000
VN: VOLUMETRIC PLOT 1 at Z=1m.
0.000000, 0.000000, 0.000000
0.000000, 0.000000, 90.0000, 0.000000
T
0.100000, 4.20000, 1.00000
0.250000, 0.250000, 0.000000
1, 71, 7

CELL 7

SG: Put the source at (4,3,1) position
4.00000, 3.00000, 1.00000
0.000000, 0.000000, 90.0000, 0.000000
-1, 0.500000, 0.000000
1.00000, 0.000000
VN: VOLUMETRIC PLOT 1 at Z=1m.
0.000000, 0.000000, 0.000000
0.000000, 0.000000, 90.0000, 0.000000
T
0.100000, 6.20000, 1.00000
0.250000, 0.250000, 0.000000
1, 19, 7

CELL 8

SG: Put the source at (4,3,1) position
4.00000, 3.00000, 1.00000
0.000000, 0.000000, 90.0000, 0.000000
-1, 0.500000, 0.000000
1.00000, 0.000000
VN: VOLUMETRIC PLOT 1 at Z=1m.
0.000000, 0.000000, 0.000000
0.000000, 0.000000, 90.0000, 0.000000
T
7.10000, 6.20000, 1.00000
0.250000, 0.250000, 0.000000
1, 7, 7

CELL 9

SG: Put the source at (4,3,1) position
4.00000, 3.00000, 1.00000

0.000000, 0.000000, 90.0000, 0.000000
-1, 0.500000, 0.000000
1.00000, 0.000000
VN: VOLUMETRIC PLOT 1 at Z=1m.
0.000000, 0.000000, 0.000000
0.000000, 0.000000, 90.0000, 0.000000
T
11.1000, 6.20000, 1.00000
0.250000, 0.250000, 0.000000
1, 7, 7

CELL 10

SG: Put the source at (4,3,1) position
4.00000, 3.00000, 1.00000
0.000000, 0.000000, 90.0000, 0.000000
-1, 0.500000, 0.000000
1.00000, 0.000000
VN: VOLUMETRIC PLOT 1 at Z=1m.
0.000000, 0.000000, 0.000000
0.000000, 0.000000, 90.0000, 0.000000
T
15.1000, 6.20000, 1.00000
0.250000, 0.250000, 0.000000
1, 11, 7

CELL 11

SG: Put the source at (4,3,1) position
4.00000, 3.00000, 1.00000
0.000000, 0.000000, 90.0000, 0.000000
-1, 0.500000, 0.000000
1.00000, 0.000000
VN: VOLUMETRIC PLOT 1 at Z=1 m.
0.000000, 0.000000, 0.000000
0.000000, 0.000000, 90.0000, 0.000000
T
0.100000, 8.20000, 1.00000
0.250000, 0.250000, 0.000000
1, 71, 3

EN: END OF FORTH LOCATION
End of all NEC-BSC files

APPENDIX C. MATHCAD FILES

MathCAD file used in the comparison with free space
(Complex Metallic Room)

Plot of the BSC Results

Read the Data

NEC_BSC_data := READPRN("C:/Temp/thesis/complex_six_plate_box_test.b

M := rows(NEC_BSC_data)

$M = 7.2 \times 10^3$

N := cols(NEC_BSC_data)

N = 9

phi := NEC_BSC_data ⁽²⁾

phi^T =

	0	1	2	3	4	5	6	7	8	9
0	1.5	1.5	1.5	1.5	1.5	1.5	1.5	1.5	1.5	1.5

$E_r := \left(\frac{\text{NEC_BSC_data}^{(3)}}{20} \right)$

$E_r^T =$

	0	1	2	3	4	5
0	3.622	1.422	0.576	3.635	4.576	4.009

$E_\theta := \frac{\text{NEC_BSC_data}^{(5)}}{20}$

$E_\theta^T =$

	0	1	2	3	4	5
0	2.999	2.996	1.856	0.121	0.622	3.614

$E_\phi := \frac{\text{NEC_BSC_data}^{(7)}}{20}$

$E_\phi^T =$

	0	1	2	3	4	5
0	14.093	20.464	15.758	18.557	17.927	17.498

$E_{\text{tot}} := \sqrt{(E_r)^2 + (E_\theta)^2 + (E_\phi)^2}$

n := 0..M - 1

$E_{\text{tot}}^T =$

	0	1	2	3	4	5	6	7	8	9
0	14.857	20.731	15.877	18.91	18.512	18.312	13.591	10.528	26.676	31.365

N.x is the # points in the outer loop

rows(E_{tot}) = 7.2×10^3



$$N_y := \frac{\text{rows}(E_{\text{tot}})}{N_x}$$

$$N_y = 60$$

$$q := 0..N_y - 1$$

$$\text{start}_q := q \cdot N_x$$

$$\text{stop}_q := \text{start}_q + N_x - 1$$

$$\text{test}_{\langle q \rangle} := \text{submatrix}(E_{\text{tot}}, \text{start}_q, \text{stop}_q, 0, 0)$$

$$\text{rows}(\text{test}) = 120$$

$$\text{cols}(\text{test}) = 60$$

$$E_{\text{tot_dB}} := 20 \cdot \log(E_{\text{tot}})$$

$$\text{test_dB}_{\langle q \rangle} := \text{submatrix}(E_{\text{tot_dB}}, \text{start}_q, \text{stop}_q, 0, 0)$$

$$\max(\text{test_dB}) = 39.564$$

$$\min(\text{test_dB}) = -195.229$$

$$\max_field_dB = \max(\text{test_dB})$$

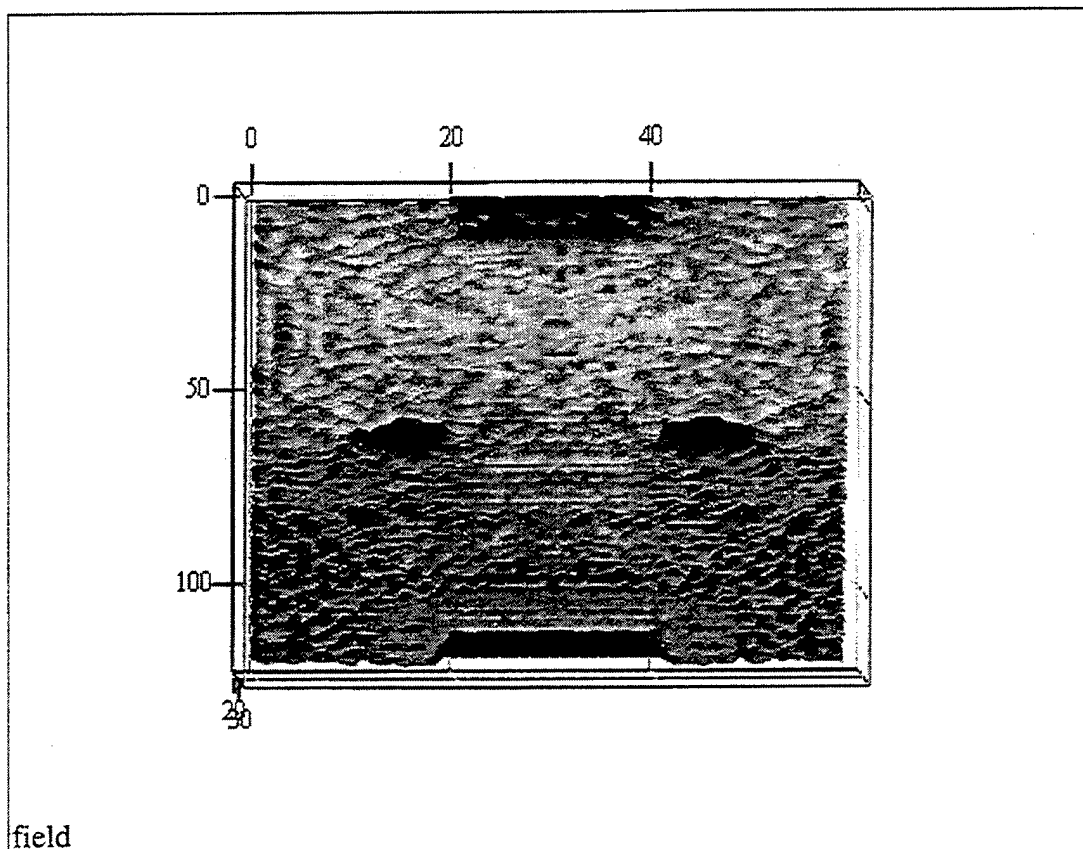
$$\text{dyn_range} := 23$$

$$\text{field_limit} = \max_field_dB - \text{dyn_range}$$

$$p := 0.. \text{rows}(\text{test_dB}) - 1$$

$$\text{field}_{p,q} := \text{if}(\text{test_dB}_{p,q} > \text{field_limit}, \text{test_dB}_{p,q}, \text{field_limit})$$

$$\text{test_lin}_{\langle q \rangle} := \text{submatrix}(E_{\text{tot}}, \text{start}_q, \text{stop}_q, 0, 0)$$



END of MathCAD file used in the comparison with free space
(Complex Metallic Room)

MathCAD file used in the comparison with free space (Room
With Two Antennas)

Plot of the BSC Results

Read the Data

NEC_BSC_data := READPRN("C:/Temp/thesis/fl_2ant_diff_zaxis.prn")

M := rows(NEC_BSC_data)

$M = 8 \times 10^4$

N := cols(NEC_BSC_data)

N = 9

phi := NEC_BSC_data ⁽²⁾

phi^T =

	0	1	2	3	4	5	6	7	8	9
0	1	1	1	1	1	1	1	1	1	1

$E_r := \left(\begin{array}{c} \overbrace{\text{NEC_BSC_data}^{(3)}}^{20} \\ 10 \end{array} \right)$

$$E_r^T = \begin{array}{|c|c|c|c|c|c|c|} \hline & 0 & 1 & 2 & 3 & 4 & 5 \\ \hline 0 & 0.015 & 1.179 & 2.438 & 2.097 & 1.952 & 2.106 \\ \hline \end{array}$$

→
NEC_BSC_data <5>

$$E_\theta := 10$$

20

$$E_\theta^T = \begin{array}{|c|c|c|c|c|c|c|} \hline & 0 & 1 & 2 & 3 & 4 & 5 \\ \hline 0 & 0.024 & 0.029 & 0.299 & 0.606 & 0.813 & 1.023 \\ \hline \end{array}$$

→
NEC_BSC_data <7>

20

$$E_\phi := 10$$

$$E_\phi^T = \begin{array}{|c|c|c|c|c|c|c|} \hline & 0 & 1 & 2 & 3 & 4 & 5 \\ \hline 0 & 0.438 & 0.219 & 0.406 & 0.241 & 0.327 & 0.201 \\ \hline \end{array}$$

$$E_{tot} := \sqrt{(E_r)^2 + (E_\theta)^2 + (E_\phi)^2}$$

$$n := 0..M-1$$

$$E_{tot}^T = \begin{array}{|c|c|c|c|c|c|c|c|c|c|c|} \hline & 0 & 1 & 2 & 3 & 4 & 5 & 6 & 7 & 8 & 9 \\ \hline 0 & 0.439 & 1.199 & 2.489 & 2.196 & 2.14 & 2.35 & 1.115 & 2.199 & 3.363 & 1.961 \\ \hline \end{array}$$

$$\text{rows}(E_{tot}) = 8 \times 10^4$$

$$N_y = 400$$

$$N_y := \frac{\text{rows}(E_{tot})}{N_x}$$

$$N_y = 400$$

$$q := 0..N_y - 1$$

$$\text{start}_q := q \cdot N_x$$

$$\text{stop}_q := \text{start}_q + N_x - 1$$

$$\text{test}^{(q)} := \text{submatrix}(E_{tot}, \text{start}_q, \text{stop}_q, 0, 0)$$

$$\text{rows}(\text{test}) = 200$$

$$\text{cols}(\text{test}) = 400$$

$$E_{tot_dB} := 20 \cdot \log(E_{tot})$$

$$\text{test_dB}^{(q)} := \text{submatrix}(E_{tot_dB}, \text{start}_q, \text{stop}_q, 0, 0)$$

$$\text{max}(\text{test_dB}) = 38.777$$

$$\text{min}(\text{test_dB}) = -195.229$$

$$\text{max_field_dB} = \text{max}(\text{test_dB})$$

When dynamic range is 30 db, we get some errors, thus we set the following:

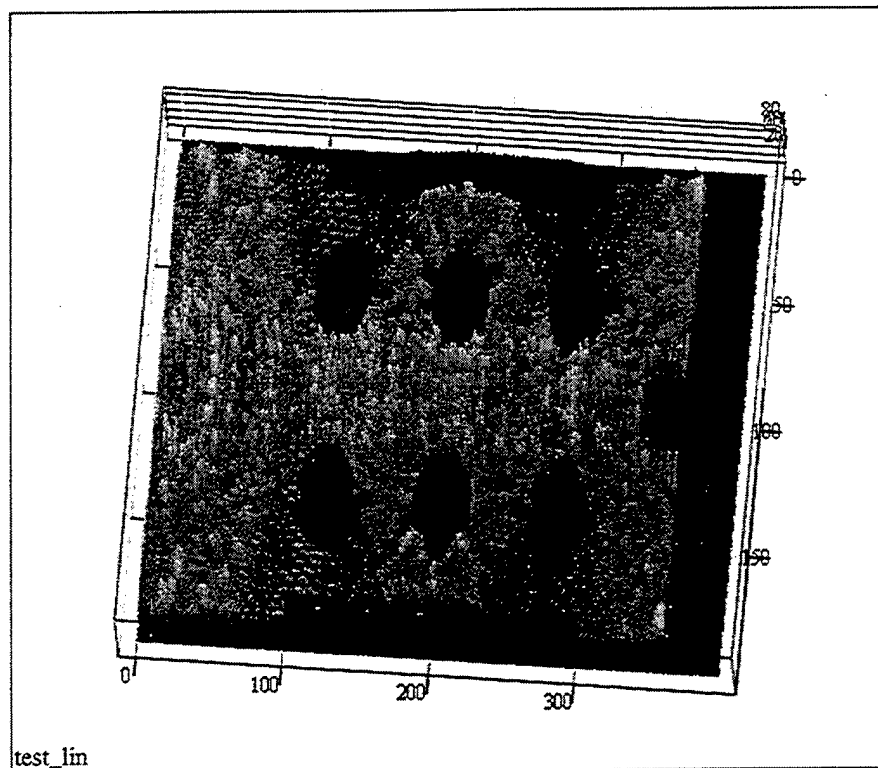
```
dyn_range := 25
```

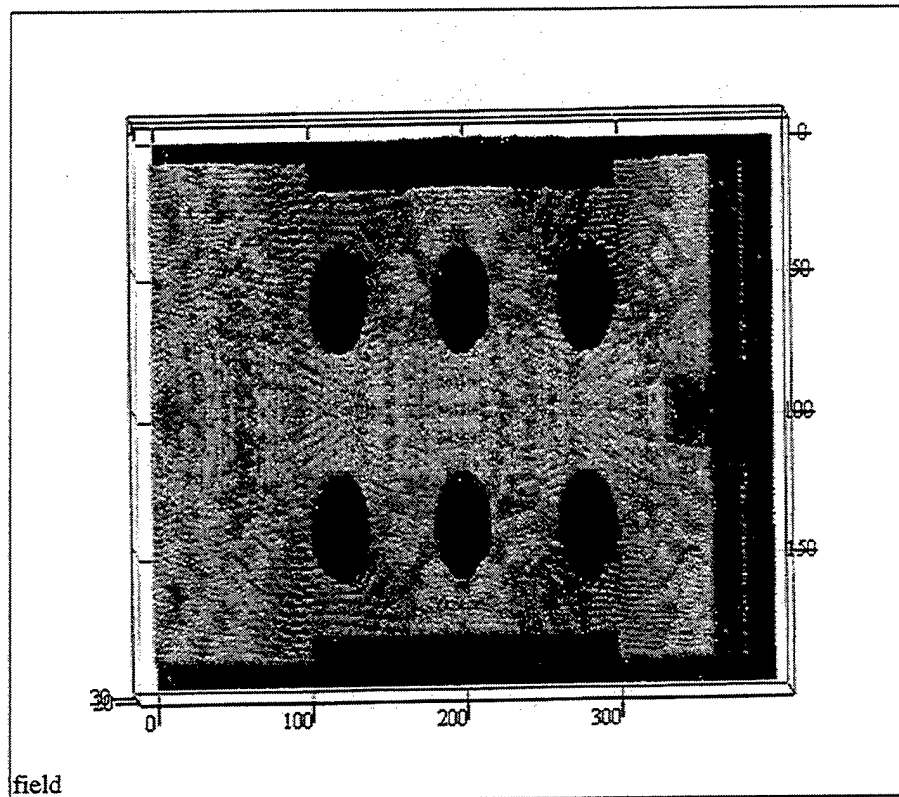
```
field_limit = max_field_dB - dyn_range
```

```
p := 0..rows(test_dB) - 1
```

```
field_p,q := if(test_dB_p,q > field_limit, test_dB_p,q, field_limit)
```

```
test_lin(q) := submatrix(E_tot, start_q, stop_q, 0, 0)
```





END of MathCAD file used in the comparison with free space
(Room With Two Antennas)

MathCAD file used in the comparison with free space
(Symmetric placement of Antenna)

Plot of the BSC Results

Read the Data

```
NEC_BSC_data := READPRN("C:/temp/Thesis/New_1f_r_op_an_pl_lant_symmetric.txt")
```

```
M := rows(NEC_BSC_data)
```

```
M =  $8 \times 10^4$ 
```

```
N := cols(NEC_BSC_data)
```

```
N = 9
```

```
phi := NEC_BSC_data <2>
```


$$\text{phi}^T = \begin{array}{|c|c|c|c|c|c|c|c|c|c|c|} \hline & 0 & 1 & 2 & 3 & 4 & 5 & 6 & 7 & 8 & 9 \\ \hline 0 & 2 & 2 & 2 & 2 & 2 & 2 & 2 & 2 & 2 & 2 \\ \hline \end{array}$$

$$E_r := \left(\frac{\text{NEC_BSC_data} \langle 3 \rangle}{20} \right)$$

$$E_r^T = \begin{array}{|c|c|c|c|c|c|c|} \hline & 0 & 1 & 2 & 3 & 4 & 5 \\ \hline 0 & 0.378 & 0.398 & 0.414 & 0.398 & 0.403 & 0.41 \\ \hline \end{array}$$

$$E_\theta := 10 \frac{\text{NEC_BSC_data} \langle 5 \rangle}{20}$$

$$E_\theta^T = \begin{array}{|c|c|c|c|c|c|c|} \hline & 0 & 1 & 2 & 3 & 4 & 5 \\ \hline 0 & 0.033 & 0.046 & 0.066 & 0.078 & 0.085 & 0.087 \\ \hline \end{array}$$

$$E_\phi := 10 \frac{\text{NEC_BSC_data} \langle 7 \rangle}{20}$$

$$E_\phi^T = \begin{array}{|c|c|c|c|c|c|c|} \hline & 0 & 1 & 2 & 3 & 4 & 5 \\ \hline 0 & 0.047 & 0.102 & 0.126 & 0.15 & 0.169 & 0.182 \\ \hline \end{array}$$

$$E_{\text{tot}} := \sqrt{(E_r)^2 + (E_\theta)^2 + (E_\phi)^2}$$

$$n := 0..M-1$$

$$E_{\text{tot}}^T = \begin{array}{|c|c|c|c|c|c|c|c|c|c|c|} \hline & 0 & 1 & 2 & 3 & 4 & 5 & 6 & 7 & 8 & 9 \\ \hline 0 & 0.382 & 0.414 & 0.438 & 0.433 & 0.446 & 0.457 & 0.436 & 0.437 & 0.426 & 0.409 \\ \hline \end{array}$$

N.x is the # points in the outer loop

$$\text{rows}(E_{\text{tot}}) = 8 \times 10^4$$

$$N_x = 200$$

$$N_y := \frac{\text{rows}(E_{\text{tot}})}{N_x}$$

$$N_y = 400$$

$$q := 0..N_y - 1$$

$$\text{start}_q := q \cdot N_x$$

$$\text{stop}_q := \text{start}_q + N_x - 1$$

$$\text{test} \langle q \rangle := \text{submatrix}(E_{\text{tot}}, \text{start}_q, \text{stop}_q, 0, 0)$$

$$\text{rows}(\text{test}) = 200$$

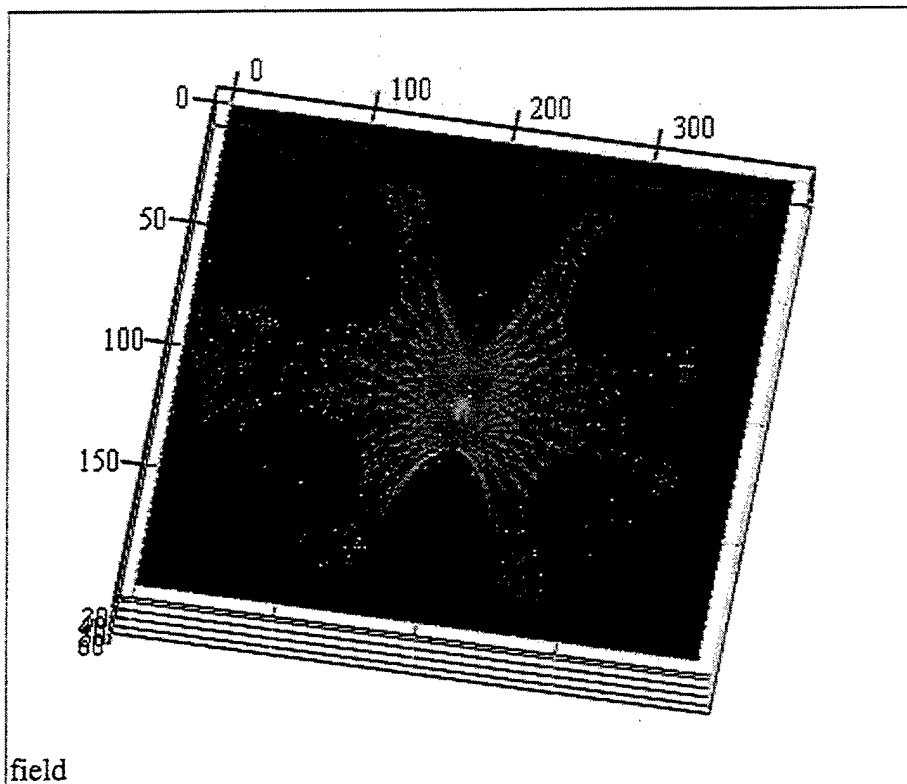
$$\text{cols}(\text{test}) = 400$$

```


$$E_{\text{tot\_dB}} := 20 \cdot \log(E_{\text{tot}})$$

test_dB < q > := submatrix(E_tot_dB, start_q, stop_q, 0, 0)
max(test_dB) = 65.84
min(test_dB) = -195.229
max_field_dB = max(test_dB)
dyn_range := 41
field_limit = max_field_dB - dyn_range
p := 0..rows(test_dB) - 1
field_p,q := if(test_dB_p,q > field_limit, test_dB_p,q, field_limit)
test_lin < q > := submatrix(E_tot, start_q, stop_q, 0, 0)

```



END of MathCAD file used in the comparison with free space
(Symmetric placement of Antenna)

MathCAD file used in the comparison with free space (Random placement of Antenna)

Plot of the BSC Results

Read the Data

NEC_BSC_data := READPRN("C:/Temp/thesis/New_1f_r_op_an_pl_1ant.txt")

M := rows(NEC_BSC_data)

M = 8×10^4

N := cols(NEC_BSC_data)

N = 9

phi := NEC_BSC_data $\langle 2 \rangle$

phi^T =

	0	1	2	3	4	5	6	7	8	9
0	1.5	1.5	1.5	1.5	1.5	1.5	1.5	1.5	1.5	1.5

$E_r := \left(\frac{\text{NEC_BSC_data} \langle 3 \rangle}{20} \right)$

E_r^T =

	0	1	2	3	4	5
0	1.247·10 ⁻³	3.051·10 ⁻⁴	3.144·10 ⁻⁴	3.24·10 ⁻⁴	3.342·10 ⁻⁴	3.447·10 ⁻⁴

$E_\theta := \frac{\text{NEC_BSC_data} \langle 5 \rangle}{20}$

E_θ^T =

	0	1	2	3	4	5
0	0.029	0.03	0.03	0.031	0.031	0.032

$E_\phi := \frac{\text{NEC_BSC_data} \langle 7 \rangle}{20}$

E_φ^T =

	0	1	2	3	4	5
0	0.39	0.247	0.252	0.257	0.263	0.268

$E_{\text{tot}} := \sqrt{(E_r)^2 + (E_\theta)^2 + (E_\phi)^2}$

n := 0..M - 1

E_{tot}^T =

	0	1	2	3	4	5	6	7	8	9
0	0.391	0.249	0.254	0.259	0.265	0.27	0.275	0.281	0.286	0.291

N.x is the # points in the outer loop

rows(E_{tot}) = 8×10^4

$\rho_{\text{tot}} := \dots$

```


$$N_y := \frac{\text{rows}(E_{\text{tot}})}{N_x}$$


$$N_y = 400$$


$$q := 0..N_y - 1$$


$$\text{start}_q := q \cdot N_x$$


$$\text{stop}_q := \text{start}_q + N_x - 1$$


$$\text{test}^{(q)} := \text{submatrix}(E_{\text{tot}}, \text{start}_q, \text{stop}_q, 0, 0)$$


$$\text{rows}(\text{test}) = 200$$


$$\text{cols}(\text{test}) = 400$$


$$E_{\text{tot\_dB}} := 20 \cdot \log(E_{\text{tot}})$$


$$\text{test\_dB}^{(q)} := \text{submatrix}(E_{\text{tot\_dB}}, \text{start}_q, \text{stop}_q, 0, 0)$$


$$\text{max}(\text{test\_dB}) = 44.709$$


$$\text{min}(\text{test\_dB}) = -195.229$$


$$\text{max\_field\_dB} = \text{max}(\text{test\_dB})$$


```

When dynamic range is 30 db, we get some errors, thus we set the following:

```


$$\text{dyn\_range} := 33$$

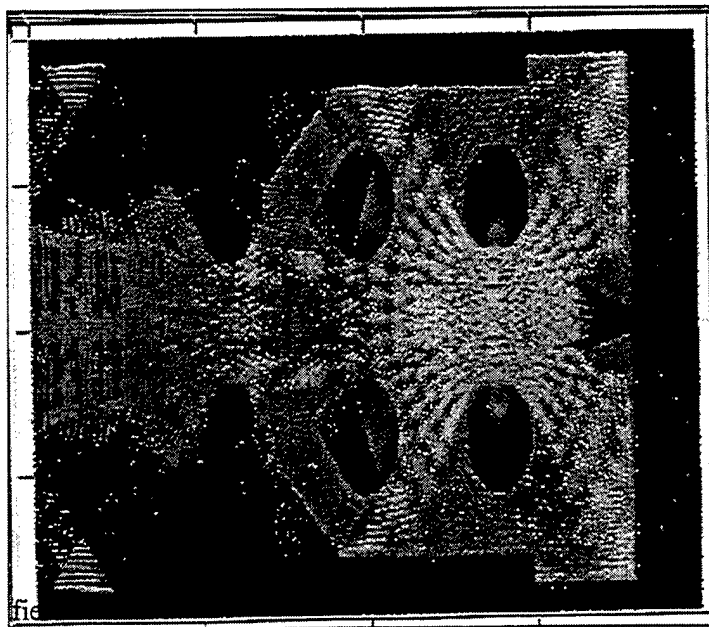
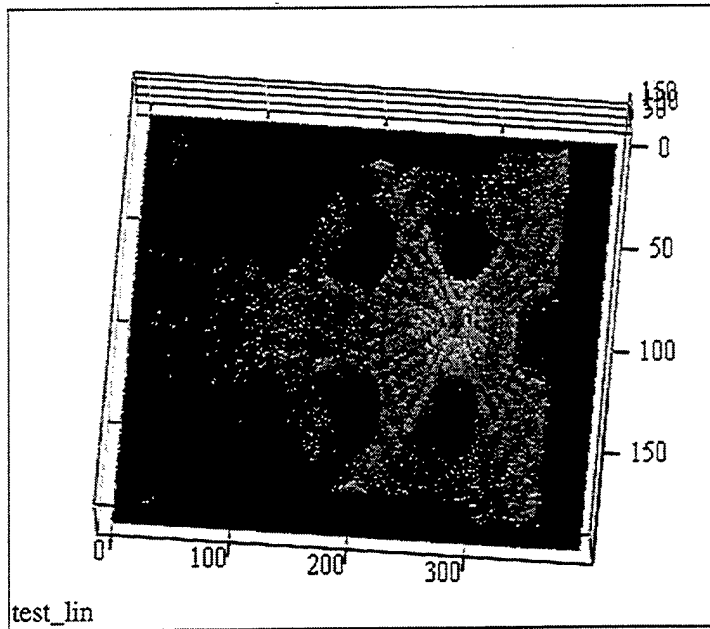

$$\text{field\_limit} = \text{max\_field\_dB} - \text{dyn\_range}$$


$$p := 0.. \text{rows}(\text{test\_dB}) - 1$$


$$\text{field}_{p,q} := \text{if}(\text{test\_dB}_{p,q} > \text{field\_limit}, \text{test\_dB}_{p,q}, \text{field\_limit})$$


$$\text{test\_lin}^{(q)} := \text{submatrix}(E_{\text{tot}}, \text{start}_q, \text{stop}_q, 0, 0)$$


```



END of MathCAD file used in the comparison with free space
(Random placement of Antenna)

MathCAD file used in the comparison with free space (Room to room scenario)

Plot of the BSC Results

Read the Data

NEC_BSC_data := READPRN ("C:/Temp/thesis/New_2F_r_op_anal_plates.txt")

M := rows(NEC_BSC_data)

M = 8×10^4

N := cols(NEC_BSC_data)

N = 9

phi := NEC_BSC_data ⁽²⁾

phi^T =

	0	1	2	3	4	5	6	7	8	9
0	6.5	6.5	6.5	6.5	6.5	6.5	6.5	6.5	6.5	6.5

E_r := $\left(\frac{\text{NEC_BSC_data}^{(3)}}{20} \right)$

E_r^T =

	0	1	2	3	4	5
0	1·10 ⁻¹⁰	1·10 ⁻¹⁰	1·10 ⁻¹⁰	1·10 ⁻¹⁰	1·10 ⁻¹⁰	1·10 ⁻¹⁰

E_θ := $\left(\frac{\text{NEC_BSC_data}^{(5)}}{20} \right)$

E_θ^T =

	0	1	2	3	4	5
0	1·10 ⁻¹⁰	1·10 ⁻¹⁰	1·10 ⁻¹⁰	1·10 ⁻¹⁰	1·10 ⁻¹⁰	1·10 ⁻¹⁰

E_φ := $\left(\frac{\text{NEC_BSC_data}^{(7)}}{20} \right)$

E_φ^T =

	0	1	2	3	4	5
0	1·10 ⁻¹⁰	1·10 ⁻¹⁰	1·10 ⁻¹⁰	1·10 ⁻¹⁰	1·10 ⁻¹⁰	1·10 ⁻¹⁰

E_{tot} := $\sqrt{(E_r)^2 + (E_\theta)^2 + (E_\phi)^2}$

n := 0..M - 1

E_{tot}^T =

	0	1	2	3	4	5
0	1.732·10 ⁻¹⁰	1.732·10 ⁻¹⁰	1.732·10 ⁻¹⁰	1.732·10 ⁻¹⁰	1.732·10 ⁻¹⁰	1.732·10 ⁻¹⁰

Nx is the # points in the outer loop

rows(E_{tot}) = 8×10^4

$$N_y := \frac{\text{rows}(E_{\text{tot}})}{N_x}$$

$$N_y = 400$$

$$q := 0..N_y - 1$$

$$\text{start}_q := q \cdot N_x$$

$$\text{stop}_q := \text{start}_q + N_x - 1$$

$$\text{test}^{(q)} := \text{submatrix}(E_{\text{tot}}, \text{start}_q, \text{stop}_q, 0, 0)$$

$$\text{rows}(\text{test}) = 200$$

$$\text{cols}(\text{test}) = 400$$

$$E_{\text{tot_dB}} := 20 \cdot \log(\overrightarrow{E_{\text{tot}}})$$

$$\text{test_dB}^{(q)} := \text{submatrix}(E_{\text{tot_dB}}, \text{start}_q, \text{stop}_q, 0, 0)$$

$$\text{max}(\text{test_dB}) = 23.308$$

$$\text{min}(\text{test_dB}) = -195.229$$

$$\text{max_field_dB} = \text{max}(\text{test_dB})$$

When dynamic range is 30 db, we get some errors, thus we set the following:

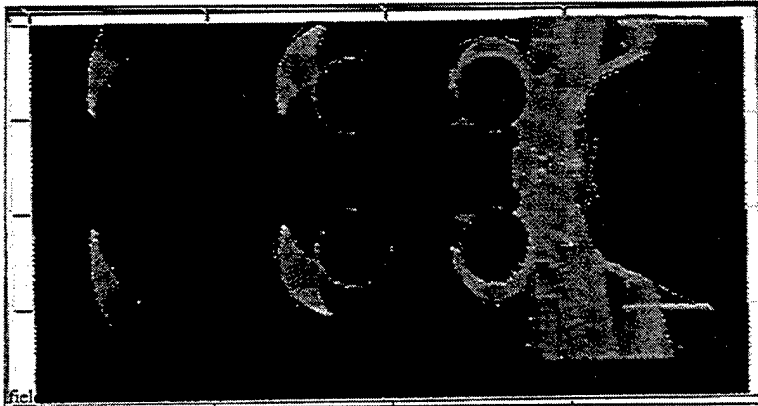
$$\text{dyn_range} := 75$$

$$\text{field_limit} = \text{max_field_dB} - \text{dyn_range}$$

$$p := 0.. \text{rows}(\text{test_dB}) - 1$$

$$\text{field}_{p,q} := \text{if}(\text{test_dB}_{p,q} > \text{field_limit}, \text{test_dB}_{p,q}, \text{field_limit})$$

$$\text{test_lin}^{(q)} := \text{submatrix}(E_{\text{tot}}, \text{start}_q, \text{stop}_q, 0, 0)$$



END of MathCAD file used in the comparison with free space
(Room to room scenario).

MathCAD file used in calculating the excess gain/loss
random variables (First location)

NEC_BSC_data := READPRN("dataroom")

$x_{\text{coord}} := \text{NEC_BSC_data} \langle 0 \rangle$

$y_{\text{coord}} := \text{NEC_BSC_data} \langle 1 \rangle$

$z_{\text{coord}} := \text{NEC_BSC_data} \langle 2 \rangle$

antenna , obser.points NOT in the same level

$\rho := \sqrt{(x_{\text{coord}} - 14.0)^2 + (y_{\text{coord}} - 5.0)^2 + (z_{\text{coord}} - 1.5)^2}$

free_space_data := READPRN("datafree")

$E_x := \left(\frac{\text{NEC_BSC_data} \langle 3 \rangle}{10 \cdot 20} \right)$

$E_y := 10 \cdot \frac{\text{NEC_BSC_data} \langle 5 \rangle}{20}$

$E_z := 10 \cdot \frac{\text{NEC_BSC_data} \langle 7 \rangle}{20}$

$$E_{tot} := \sqrt{(E_x)^2 + (E_y)^2 + (E_z)^2}$$

$$\text{rows}(E_{tot}) = 1.539 \times 10^3$$

$$E_{x_free} := \left(\frac{\text{free_space_data}^{(3)}}{10^{20}} \right)$$

$$E_{y_free} := 10 \frac{\text{free_space_data}^{(5)}}{20}$$

$$E_{z_free} := 10 \frac{\text{free_space_data}^{(7)}}{20}$$

$$E_{tot_free} := \sqrt{(E_{x_free})^2 + (E_{y_free})^2 + (E_{z_free})^2}$$

Since the **NEC-BSC dynamic range** is only 30dB, we will have to account for this fact by "filtering" out all values which are out of that range. This is done in the following fashion:

$$E_{tot_dB} := (20 \log(E_{tot}))$$

$$\text{dyn_range} = 30$$

$$jj := 0.. \text{rows}(E_{tot_dB}) - 1$$

$$\text{lowest_allowed_Etot_value} := \max(E_{tot_dB}) - \text{dyn_range}$$

$$\text{lowest_allowed_Etot_value} = 12.948$$

$$E_{tot_free_dB} := (20 \log(E_{tot_free}))$$

$$\text{lowest_allowed_Etot_fr_val} := \max(E_{tot_free_dB}) - \text{dyn_range}$$

$$\text{lowest_allowed_Etot_fr_val} = 7.82$$

$$E_{total_dB_jj} := \text{if}(E_{tot_dB_jj} < \text{lowest_allowed_Etot_value}, \text{lowest_allowed_Etot_value}, E_{tot_dB_jj})$$

$$E_{total_free_dB_jj} := \text{if}(E_{tot_free_dB_jj} < \text{lowest_allowed_Etot_fr_val}, \text{lowest_allowed_Etot_fr_val}, E_{tot_free_dB_jj})$$

Converting to linear:

$$E_{total} := 10 \frac{E_{total_dB}}{20}$$

$$E_{total_free} := 10 \frac{E_{total_free_dB}}{20}$$

Let us now create the two data matrices, namely the "datamatrix" which consists of the room's field strength values for every observed point and the "freespacedata01" which includes the corresponding data for the free space case.

$$\text{datamatrix} := \text{augment}(\rho, E_{total})$$

$$\text{freespacedata01} := \text{augment}(\rho, E_{total_free})$$

At this point, owing to the nonuniform layout of the distance (from the antenna) points in the \square array, we will have to distinguish them into several different groups using the following approach:

$\text{lower} := \text{floor}(\min(\rho))$

$\text{upper} := \text{ceil}(\max(\rho))$

Maximum and minimum distance for this antenna location:

$\text{upper} = 15$

$\text{lower} = 0$

Groups separation for this calculation (in cm):

$\text{separation} := 50$

"Step factor" for this calculation:

$\text{factor} := \text{ceil}\left(\frac{100}{\text{separation}}\right)$

$\text{factor} = 2$

Number of distance bins for this calculation:

$\text{bins} := \text{upper} \cdot \text{factor}$

$\text{bins} = 30$

$h := \frac{\text{upper} - \text{lower}}{\text{bins}}$

$h = 0.5$

$n := 0.. \text{bins}$

$k_n := \text{lower} + n \cdot h$

It should be noted that the number of bins may be chosen in a fashion which best suits our desirable "distance steps".

For instance, **should we choose to have groups points separated by 50cm**, where the maximum distance from the

antenna is 49m, our intuitive selection should be 98.

We next introduce a new function which shall be utilized several times in our subsequent calculations. As input, it expects a two column matrix and an array. It looks for those values of the first column (i.e., in our problem, the distance array which fall within our made-up groups and then creates a new matrix that contains all those second column's values whose respective first column value satisfy our requirement. It finally returns this new matrix which, it should be underlined, normally has a **different number of elements in each row**.

```

build(M,binvector) :=
  A ← M <0>
  B ← M <1>
  k ← binvector
  for l ∈ 0..rows(k) - 2
    Dl ← 0
  for i ∈ 0..rows(k) - 2
    for j ∈ 0..rows(M) - 1
      Di ← augment(Bj,Di) if ki < Aj ≤ ki+1
  for i ∈ 0..rows(D) - 1
    Di ← submatrix(Di,0,rows(Di) - 1,0,cols(Di) - 2) if Di ≠ 0
  D

```

It is high time we used this helping function.

```
datamatrix02 := build(datamatrix,k)
```

```
freespacedata02 := build(freespacedata01,k)
```

```
datamatrix02T =
```

	0	1	2	3	4	5	6
0	[1,13]	[1,35]	[1,31]	[1,40]	[1,67]	[1,93]	[1,127]

The following new function is, seemingly, of high importance since it is the one which calculates the "normalized difference" random variables. It receives two matrices of the same dimensions and returns a new matrix which in each row contains the values of the random variable pertinent to that row's "distance group."

```

difference(X, Y) :=
  for k ∈ 0..rows(X) - 1
    Ck ← 0
    (
      for j ∈ 0..rows(X) - 1
        n ← cols(Xj)
        A ← Xj
        B ← Yj
        i ← 0
        for i ∈ 0..n - 1
          diffi ← 20·log( $\frac{A_{0,i}}{B_{0,i}}$ )
        n ← cols(Xj)
        Cj ← stack(Cj, diff)
        Cj ← (Cj)T
        k ← rows(Cj)
        l ← cols(Cj)
        Cj ← submatrix(Cj, 0, k - 1, l, l - 1)
    )
  C

```

The "room gain" is defined here in dB

We now get rid of the redundant first row zeros and then calculate the normalized difference variables.

```

new_datamatrix02 := submatrix(datamatrix02, 1, rows(datamatrix02) - 2, 0, cols(datamatrix02) - 1)
new_freespacedata02 := submatrix(freespacedata02, 1, rows(freespacedata02) - 2, 0, cols(freespacedata02) - 1)
norm_diff := difference(new_datamatrix02, new_freespacedata02)

```

norm_diff^T =

	0	1	2	3	4	5	6
0	[1,35]	[1,35]	[1,40]	[1,67]	[1,93]	[1,127]	[1,134]

Surprisingly and unexpectedly the Mathcad appears to suffer from a bug for it returns an erroneous matrix. The cause of this weird occurrence remains unknown, however we shall attempt to effectively overcome this mishap by applying an easy trick.

```

i := 0..rows(new_datamatrix02) - 1
ri := cols(new_datamatrix02)
corr_norm_diffi := submatrix(norm_diffi, 0, rows(norm_diffi) - 1, 0, ri - 1)

```

corr_norm_diff^T =

	0	1	2	3	4	5	6
0	[1,35]	[1,31]	[1,40]	[1,67]	[1,93]	[1,127]	[1,134]

This last matrix named "corr_norm_diff" is the one we intended to find. In each row of unequal element number, it contains a different random variable as function of our

"devised" groups. Let us take a closer look in one of them, say the 5th.

$\text{test}_0 := (\text{corr_norm_diff}^T)^{(0)}$

$\text{test}_0 =$	0	1	2	3	4	5	6	7	8
0	-2.506	1.357	0.4	3.603	4.162	4.647	1.404	-1.316	-0.902

$\text{mean}(\text{test}_0) = 0.878$

$\text{test}_1 := (\text{corr_norm_diff}^T)^{(1)}$

$\text{test}_1 =$	0	1	2	3	4	5	6	7	8
0	4.37	2.399	-2.935	0.109	-0.481	-2.83	1.088	1.898	-1.193

$\text{mean}(\text{test}_1) = 0.592$

THESE ARE % DIFFERENCE

Defining the number of the bins:

$N_{\text{points}} := 200$

$ii := 0..N_{\text{points}} - 1$

$j := 0.. \text{rows}(\text{corr_norm_diff}) - 1$

$\text{upper}_j := \max(\text{corr_norm_diff}_j)$

$\text{lower}_j := \min(\text{corr_norm_diff}_j)$

$\text{upper_max} := \max(\text{upper})$

$\text{lower_min} := \min(\text{lower})$

$\text{step} := \frac{\text{upper_max} - \text{lower_min}}{N_{\text{points}}}$

$\text{upper_max} = 13.584$

$\text{lower_min} = -17.064$

$\text{step} = 0.153$

$\text{gen_intervals}_{ii} := \text{lower_min} + \text{step} \cdot ii$

$I_j = \frac{\text{hist}(\text{gen_intervals}, \text{corr_norm_diff}_j)}{\text{cols}(\text{corr_norm_diff}_j)}$

$\text{rows}(\text{gen_intervals}) = 200$

$\text{buildL}(L) := \begin{array}{l} L_{\text{new}} \leftarrow L_0^T \\ \text{for } q \in 1.. \text{rows}(L) - 1 \\ \quad A \leftarrow L_q^T \\ \quad L_{\text{new}} \leftarrow \text{stack}(L_{\text{new}}, A) \end{array}$

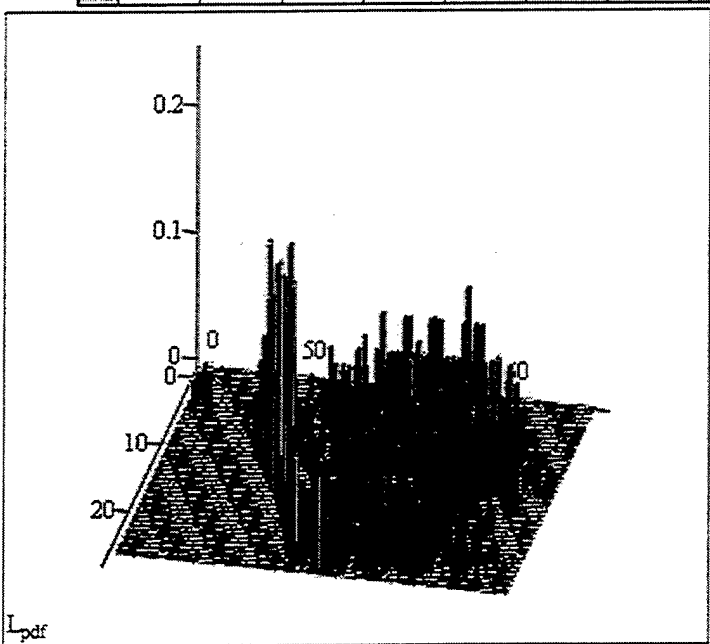
$L_{\text{pdf}} := \text{buildL}(L)$

$\text{rows}(L_{\text{pdf}}) = 28$

$\text{cols}(L_{\text{pdf}}) = 199$

$$L_{pdf} =$$

	0	1	2	3	4	5	6	7	8	9
0	0	0	0	0	0	0	0	0	0	0
1	0	0	0	0	0	0	0	0	0	0
2	0	0	0	0	0	0	0	0	0	0
3	0	0	0	0	0	0	0	0	0	0
4	0.011	0	0	0	0	0	0	0	0	0
5	0	0	0	0	0.024	0	0	0	0.031	0
6	0	0	0	0	0	0	0	0	0	0
7	0	0	0	0	0	0	0	0	0	0
8	0	0	0	0	0	0	0	0	0	0
9	0	0	0	0	0	0	0	0	0	0
10	0	0	0	0	0	0	0	0	0	0
11	0	0	0	0	0	0	0	0	0	0
12	0	0	0	0	0	0	0	0	0	0
13	0	0	0	0	0	0	0	0	0	0
14	0	0	0	0	0	0	0	0	0	0
15	0	0	0	0	0	0	0	0	0	0



```

N_pdfs := cols(L_pdf) - 1
qq := 0..N_pdfs - 1
avg_pdf_qq := mean(L_pdf<qq>)
Σ avg_pdf = 0.998

```

$$avg_pdf^T =$$

	0	1	2	3	4	5
0	$3.84 \cdot 10^{-4}$	0	0	0	$8.436 \cdot 10^{-4}$	0

$$\text{mean_rv} := \sum_{qq=0}^{N_{\text{pdfs}}-1} \text{gen_intervals}_{qq} \cdot \text{avg_pdf}_{qq}$$

$$\text{mean_rv} = -0.108$$

$$\text{step} = 0.153$$

$$\text{mean_sq_rv} := \sum_{qq=0}^{N_{\text{pdfs}}-1} (\text{gen_intervals}_{qq})^2 \cdot \text{avg_pdf}_{qq}$$

$$\text{mean_sq_rv} = 28.219$$

$$\text{var_rv} := \text{mean_sq_rv} - \text{mean_rv}^2$$

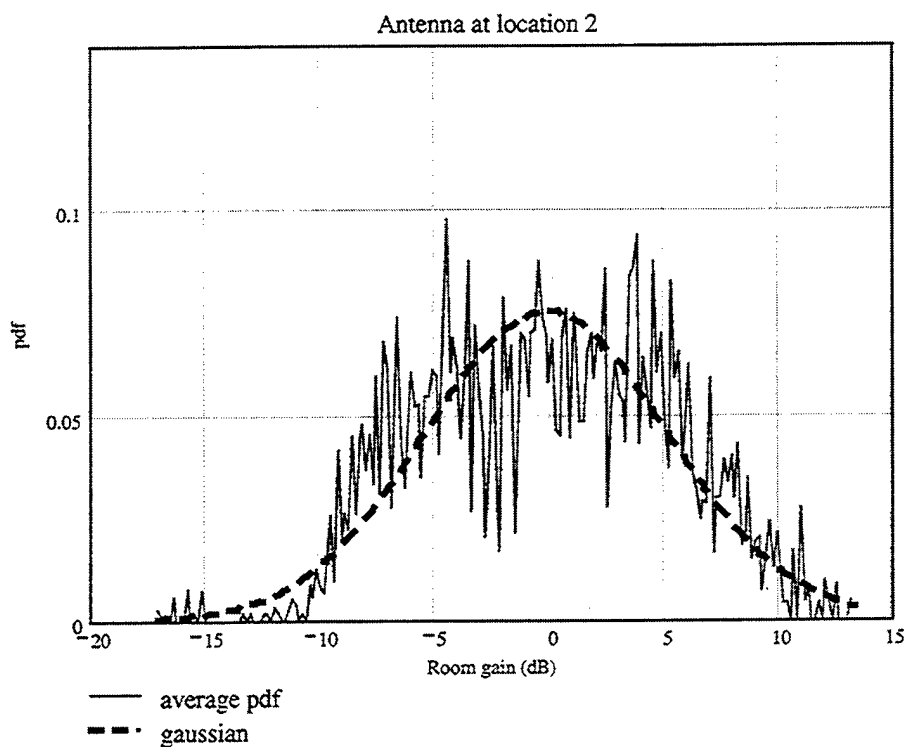
$$\text{var_rv} = 28.197$$

$$\text{mean_rv} = -0.108$$

Defining **Gaussian** pdf:

$$\text{gauss}_{ii} := \frac{1}{\sqrt{2 \cdot \pi \cdot \text{var_rv}}} \cdot e^{-\frac{(\text{gen_intervals}_i - \text{mean_rv})^2}{2 \cdot \text{var_rv}}}$$

$$\text{room_gain}_{\text{dB}} := \text{gen_intervals}$$



$$\text{avg_pdf}^T =$$

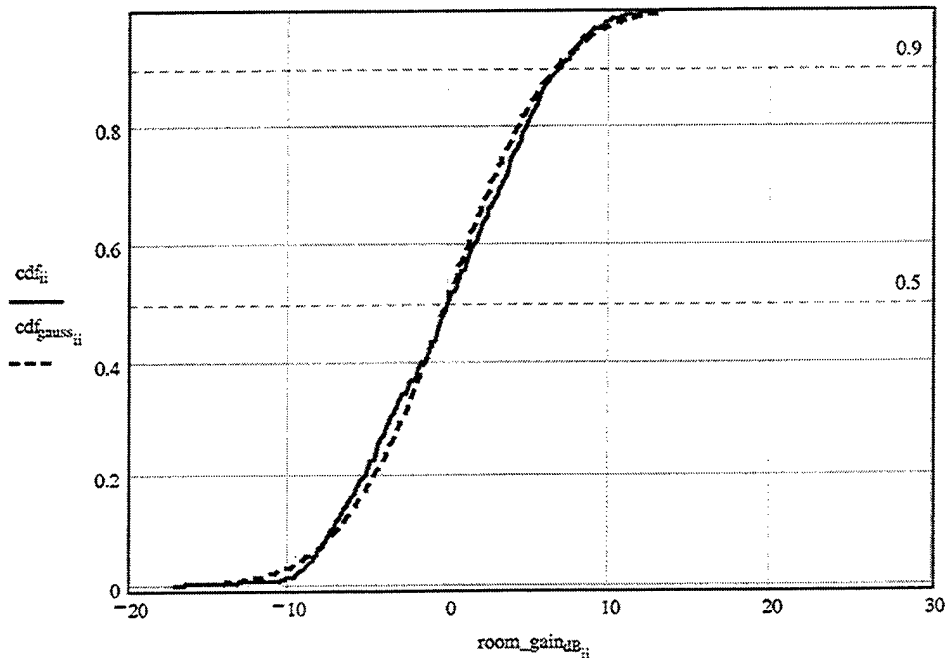
	0	1	2	3	4	5
0	$3.84 \cdot 10^{-4}$	0	0	0	$8.436 \cdot 10^{-4}$	0

$$\text{gauss}^T =$$

	0	1	2	3	4	5
0	$4.701 \cdot 10^{-4}$	$5.152 \cdot 10^{-4}$	$5.641 \cdot 10^{-4}$	$6.171 \cdot 10^{-4}$	$6.746 \cdot 10^{-4}$	$7.367 \cdot 10^{-4}$

$$cdf_{qq} := \sum_{m=0}^{qq} avg_pdf_m$$

$$cdf_{gauss_ii} := step \cdot \left(\sum_{m=0}^{ii} gauss_m \right)$$



END of MathCAD file used in calculating the excess gain/loss random variables (First location)

MathCAD file used in calculating the excess gain/loss random variables (Second location)

Calculating the normalized difference random variables

Random position STACK

In this program we are aiming at calculating all the random variables of the normalized difference between the room's and the free space field strength (Etot and Etot_free respectively). We start by reading the associated data files generated by NEC_BSC.

```
NEC_BSC_data1:=READPRN"C:/temp/Thesis/x1a.txt")
```

```
M1:=rows(NEC_BSC_data1)
```

```
M1=213
```

```
N1:=cols(NEC_BSC_data1)
```

```
N1=9
```

```
NEC_BSC_data2:=READPRN"C:/temp/Thesis/x2a.txt")
```

```
M2:=rows(NEC_BSC_data2)
```



```

M2 = 133
N2 := cols(NEC_BSC_data2)
N2 = 9
NEC_BSC_data3 := READPRN("C:/temp/Thesis/x3a.txt")
M3 := rows(NEC_BSC_data3)
M3 = 49
N3 := cols(NEC_BSC_data3)
N3 = 9
NEC_BSC_data4 := READPRN("C:/temp/Thesis/x4a.txt")
M4 := rows(NEC_BSC_data4)
M4 = 49
N4 := cols(NEC_BSC_data4)
N4 = 9
NEC_BSC_data5 := READPRN("C:/temp/Thesis/x5a.txt")
M5 := rows(NEC_BSC_data5)
M5 = 77
N5 := cols(NEC_BSC_data5)
N5 = 9
NEC_BSC_data6 := READPRN("C:/temp/Thesis/x6a.txt")
M6 := rows(NEC_BSC_data6)
M6 = 497
N6 := cols(NEC_BSC_data6)
N6 = 9
NEC_BSC_data7 := READPRN("C:/temp/Thesis/x7a.txt")
M7 := rows(NEC_BSC_data7)
M7 = 133
N7 := cols(NEC_BSC_data7)
N7 = 9
NEC_BSC_data8 := READPRN("C:/temp/Thesis/x8a.txt")
M8 := rows(NEC_BSC_data8)
M8 = 49
N8 := cols(NEC_BSC_data8)
N8 = 9
NEC_BSC_data9 := READPRN("C:/temp/Thesis/x9a.txt")
M9 := rows(NEC_BSC_data9)
M9 = 49
N9 := cols(NEC_BSC_data9)
N9 = 9
NEC_BSC_data10 := READPRN("C:/temp/Thesis/x10a.txt")
M10 := rows(NEC_BSC_data10)
M10 = 77
N10 := cols(NEC_BSC_data10)
N10 = 9
NEC_BSC_data11 := READPRN("C:/temp/Thesis/x11a.txt")

```

```

M11 := rows(NEC_BSC_data1)
M11 = 213
N11 := cols(NEC_BSC_data1)
N11 = 9

x_coord := NEC_BSC_data <0>
y_coord := NEC_BSC_data <1>
z_coord := NEC_BSC_data <2>


$$\rho := \sqrt{(x_{\text{coord}} - 2)^2 + (y_{\text{coord}} - 2)^2 + (z_{\text{coord}} - 2)^2}$$

free_space_data1 := READPRN"C:/temp/Thesis/fs1a.txt" )
MM1 := rows(free_space_data1 )
MM1 = 213
NN1 := cols(free_space_data1 )
NN1 = 9
free_space_data2 := READPRN"C:/temp/Thesis/fs2a.txt" )
MM2 := rows(free_space_data2 )
MM2 = 133
NN2 := cols(free_space_data2 )
NN2 = 9
free_space_data3 := READPRN"C:/temp/Thesis/fs3a.txt" )
MM3 := rows(free_space_data3 )
MM3 = 49
NN3 := cols(free_space_data3 )
NN3 = 9
free_space_data4 := READPRN"C:/temp/Thesis/fs4a.txt" )
MM4 := rows(free_space_data4 )
MM4 = 49
NN4 := cols(free_space_data4 )
NN4 = 9
free_space_data5 := READPRN"C:/temp/Thesis/fs5a.txt" )
MM5 := rows(free_space_data5 )
MM5 = 77
NN5 := cols(free_space_data5 )
NN5 = 9
free_space_data6 := READPRN"C:/temp/Thesis/fs6a.txt" )
MM6 := rows(free_space_data6 )
MM6 = 497
NN6 := cols(free_space_data6 )
NN6 = 9
free_space_data7 := READPRN"C:/temp/Thesis/fs7a.txt" )
MM7 := rows(free_space_data7 )
MM7 = 133

```

```

NN7 := cols(free_space_data7 )
NN7 = 9
free_space_data8 := READPRN("C:/temp/Thesis/fs8a.txt" )
MM8 := rows(free_space_data8 )
MM8 = 49
NN8 := cols(free_space_data8 )
NN8 = 9
free_space_data9 := READPRN("C:/temp/Thesis/fs9a.txt" )
MM9 := rows(free_space_data9 )
MM9 = 49
NN9 := cols(free_space_data9 )
NN9 = 9
free_space_data10 := READPRN("C:/temp/Thesis/fs10a.txt" )
MM10 := rows(free_space_data10 )
MM10 = 77
NN10 := cols(free_space_data10 )
NN10 = 9
free_space_data11 := READPRN("C:/temp/Thesis/fs11a.txt" )
MM11 := rows(free_space_data11 )
MM11 = 213
NN11 := cols(free_space_data11 )
NN11 = 9

```

$$E_x := \left(\frac{\text{NEC_BSC_data}^{(s)}}{10 \quad 20} \right)$$

$$E_y := 10 \quad \frac{\text{NEC_BSC_data}^{(s)}}{20}$$

$$E_z := 10 \quad \frac{\text{NEC_BSC_data}^{(7)}}{20}$$

$$E_{\text{tot}} := \sqrt{(E_x)^2 + (E_y)^2 + (E_z)^2}$$

$$\text{rows}(E_{\text{tot}}) = 1.539 \times 10^3$$

$$E_{x_free} := \left(\frac{\text{free_space_data}^{(s)}}{10 \quad 20} \right)$$

$$E_{y_free} := 10 \quad \frac{\text{free_space_data}^{(s)}}{20}$$

$$E_{z_free} := 10 \quad \frac{\text{free_space_data}^{(7)}}{20}$$

$$E_{\text{tot_free}} := \sqrt{(E_{x_free})^2 + (E_{y_free})^2 + (E_{z_free})^2}$$

Since the **NEC-BSC dynamic range** is only 30dB, we will have to account for this fact by "filtering" out all values which are out of that range. This is done in the following fashion:

$$E_{\text{tot_dB}} := (20 \cdot \log(E_{\text{tot}}))$$

$$\text{dyn_range} := 30$$

$$jj := 0.. \text{rows}(E_{\text{tot_dB}}) - 1$$

$$\text{lowest_allowed_Etot_value} := \max(E_{\text{tot_dB}}) - \text{dyn_range}$$

$$\text{lowest_allowed_Etot_value} = 22.107$$

$$E_{\text{tot_free_dB}} := (20 \cdot \log(E_{\text{tot_free}}))$$

$$\text{lowest_allowed_Etot_fr_val} := \max(E_{\text{tot_free_dB}}) - \text{dyn_range}$$

$$\text{lowest_allowed_Etot_fr_val} = 22.47$$

$$E_{\text{total_dB_jj}} := \text{if}(E_{\text{tot_dB_jj}} < \text{lowest_allowed_Etot_value}, \text{lowest_allowed_Etot_value}, E_{\text{tot_dB_jj}})$$

$$E_{\text{total_free_dB_jj}} := \text{if}(E_{\text{tot_free_dB_jj}} < \text{lowest_allowed_Etot_fr_val}, \text{lowest_allowed_Etot_fr_val}, E_{\text{tot_free_dB_jj}})$$

Converting to linear:

$$E_{\text{total}} := 10^{\frac{E_{\text{total_dB}}}{20}}$$

$$E_{\text{total_free}} := 10^{\frac{E_{\text{total_free_dB}}}{20}}$$

Let us now create the two datamatrices, namely the "datamatrix" which consists of the room's field strength values for every observed point and the "freespacedata01" which includes the corresponding data for the free space case.

$$\text{datamatrix} := \text{augment}(\rho, E_{\text{total}})$$

$$\text{freespacedata01} := \text{augment}(\rho, E_{\text{total_free}})$$

At this point, owing to the nonuniform layout of the distance (from the antenna) points in the ρ array, we will have to distinguish them into several different groups using the following approach:

$$\text{lower} := \text{floor}(\min(\rho))$$

$$\text{upper} := \text{ceil}(\max(\rho))$$

Maximum and minimum distance for this antenna location:

$$\text{upper} = 17$$

$$\text{lower} = 0$$

Groups separation for this calculation (in cm):

$$\text{separation} := 50$$

"Step factor" for this calculation:

$$\text{factor} := \text{ceil}\left(\frac{100}{\text{separation}}\right)$$

factor = 2

Number of distance bins for this calculation:

bins := upper · factor

bins = 34

$$h := \frac{\text{upper} - \text{lower}}{\text{bins}}$$

h = 0.5

n := 0..bins

$k_n := \text{lower} + n \cdot h$

It should be noted that the number of bins may be chosen in a fashion which best suits our desirable "distance steps".

For instance, **should we choose to have groups points separated by 50cm**, where the maximum distance from the antenna is 49m, our intuitive selection should be 98.

We next introduce a new function which shall be utilized several times in our subsequent calculations. As input, it expects a two column matrix and an array. It looks for those values of the first column (i.e., in our problem, the distance array \square), which fall within our made-up groups and then creates a new matrix that contains all those second column's values whose respective first column value satisfy our requirement. It finally returns this new matrix which, it should be underlined, normally has a **different number of elements in each row**.

```

build(M, binvector) :=
  A ← M <0>
  B ← M <1>
  k ← binvector
  for l ∈ 0..rows(k) - 2
    Dl ← 0
  for i ∈ 0..rows(k) - 2
    for j ∈ 0..rows(M) - 1
      Di ← augment(Bj, Di) if ki < Aj ≤ ki+1
  for i ∈ 0..rows(D) - 1
    Di ← submatrix(Di, 0, rows(Di) - 1, 0, cols(Di) - 2) if Di ≠ 0
  D

```

It is high time we used this helping function.

datamatrix02 := build(datamatrix, k)

freespacedata02 := build(freespacedata01, k)

datamatrix02^T =

	0	1	2	3	4	5	6
0	[1,10]	[1,32]	[1,46]	[1,51]	[1,47]	[1,50]	[1,48]

The following new function is, seemingly, of high importance since it is the one which calculates the "normalized difference" random variables. It receives two matrices of the same dimensions and returns a new matrix which in each row contains the values of the random variable pertinent to that row's "distance group."

```

difference(X, Y) :=
  for k ∈ 0..rows(X) - 1
    Ck ← 0
    (
      for j ∈ 0..rows(X) - 1
        n ← cols(Xj)
        A ← Xj
        B ← Yj
        i ← 0
        for i ∈ 0..n - 1
          diffi ← 20·log( $\frac{A_{0,i}}{B_{0,i}}$ )
        n ← cols(Xj)
        Cj ← stack(Cj, diff)
        Cj ← (Cj)T
        k ← rows(Cj)
        l ← cols(Cj)
        Cj ← submatrix(Cj, 0, k - 1, l - 1)
    )
  C

```

The "room gain" is defined here in dB

We now get rid of the redundant first row zeros and then calculate the normalized difference variables.

```
new_datamatrix02 := submatrix(datamatrix02, 1, rows(datamatrix02) - 2, 0, cols(datamatrix02) - 1)
```

```
new_freespacedata02 := submatrix(freespacedata02, 1, rows(freespacedata02) - 2, 0, cols(freespacedata02) - 1)
```

```
norm_diff := difference(new_datamatrix02, new_freespacedata02)
```

```
norm_diffT =
```

	0	1	2	3	4	5	6
0	[1,32]	[1,46]	[1,51]	[1,51]	[1,51]	[1,51]	[1,51]

Surprisingly and unexpectedly the Mathcad appears to suffer from a bug for it returns an erroneous matrix. The cause of this weird occurrence remains unknown, however we shall attempt to effectively overcome this mishap by applying an easy trick.

```
i := 0..rows(new_datamatrix02) - 1
```

```
ri := cols(new_datamatrix02)
```

```
corr_norm_diffi := submatrix(norm_diff, 0, rows(norm_diff) - 1, 0, ri - 1)
```

$$\text{corr_norm_diff}^T = \begin{array}{c|cccccc} & 0 & 1 & 2 & 3 & 4 & 5 & 6 \\ \hline 0 & [1,32] & [1,46] & [1,51] & [1,47] & [1,50] & [1,48] & [1,48] \end{array}$$

This last matrix named "corr_norm_diff" is the one we intended to find. In each row of unequal element number, it contains a different random variable as function of our "devised" groups. Let us take a closer look in one of them, say the 5th.

$$\text{test}_0 := (\text{corr_norm_diff}^T)^{(0)}$$

$$\text{test}_{0_0} = \begin{array}{c|ccccccccc} & 0 & 1 & 2 & 3 & 4 & 5 & 6 & 7 & 8 \\ \hline 0 & 2.395 & -0.754 & 2.494 & -1.278 & -0.751 & -0.465 & 0.245 & -2.726 & -0.447 \end{array}$$

$$\text{mean}(\text{test}_{0_0}) = 0.338$$

$$\text{test}_1 := (\text{corr_norm_diff}^T)^{(1)}$$

$$\text{test}_{1_0} = \begin{array}{c|ccccccccc} & 0 & 1 & 2 & 3 & 4 & 5 & 6 & 7 & 8 \\ \hline 0 & 2.38 & 1.31 & -0.076 & 2.766 & 3.854 & -6.99 & 2.108 & 2.363 & 5.748 \end{array}$$

$$\text{mean}(\text{test}_{1_0}) = 1.121$$

THESE ARE % DIFFERENCE

Defining the number of the bins:

$$N_{\text{points}} := 200$$

$$ii := 0..N_{\text{points}} - 1$$

$$j := 0..\text{rows}(\text{corr_norm_diff}) - 1$$

$$\text{upper}_j := \max(\text{corr_norm_diff}_j)$$

$$\text{lower}_j := \min(\text{corr_norm_diff}_j)$$

$$\text{upper_max} := \max(\text{upper})$$

$$\text{lower_min} := \min(\text{lower})$$

$$\text{step} := \frac{\text{upper_max} - \text{lower_min}}{N_{\text{points}}}$$

$$\text{upper_max} = 13.48$$

$$\text{lower_min} = -11.543$$

$$\text{step} = 0.125$$

$$\text{gen_intervals}_{ii} := \text{lower_min} + \text{step} \cdot ii$$

$$L_j := \frac{\text{hist}(\text{gen_intervals}, \text{corr_norm_diff}_j)}{\text{cols}(\text{corr_norm_diff}_j)}$$

$$\text{rows}(\text{gen_intervals}) = 200$$

$$\text{buildL}(L) := \begin{array}{l} L_{\text{new}} \leftarrow L_0^T \\ \text{for } q \in 1..\text{rows}(L) - 1 \\ \quad A \leftarrow L_q^T \\ \quad L_{\text{new}} \leftarrow \text{stack}(L_{\text{new}}, A) \end{array}$$

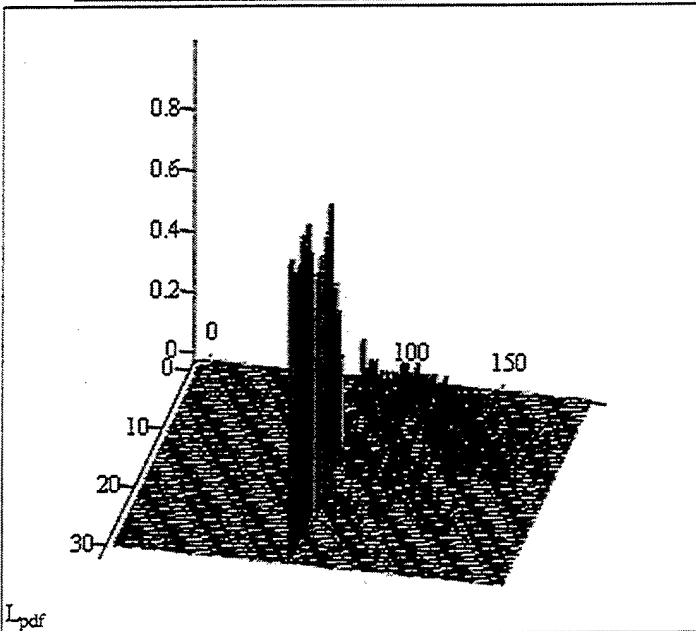
$$L_{\text{pdf}} := \text{buildL}(L)$$

$\text{rows}(L_{\text{pdf}}) = 32$

$\text{cols}(L_{\text{pdf}}) = 199$

$L_{\text{pdf}} =$

	0	1	2	3	4	5	6	7	8	9
0	0	0	0	0	0	0	0	0	0	0
1	0	0	0	0	0	0	0	0	0	0
2	0.02	0	0	0	0	0	0	0	0	0
3	0	0	0.021	0	0	0	0	0	0	0
4	0	0	0	0	0	0	0	0	0	0
5	0	0	0	0	0	0	0	0	0	0
6	0	0	0	0	0	0	0	0	0	0
7	0	0	0	0	0	0	0	0	0	0
8	0	0	0	0	0	0	0	0	0	0
9	0	0	0	0	0	0	0	0	0	0
10	0	0	0	0	0	0	0	0	0	0
11	0	0	0	0	0	0	0	0	0	0
12	0	0	0	0	0	0	0	0	0	0
13	0	0	0	0	0	0	0	0	0	0
14	0	0	0	0	0	0	0	0	0	0
15	0	0	0	0	0	0	0	0	0	0



L_{pdf}

$N_{\text{pdfs}} := \text{cols}(L_{\text{pdf}}) - 1$

$qq := 0..N_{\text{pdfs}} - 1$

$\text{avg_pdf}_{qq} := \text{mean}(L_{\text{pdf}}^{\langle qq \rangle})$

$\sum \text{avg_pdf} = 1$

$$\text{avg_pdf}^T =$$

	88	89	90	91	92	93
0	$5.894 \cdot 10^{-3}$	0.474	$5.24 \cdot 10^{-3}$	$5.734 \cdot 10^{-3}$	$5.304 \cdot 10^{-3}$	$7.015 \cdot 10^{-3}$

$$\text{mean_rv} := \sum_{qq=0}^{N_{\text{pdfs}}-1} \text{gen_intervals}_{qq} \cdot \text{avg_pdf}_{qq}$$

$$\text{mean_rv} = 1.435$$

$$\text{step} = 0.125$$

$$\text{avg_pdf}_{89} := 0.005$$

$$\sum \text{avg_pdf} = 0.531$$

$$\text{avg_pdf} := \frac{\text{avg_pdf}}{\sum \text{avg_pdf}}$$

$$\sum \text{avg_pdf} = 1$$

$$\text{mean_sq_rv} := \sum_{qq=0}^{N_{\text{pdfs}}-1} (\text{gen_intervals}_{qq})^2 \cdot \text{avg_pdf}_{qq}$$

$$\text{mean_sq_rv} = 25.604$$

$$\text{var_rv} := \text{mean_sq_rv} - \text{mean_rv}^2$$

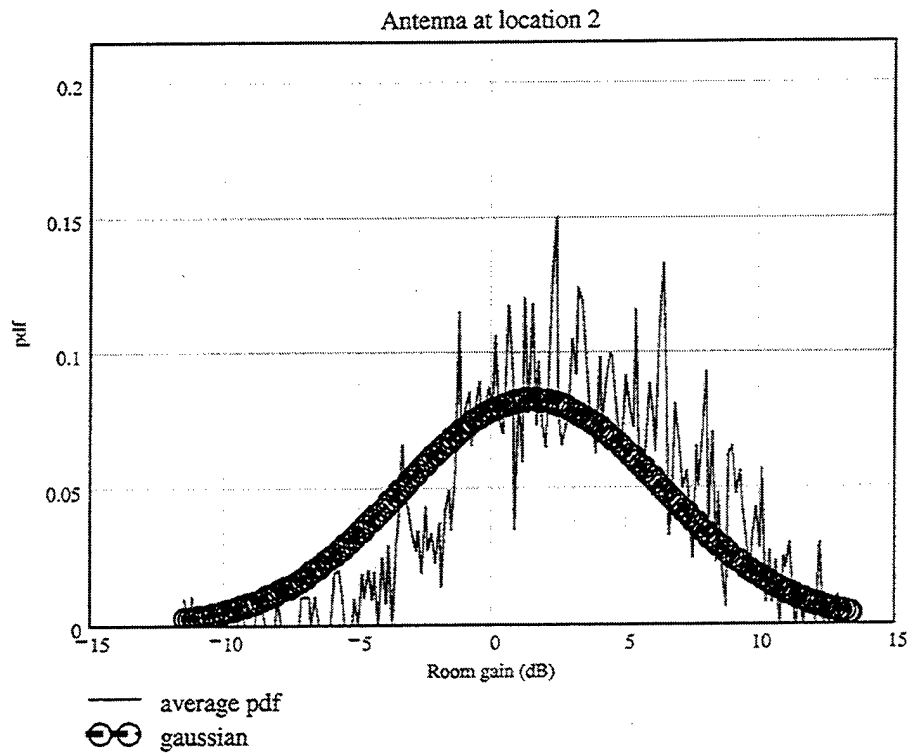
$$\text{var_rv} = 23.545$$

$$\text{mean_rv} = 1.435$$

Defining **Gaussian pdf**:

$$\text{gauss}_{ii} := \frac{1}{\sqrt{2 \cdot \pi \cdot \text{var_rv}}} \cdot e^{\frac{-(\text{gen_intervals}_{ii} - \text{mean_rv})^2}{2 \cdot \text{var_rv}}}$$

$$\text{room_gain}_{\text{dB}} := \text{gen_intervals}$$



$$\text{avg_pdf}^T =$$

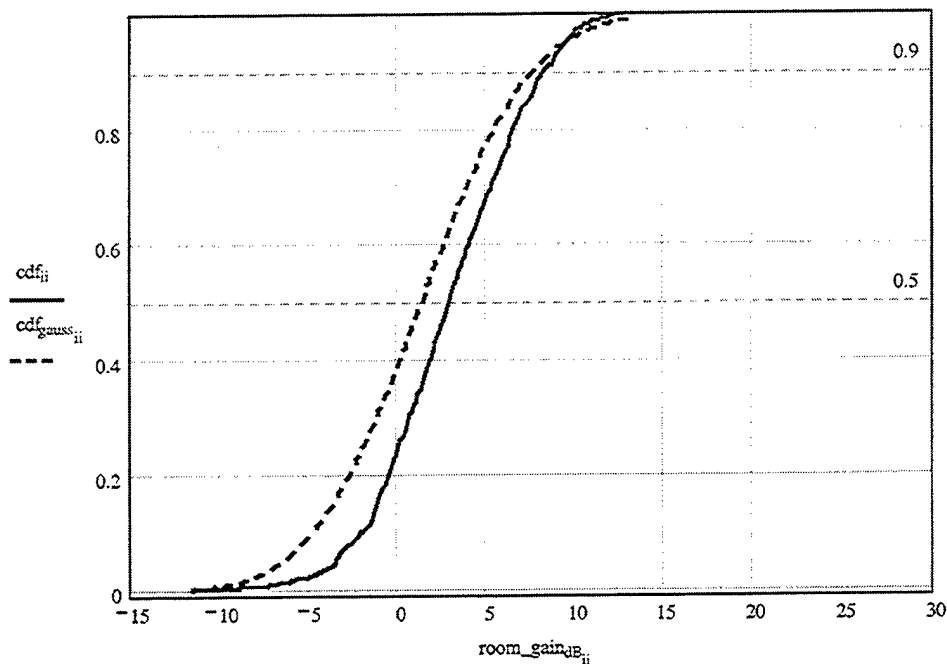
	0	1	2	3	4	5
0	$1.154 \cdot 10^{-3}$		$1.252 \cdot 10^{-3}$	0	0	0

$$\text{gauss}^T =$$

	0	1	2	3	4	5
0	$2.299 \cdot 10^{-3}$	$2.462 \cdot 10^{-3}$	$2.636 \cdot 10^{-3}$	$2.819 \cdot 10^{-3}$	$3.013 \cdot 10^{-3}$	$3.219 \cdot 10^{-3}$

$$\text{cdf}_{\text{qq}} := \sum_{m=0}^{\text{qq}} \text{avg_pdf}_m$$

$$\text{cdf}_{\text{gauss}} := \text{step} \cdot \left(\sum_{m=0}^{\text{ii}} \text{gauss}_m \right)$$



END of MathCAD file used in calculating the excess gain/loss random variables (Second location)

MathCAD file used in calculating the excess gain/loss random variables (Third location)

```

NEC_BSC_data := READPRN("dataroom_b" )
x_coord := NEC_BSC_data <0>
y_coord := NEC_BSC_data <1>
z_coord := NEC_BSC_data <2>
antenna , obser.points in same level

$$\rho := \sqrt{(x_{\text{coord}} - 2)^2 + (y_{\text{coord}} - 2)^2 + (z_{\text{coord}} - 2.2)^2}$$

free_space_data := READPRN("datafree_b" )

$$E_x := \frac{\frac{\text{NEC\_BSC\_data} \langle 3 \rangle}{20}}{10}$$


$$E_y := \frac{\frac{\text{NEC\_BSC\_data} \langle 5 \rangle}{20}}{10}$$


$$E_z := \frac{\frac{\text{NEC\_BSC\_data} \langle 7 \rangle}{20}}{10}$$


```

$$E_{\text{tot}} := \sqrt{(E_x)^2 + (E_y)^2 + (E_z)^2}$$

$$\text{rows}(E_{\text{tot}}) = 1.539 \times 10^3$$

$$E_{x_free} := \left(\frac{\text{free_space_data}^{(3)}}{10^{20}} \right)$$

$$E_{y_free} := 10^{\frac{\text{free_space_data}^{(5)}}{20}}$$

$$E_{z_free} := 10^{\frac{\text{free_space_data}^{(7)}}{20}}$$

$$E_{\text{tot_free}} := \sqrt{(E_{x_free})^2 + (E_{y_free})^2 + (E_{z_free})^2}$$

Since the **NEC-BSC dynamic range** is only 30dB, we will have to account for this fact by "filtering" out all values which are out of that range. This is done in the following fashion:

$$E_{\text{tot_dB}} := (20 \log(E_{\text{tot}}))$$

$$\text{dyn_range} := 30$$

$$jj := 0.. \text{rows}(E_{\text{tot_dB}}) - 1$$

$$\text{lowest_allowed_Etot_value} := \max(E_{\text{tot_dB}}) - \text{dyn_range}$$

$$\text{lowest_allowed_Etot_value} = 22.115$$

$$E_{\text{tot_free_dB}} := (20 \log(E_{\text{tot_free}}))$$

$$\text{lowest_allowed_Etot_fr_val} := \max(E_{\text{tot_free_dB}}) - \text{dyn_range}$$

$$\text{lowest_allowed_Etot_fr_val} = 22.47$$

$$E_{\text{total_dB_jj}} := \text{if}(E_{\text{tot_dB_jj}} < \text{lowest_allowed_Etot_value}, \text{lowest_allowed_Etot_value}, E_{\text{tot_dB_jj}})$$

$$E_{\text{total_free_dB_jj}} := \text{if}(E_{\text{tot_free_dB_jj}} < \text{lowest_allowed_Etot_fr_val}, \text{lowest_allowed_Etot_fr_val}, E_{\text{tot_free_dB_jj}})$$

Converting to linear:

$$E_{\text{total}} := 10^{\frac{E_{\text{total_dB}}}{20}}$$

$$E_{\text{total_free}} := 10^{\frac{E_{\text{total_free_dB}}}{20}}$$

Let us now create the two datamatrices, namely the "datamatrix" which consists of the room's field strength values for every observed point and the "freespacedata01" which includes the corresponding data for the free space case.

$$\text{datamatrix} := \text{augment}(\rho, E_{\text{total}})$$

$$\text{freespacedata01} := \text{augment}(\rho, E_{\text{total_free}})$$

At this point, owing to the nonuniform layout of the distance (from the antenna) points in the \square array, we will have to distinguish them into several different groups using the following approach:

$\text{lower} := \text{floor}(\min(\rho))$

$\text{upper} := \text{ceil}(\max(\rho))$

Maximum and minimum distance for this antenna location:

$\text{upper} = 17$

$\text{lower} = 0$

Groups separation for this calculation (in cm):

$\text{separation} := 50$

"Step factor" for this calculation:

$\text{factor} := \text{ceil}\left(\frac{100}{\text{separation}}\right)$

$\text{factor} = 2$

Number of distance bins for this calculation:

$\text{bins} := \text{upper} \cdot \text{factor}$

$\text{bins} = 34$

$h := \frac{\text{upper} - \text{lower}}{\text{bins}}$

$h = 0.5$

$n := 0.. \text{bins}$

$k_n := \text{lower} + n \cdot h$

It should be noted that the number of bins may be chosen in a fashion which best suits our desirable "distance steps".

For instance, **should we choose to have groups points separated by 50cm**, where the maximum distance from the antenna is 49m, our intuitive selection should be 98.

We next introduce a new function which shall be utilized several times in our subsequent calculations. As input, it expects a two column matrix and an array. It looks for those values of the first column (i.e., in our problem, the distance array \square ..which fall within our made-up groups and then creates a new matrix that contains all those second column's values whose respective first column value satisfy our requirement. It finally returns this new matrix which, it should be underlined, normally has a **different number of elements in each row**.

```

build(M,binvector) :=
  A ← M <0>
  B ← M <1>
  k ← binvector
  for l ∈ 0..rows(k) - 2
    Dl ← 0
  for i ∈ 0..rows(k) - 2
    for j ∈ 0..rows(M) - 1
      Di ← augment(Bj,Di) if ki < Aj ≤ ki+1
  for i ∈ 0..rows(D) - 1
    Di ← submatrix(Di,0,rows(Di) - 1,0,cols(Di) - 2) if Di ≠ 0
  D

```

It is high time we used this helping function.

datamatrix02 := build(datamatrix,k)

freespacedata02 := build(freespacedata01,k)

datamatrix02^T =

	0	1	2	3	4	5	6
0	[1,10]	[1,32]	[1,46]	[1,51]	[1,47]	[1,50]	[1,48]

The following new function is, seemingly, of high importance since it is the one which calculates the "normalized difference" random variables. It receives two matrices of the same dimensions and returns a new matrix which in each row contains the values of the random variable pertinent to that row's "distance group."

```

difference(X, Y) :=
  for k ∈ 0..rows(X) - 1
    Ck ← 0
    (
      for j ∈ 0..rows(X) - 1
        n ← cols(Xj)
        A ← Xj
        B ← Yj
        i ← 0
        for i ∈ 0..n - 1
          diffi ← 20·log( $\frac{A_{0,i}}{B_{0,i}}$ )
        n ← cols(Xj)
        Cj ← stack(Cj, diff)
        Cj ← (Cj)T
        k ← rows(Cj)
        l ← cols(Cj)
        Cj ← submatrix(Cj, 0, k - 1, l - 1)
    )
  C

```

The "room gain" is defined here in dB

We now get rid of the redundant first row zeros and then calculate the normalized difference variables.

```
new_datamatrix02 := submatrix(datamatrix02, 1, rows(datamatrix02) - 2, 0, cols(datamatrix02) - 1)
```

```
new_freespacedata02 := submatrix(freespacedata02, 1, rows(freespacedata02) - 2, 0, cols(freespacedata02) - 1)
```

```
norm_diff := difference(new_datamatrix02, new_freespacedata02)
```

```
norm_diffT =
```

	0	1	2	3	4	5	6
0	[1,32]	[1,46]	[1,51]	[1,51]	[1,51]	[1,51]	[1,51]

Surprisingly and unexpectedly the Mathcad appears to suffer from a bug for it returns an erroneous matrix. The cause of this weird occurrence remains unknown, however we shall attempt to effectively overcome this mishap by applying an easy trick.

```
i := 0..rows(new_datamatrix02) - 1
```

```
ri := cols(new_datamatrix02)
```

```
corr_norm_diffi := submatrix(norm_diffi, 0, rows(norm_diffi) - 1, 0, ri - 1)
```

```
corr_norm_diffT =
```

	0	1	2	3	4	5	6
0	[1,32]	[1,46]	[1,51]	[1,47]	[1,50]	[1,48]	[1,48]

This last matrix named "corr_norm_diff" is the one we intended to find. In each row of unequal element number, it contains a different random variable as function of our

"devised" groups. Let us take a closer look in one of them, say the 5th.

$\text{test}_0 := (\text{corr_norm_diff}^T)^{(0)}$

test_0_0 =	0	1	2	3	4	5	6	7	8
	0	2.195	-1.009	1.082	-2.183	-2.128	-1.118	0.944	-3.434

$\text{mean}(\text{test}_0) = 0.197$

$\text{test}_1 := (\text{corr_norm_diff}^T)^{(1)}$

test_1_0 =	0	1	2	3	4	5	6	7	8
	0	1.067	-2.39	1.257	4.745	4.002	-3.704	2.847	1.616

$\text{mean}(\text{test}_1) = 1.387$

THESE ARE % DIFFERENCE

Defining the number of the bins:

$N_{\text{points}} := 200$

$ii := 0..N_{\text{points}} - 1$

$j := 0.. \text{rows}(\text{corr_norm_diff}) - 1$

$\text{upper}_j := \max(\text{corr_norm_diff}_j)$

$\text{lower}_j := \min(\text{corr_norm_diff}_j)$

$\text{upper_max} := \max(\text{upper})$

$\text{lower_min} := \min(\text{lower})$

$\text{step} := \frac{\text{upper_max} - \text{lower_min}}{N_{\text{points}}}$

$\text{upper_max} = 14.215$

$\text{lower_min} = -10.339$

$\text{step} = 0.123$

$\text{gen_intervals}_{ii} := \text{lower_min} + \text{step} \cdot ii$

$L_j = \frac{\text{hist}(\text{gen_intervals}, \text{corr_norm_diff}_j)}{\text{cols}(\text{corr_norm_diff}_j)}$

$\text{rows}(\text{gen_intervals}) = 200$

$\text{buildL}(L) := \begin{cases} L_{\text{new}} \leftarrow L_0^T \\ \text{for } q \in 1.. \text{rows}(L) - 1 \\ \quad \begin{cases} A \leftarrow L_q^T \\ L_{\text{new}} \leftarrow \text{stack}(L_{\text{new}}, A) \end{cases} \end{cases}$

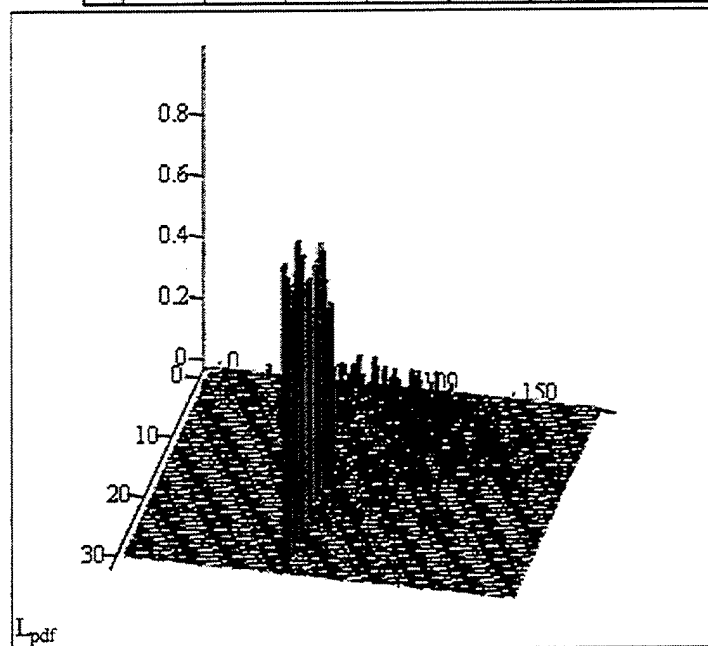
$L_{\text{pdf}} := \text{buildL}(L)$

$\text{rows}(L_{\text{pdf}}) = 32$

$\text{cols}(L_{\text{pdf}}) = 199$

	0	1	2	3	4	5	6	7	8	9
0	0	0	0	0	0	0	0	0	0	0
1	0	0	0	0	0	0	0	0	0	0
2	0	0	0	0	0	0	0	0	0.02	0
3	0.021	0	0	0	0	0	0	0	0	0
4	0	0	0	0	0	0	0	0	0	0
5	0	0	0	0	0	0	0	0	0	0
6	0	0	0	0	0	0	0	0	0	0
7	0	0	0	0	0	0	0	0	0	0
8	0	0	0	0	0	0	0	0	0	0
9	0	0	0	0	0	0	0	0	0	0
10	0	0	0	0	0	0	0	0	0	0
11	0	0	0	0	0	0	0	0	0	0
12	0	0	0	0	0	0	0	0	0	0
13	0	0	0	0	0	0	0	0	0	0
14	0	0	0	0	0	0	0	0	0	0
15	0	0	0	0	0	0	0	0	0	0

$L_{pdf} =$



L_{pdf}

$$N_{pdfs} := \text{cols}(L_{pdf}) - 1$$

$$qq := 0..N_{pdfs} - 1$$

$$\text{avg_pdf}_{qq} := \text{mean}(L_{pdf}^{(qq)})$$

$$\sum \text{avg_pdf} = 0.998$$

gen_intervals ^T =		0	1	2	3	4	5	6	7
	0	-10.339	-10.216	-10.094	-9.971	-9.848	-9.725	-9.603	-9.48

$$\text{avg_pdf}^T =$$

	81	82	83	84	85	86	87
0	0.463	$5.015 \cdot 10^{-3}$	$6.468 \cdot 10^{-3}$	$4.614 \cdot 10^{-3}$	$3.483 \cdot 10^{-3}$	$7.664 \cdot 10^{-3}$	$5.727 \cdot 10^{-3}$

$$\text{avg_pdf}_{s_1} := 0.005$$

$$\sum \text{avg_pdf} = 0.54$$

$$\text{avg_pdf} := \frac{\text{avg_pdf}}{\sum \text{avg_pdf}}$$

$$\sum \text{avg_pdf} = 1$$

$$\text{mean_rv} := \sum_{qq=0}^{N_{\text{pdfs}}-1} \text{gen_intervals}_{qq} \cdot \text{avg_pdf}_{qq}$$

$$\text{step} = 0.123$$

$$\text{mean_rv} = 2.926$$

$$\text{mean_sq_rv} := \sum_{qq=0}^{N_{\text{pdfs}}-1} (\text{gen_intervals}_{qq})^2 \cdot \text{avg_pdf}_{qq}$$

$$\text{mean_sq_rv} = 24.219$$

$$\text{var_rv} := \text{mean_sq_rv} - \text{mean_rv}^2$$

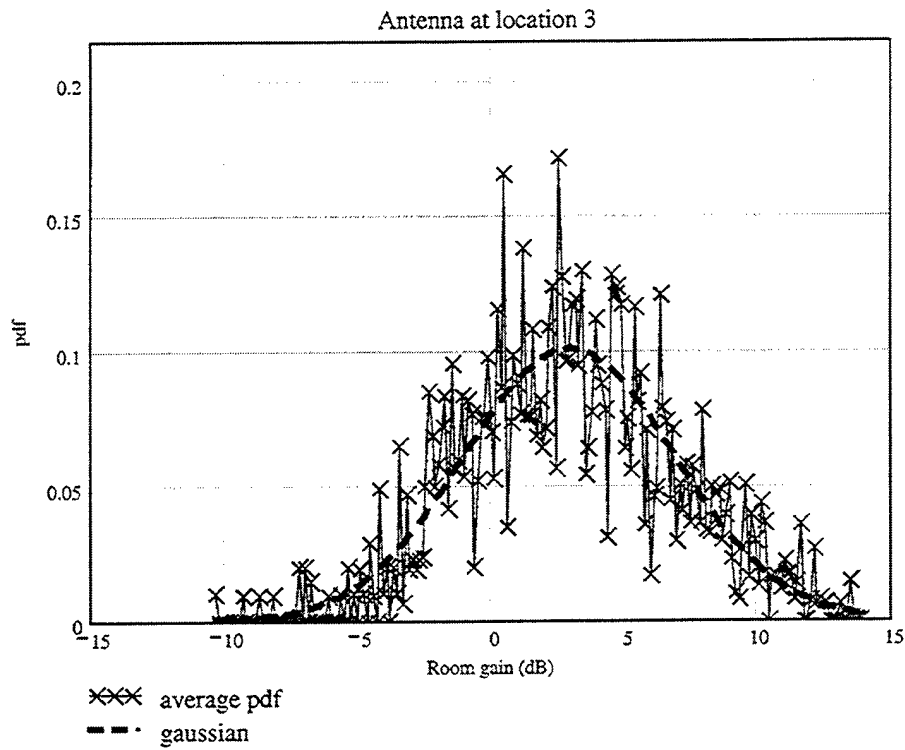
$$\text{var_rv} = 15.658$$

$$\text{mean_rv} = 2.926$$

Defining Gaussian pdf:

$$\text{gauss}_{ii} := \frac{1}{\sqrt{2 \cdot \pi \cdot \text{var_rv}}} \cdot e^{\frac{-(\text{gen_intervals}_{ii} - \text{mean_rv})^2}{2 \cdot \text{var_rv}}}$$

$$\text{room_gain}_{\text{dB}} := \text{gen_intervals}$$



$$\text{avg_pdf}^T =$$

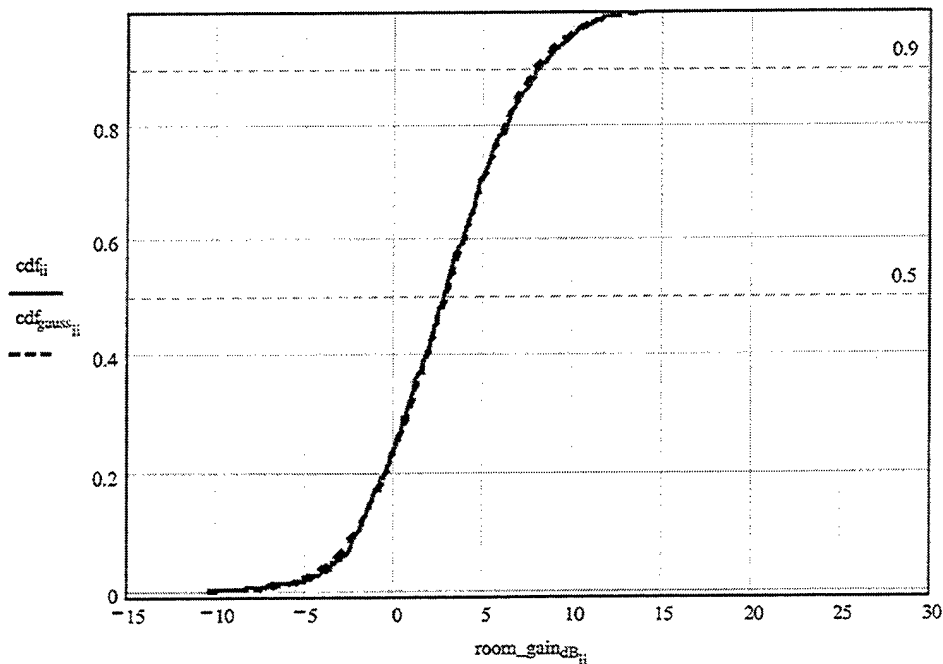
	0	1	2	3	4	5
0	$1.23 \cdot 10^{-3}$	0	0	0	0	0

$$\text{gauss}^T =$$

	0	1	2	3	4	5
0	$3.658 \cdot 10^{-4}$	$4.057 \cdot 10^{-4}$	$4.495 \cdot 10^{-4}$	$4.975 \cdot 10^{-4}$	$5.502 \cdot 10^{-4}$	$6.079 \cdot 10^{-4}$

$$\text{cdf}_{\text{qq}} := \sum_{m=0}^{\text{qq}} \text{avg_pdf}_m$$

$$\text{cdf}_{\text{gauss}_{\text{ii}}} := \text{step} \cdot \left(\sum_{m=0}^{\text{ii}} \text{gauss}_m \right)$$



END of MathCAD file used in calculating the excess gain/loss random variables (Third location)

MathCAD file used in calculating the excess gain/loss random variables (Forth location)

Calculating the normalized difference random variables random position STACK

In this program we are aiming at calculating all the random variables of the normalized difference between the room's and the free space field strength (E_{tot} and E_{tot_free} respectively). We start by reading the associated data files generated by NEC_BSC.

```
NEC_BSC_data1 := READPRN("C:/temp/Thesis/x1c.txt")
```

```
M1 := rows(NEC_BSC_data1)
```

```
M1 = 213
```

```
N1 := cols(NEC_BSC_data1)
```

```
N1 = 9
```

```
NEC_BSC_data2 := READPRN("C:/temp/Thesis/x2c.txt")
```

```
M2 := rows(NEC_BSC_data2)
```

```
M2 = 133
```

```
N2 := cols(NEC_BSC_data2)
```

```
N2 = 9
```

```
NEC_BSC_data3 := READPRN("C:/temp/Thesis/x3c.txt")
```

```

M3 := rows(NEC_BSC_data3)
M3 = 49
N3 := cols(NEC_BSC_data3)
N3 = 9
NEC_BSC_data4 := READPRN("C:/temp/Thesis/x4c.txt")
M4 := rows(NEC_BSC_data4)
M4 = 49
N4 := cols(NEC_BSC_data4)
N4 = 9
NEC_BSC_data5 := READPRN("C:/temp/Thesis/x5c.txt")
M5 := rows(NEC_BSC_data5)
M5 = 77
N5 := cols(NEC_BSC_data5)
N5 = 9
NEC_BSC_data6 := READPRN("C:/temp/Thesis/x6c.txt")
M6 := rows(NEC_BSC_data6)
M6 = 497
N6 := cols(NEC_BSC_data6)
N6 = 9
NEC_BSC_data7 := READPRN("C:/temp/Thesis/x7c.txt")
M7 := rows(NEC_BSC_data7)
M7 = 133
N7 := cols(NEC_BSC_data7)
N7 = 9
NEC_BSC_data8 := READPRN("C:/temp/Thesis/x8c.txt")
M8 := rows(NEC_BSC_data8)
M8 = 49
N8 := cols(NEC_BSC_data8)
N8 = 9
NEC_BSC_data9 := READPRN("C:/temp/Thesis/x9c.txt")
M9 := rows(NEC_BSC_data9)
M9 = 49
N9 := cols(NEC_BSC_data9)
N9 = 9
NEC_BSC_data10 := READPRN("C:/temp/Thesis/x10c.txt")
M10 := rows(NEC_BSC_data10)
M10 = 77
N10 := cols(NEC_BSC_data10)
N10 = 9
NEC_BSC_data11 := READPRN("C:/temp/Thesis/x11c.txt")
M11 := rows(NEC_BSC_data11)
M11 = 213
N11 := cols(NEC_BSC_data11)
N11 = 9

```

```

-----
x_coord := NEC_BSC_data <0>
y_coord := NEC_BSC_data <1>
z_coord := NEC_BSC_data <2>

$$\rho := \sqrt{(x_{\text{coord}} - 4)^2 + (y_{\text{coord}} - 3)^2 + (z_{\text{coord}} - 1)^2}$$

free_space_data1 := READPRN"C:/temp/Thesis/fs1c.txt" )
MM1 := rows(free_space_data1 )
MM1 = 213
NN1 := cols(free_space_data1 )
NN1 = 9
free_space_data2 := READPRN"C:/temp/Thesis/fs2c.txt" )
MM2 := rows(free_space_data2 )
MM2 = 133
NN2 := cols(free_space_data2 )
NN2 = 9
free_space_data3 := READPRN"C:/temp/Thesis/fs3c.txt" )
MM3 := rows(free_space_data3 )
MM3 = 49
NN3 := cols(free_space_data3 )
NN3 = 9
free_space_data4 := READPRN"C:/temp/Thesis/fs4c.txt" )
MM4 := rows(free_space_data4 )
MM4 = 49
NN4 := cols(free_space_data4 )
NN4 = 9
free_space_data5 := READPRN"C:/temp/Thesis/fs5c.txt" )
MM5 := rows(free_space_data5 )
MM5 = 77
NN5 := cols(free_space_data5 )
NN5 = 9
free_space_data6 := READPRN"C:/temp/Thesis/fs6c.txt" )
MM6 := rows(free_space_data6 )
MM6 = 497
NN6 := cols(free_space_data6 )
NN6 = 9
free_space_data7 := READPRN"C:/temp/Thesis/fs7c.txt" )
MM7 := rows(free_space_data7 )
MM7 = 133
NN7 := cols(free_space_data7 )
NN7 = 9
free_space_data8 := READPRN"C:/temp/Thesis/fs8c.txt" )
MM8 := rows(free_space_data8 )

```

```

MM8 = 49
NN8 := cols(free_space_data8 )
NN8 = 9
free_space_data9 := READPRN("C:/temp/Thesis/fs9c.txt" )
MM9 := rows(free_space_data9 )
MM9 = 49
NN9 := cols(free_space_data9 )
NN9 = 9
free_space_data10 := READPRN("C:/temp/Thesis/fs10c.txt" )
MM10 := rows(free_space_data10 )
MM10 = 77
NN10 := cols(free_space_data10 )
NN10 = 9
free_space_data11 := READPRN("C:/temp/Thesis/fs11c.txt" )
MM11 := rows(free_space_data11 )
MM11 = 213
NN11 := cols(free_space_data11 )
NN11 = 9

```

$$E_x := \left(\frac{\text{NEC_BSC_data}^{(3)}}{10} \right)$$

$$E_y := 10 \frac{\text{NEC_BSC_data}^{(5)}}{20}$$

$$E_z := 10 \frac{\text{NEC_BSC_data}^{(7)}}{20}$$

$$E_{\text{tot}} := \sqrt{(E_x)^2 + (E_y)^2 + (E_z)^2}$$

$$\text{rows}(E_{\text{tot}}) = 1.539 \times 10^3$$

$$E_{x_free} := \left(\frac{\text{free_space_data}^{(3)}}{10} \right)$$

$$E_{y_free} := 10 \frac{\text{free_space_data}^{(5)}}{20}$$

$$E_{z_free} := 10 \frac{\text{free_space_data}^{(7)}}{20}$$

$$E_{\text{tot_free}} := \sqrt{(E_{x_free})^2 + (E_{y_free})^2 + (E_{z_free})^2}$$

Since the **NEC-BSC dynamic range** is only 30dB, we will have to account for this fact by "filtering" out all values

which are out of that range. This is done in the following fashion:

```


$$E_{\text{tot\_dB}} := \overrightarrow{(20 \log(E_{\text{tot}}))}$$


$$\text{dyn\_range} := 30$$


$$jj := 0.. \text{rows}(E_{\text{tot\_dB}}) - 1$$


$$\text{lowest\_allowed\_Etot\_value} := \max(E_{\text{tot\_dB}}) - \text{dyn\_range}$$


$$\text{lowest\_allowed\_Etot\_value} = 28.39$$


$$E_{\text{tot\_free\_dB}} := \overrightarrow{(20 \log(E_{\text{tot\_free}}))}$$


$$\text{lowest\_allowed\_Etot\_fr\_val} := \max(E_{\text{tot\_free\_dB}}) - \text{dyn\_range}$$


$$\text{lowest\_allowed\_Etot\_fr\_val} = 28.51$$


$$E_{\text{total\_dB}}_{jj} := \text{if} \left[ (E_{\text{tot\_dB}}_{jj}) < \text{lowest\_allowed\_Etot\_value}, \text{lowest\_allowed\_Etot\_value}, E_{\text{tot\_dB}}_{jj} \right]$$


$$E_{\text{total\_free\_dB}}_{jj} := \text{if} \left( E_{\text{tot\_free\_dB}}_{jj} < \text{lowest\_allowed\_Etot\_fr\_val}, \text{lowest\_allowed\_Etot\_fr\_val}, E_{\text{tot\_free\_dB}}_{jj} \right)$$


```

Converting to linear:

```


$$E_{\text{total}} := 10^{\frac{E_{\text{total\_dB}}}{20}}$$


$$E_{\text{total\_free}} := 10^{\frac{E_{\text{total\_free\_dB}}}{20}}$$


```

Let us now create the two datamatrices, namely the "datamatrix" which consists of the room's field strength values for every observed point and the "freespacedata01" which includes the corresponding data for the free space case.

```

datamatrix := augment( $\rho$ ,  $E_{\text{total}}$ )
freespacedata01 := augment( $\rho$ ,  $E_{\text{total\_free}}$ )

```

At this point, owing to the nonuniform layout of the distance (from the antenna) points in the \square array, we will have to distinguish them into several different groups using the following approach:

```

lower := floor(min( $\rho$ ))
upper := ceil(max( $\rho$ ))

```

Maximum and minimum distance for this antenna location:

```

upper = 15
lower = 0

```

Groups separation for this calculation (in cm):

```

separation := 50

```

"Step factor" for this calculation:

```

factor := ceil( $\frac{100}{\text{separation}}$ )
factor = 2

```

Number of distance bins for this calculation:


```
bins := upper-factor
```

```
bins = 30
```

```
h :=  $\frac{\text{upper} - \text{lower}}{\text{bins}}$ 
```

```
h = 0.5
```

```
n := 0..bins
```

```
 $k_n := \text{lower} + n \cdot h$ 
```

It should be noted that the number of bins may be chosen in a fashion which best suits our desirable "distance steps".

For instance, **should we choose to have groups points separated by 50cm**, where the maximum distance from the antenna is 49m, our intuitive selection should be 98.

We next introduce a new function which shall be utilized several times in our subsequent calculations. As input, it expects a two column matrix and an array. It looks for those values of the first column (i.e., in our problem, the distance array \square), which fall within our made-up groups and then creates a new matrix that contains all those second column's values whose respective first column value satisfy our requirement. It finally returns this new matrix which, it should be underlined, normally has a **different number of elements in each row**.

```
build(M, binvector) :=  $\left\{ \begin{array}{l} A \leftarrow M^{(0)} \\ B \leftarrow M^{(1)} \\ k \leftarrow \text{binvector} \\ \text{for } l \in 0.. \text{rows}(k) - 2 \\ \quad D_l \leftarrow 0 \\ \text{for } i \in 0.. \text{rows}(k) - 2 \\ \quad \text{for } j \in 0.. \text{rows}(M) - 1 \\ \quad \quad D_i \leftarrow \text{augment}(B_j, D_i) \text{ if } k_i < A_j \leq k_{i+1} \\ \text{for } i \in 0.. \text{rows}(D) - 1 \\ \quad D_i \leftarrow \text{submatrix}(D_i, 0, \text{rows}(D_i) - 1, 0, \text{cols}(D_i) - 2) \text{ if } D_i \neq 0 \end{array} \right.$ 
```

It is high time we used this helping function.

```
datamatrix02 := build(datamatrix, k)
```

```
freespacedata02 := build(freespacedata01, k)
```

```
datamatrix02T = 

|   |        |        |        |        |        |        |        |
|---|--------|--------|--------|--------|--------|--------|--------|
|   | 0      | 1      | 2      | 3      | 4      | 5      | 6      |
| 0 | [1,14] | [1,30] | [1,33] | [1,63] | [1,71] | [1,76] | [1,94] |


```

The following new function is, seemingly, of high importance since it is the one which calculates the "normalized difference" random variables. It receives two matrices of the same dimensions and returns a new matrix

which in each row contains the values of the random variable pertinent to that row's "distance group."

```

difference(X,Y) :=
  for k ∈ 0..rows(X) - 1
    Ck ← 0
    (
      for j ∈ 0..rows(X) - 1
        n ← cols(Xj)
        A ← Xj
        B ← Yj
        i ← 0
        for i ∈ 0..n - 1
          diffi ← 20·log( $\frac{A_{0,i}}{B_{0,i}}$ )
          n ← cols(Xj)
          Cj ← stack(Cj, diff)
          Cj ← (Cj)T
          k ← rows(Cj)
          l ← cols(Cj)
          Cj ← submatrix(Cj, 0, k - 1, 1, l - 1)
    )
  C

```

The "room gain" is defined here in dB

We now get rid of the redundant first row zeros and then calculate the normalized difference variables.

```

new_datamatrix02 := submatrix(datamatrix02, 1, rows(datamatrix02) - 2, 0, cols(datamatrix02) - 1)
new_freespacedata02 := submatrix(freespacedata02, 1, rows(freespacedata02) - 2, 0, cols(freespacedata02) - 1)
norm_diff := difference(new_datamatrix02, new_freespacedata02)

```

norm_diff^T =

	0	1	2	3	4	5	6
0	[1,30]	[1,33]	[1,63]	[1,71]	[1,76]	[1,94]	[1,99]

Surprisingly and unexpectedly the Mathcad appears to suffer from a bug for it returns an erroneous matrix. The cause of this weird occurrence remains unknown, however we shall attempt to effectively overcome this mishap by applying an easy trick.

```

i := 0..rows(new_datamatrix02) - 1
ri := cols(new_datamatrix02)
corr_norm_diffi := submatrix(norm_diffi, 0, rows(norm_diffi) - 1, 0, ri - 1)

```

corr_norm_diff^T =

	0	1	2	3	4	5	6
0	[1,30]	[1,33]	[1,63]	[1,71]	[1,76]	[1,94]	[1,99]

This last matrix named "corr_norm_diff" is the one we intended to find. In each row of unequal element number, it

contains a different random variable as function of our "devised" groups. Let us take a closer look in one of them, say the 5th.

$\text{test}_0 := (\text{corr_norm_diff}^T)^{(0)}$

test_0_0 =		0	1	2	3	4	5	6	7
	0	0.078	-2.592	0.235	-0.191	3.503	3.511	-10.335	-0.102

$\text{mean}(\text{test}_{00}) = 0.529$

$\text{test}_1 := (\text{corr_norm_diff}^T)^{(1)}$

	0	1	2	3	4	5	6	7	8	
test_10 =	0	0.171	-4.62	0.389	-0.842	-2.145	3.178	2.166	-3.219	1.823

$\text{mean}(\text{test}_{10}) = -0.346$

THESE ARE % DIFFERENCE

Defining the number of the bins:

$N_{\text{points}} := 200$

$ii := 0..N_{\text{points}} - 1$

$j := 0.. \text{rows}(\text{corr_norm_diff}) - 1$

$\text{upper}_j := \max(\text{corr_norm_diff}_j)$

$\text{lower}_j := \min(\text{corr_norm_diff}_j)$

$\text{upper_max} := \max(\text{upper})$

$\text{lower_min} := \min(\text{lower})$

$\text{step} := \frac{\text{upper_max} - \text{lower_min}}{N_{\text{points}}}$

$\text{upper_max} = 12.092$

$\text{lower_min} = -10.335$

$\text{step} = 0.112$

$\text{gen_intervals}_{ii} := \text{lower_min} + \text{step} \cdot ii$

$L_j := \frac{\text{hist}(\text{gen_intervals}, \text{corr_norm_diff}_j)}{\text{cols}(\text{corr_norm_diff}_j)}$

$\text{rows}(\text{gen_intervals}) = 200$

$\text{buildL}(L) := \begin{array}{l} L_{\text{new}} \leftarrow L_0^T \\ \text{for } q \in 1.. \text{rows}(L) - 1 \\ \quad A \leftarrow L_q^T \\ \quad L_{\text{new}} \leftarrow \text{stack}(L_{\text{new}}, A) \end{array}$

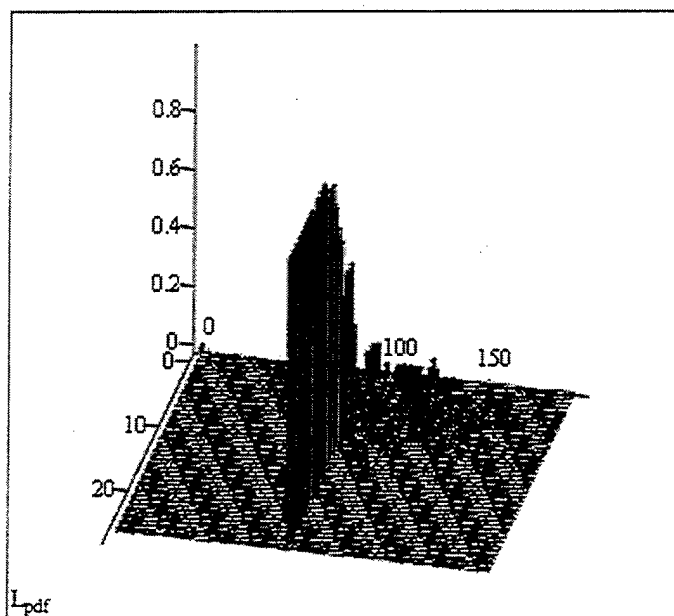
$L_{\text{pdf}} := \text{buildL}(L)$

$\text{rows}(L_{\text{pdf}}) = 28$

$\text{cols}(L_{\text{pdf}}) = 199$

$$L_{pdf} =$$

	0	1	2	3	4	5	6	7	8	9
0	0.033	0	0	0	0	0	0	0	0	0
1	0	0	0	0	0	0.03	0	0	0	0
2	0	0	0	0	0	0	0	0	0	0
3	0	0	0	0	0	0	0	0	0	0
4	0	0	0	0	0	0	0	0	0	0
5	0	0	0	0	0	0	0	0	0	0
6	0	0	0	0	0	0	0	0	0	0
7	0	0	0	0	0	0	0	0	0	0
8	0	0	0	0	0	0	0	0	0	0
9	0	0	0	0	0	0	0	0	0	0
10	0	0	0	0	0	0	0	0	0	0
11	0	0	0	0	0	0	0	0	0	0
12	0	0	0	0	0	0	0	0	0	0
13	0	0	0	0	0	0	0	0	0	0
14	0	0	0	0	0	0	0	0	0	0
15	0	0	0	0	0	0	0	0	0	0



$$N_{pdfs} := \text{cols}(L_{pdf}) - 1$$

$$qq := 0..N_{pdfs} - 1$$

$$\text{avg_pdf}_{qq} := \text{mean}(L_{pdf}^{(qq)})$$

$$\sum \text{avg_pdf} = 1$$

$$\text{avg_pdf}^T =$$

	4	5	6	7	8	9
0	0	$1.082 \cdot 10^{-3}$	0	0	0	0

$$\text{mean_rv} := \sum_{qq=0}^{N_{\text{pdfs}}-1} \text{gen_intervals}_{qq} \cdot \text{avg_pdf}_{qq}$$

$$\text{mean_rv} = 0.577$$

$$\text{step} = 0.112$$

$$\text{avg_pdf}_{91} := 0.005$$

$$\sum \text{avg_pdf} = 0.329 \quad \text{avg_pdf} := \frac{\text{avg_pdf}}{\sum \text{avg_pdf}}$$

$$\sum \text{avg_pdf} = 1$$

$$\text{mean_sq_rv} := \sum_{qq=0}^{N_{\text{pdfs}}-1} (\text{gen_intervals}_{qq})^2 \cdot \text{avg_pdf}_{qq}$$

$$\text{mean_sq_rv} = 15.621$$

$$\text{var_rv} := \text{mean_sq_rv} - \text{mean_rv}^2$$

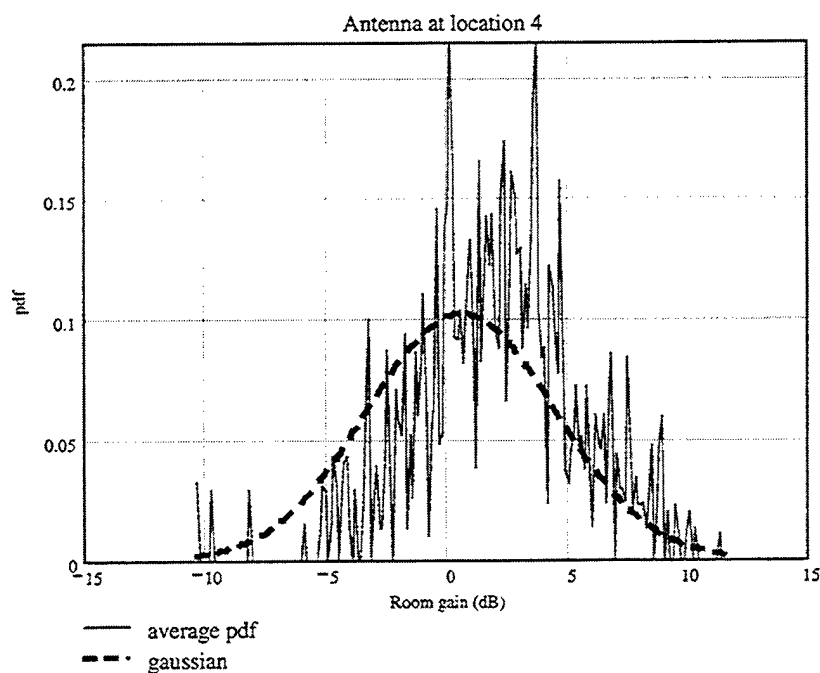
$$\text{var_rv} = 15.288$$

$$\text{mean_rv} = 0.577$$

Defining **Gaussian pdf**:

$$\text{gauss}_{ii} := \frac{1}{\sqrt{2 \cdot \pi \cdot \text{var_rv}}} \cdot e^{\frac{-(\text{gen_intervals}_{ii} - \text{mean_rv})^2}{2 \cdot \text{var_rv}}}$$

$$\text{room_gain}_{\text{dB}} := \text{gen_intervals}$$



$$\text{avg_pdf}^T =$$

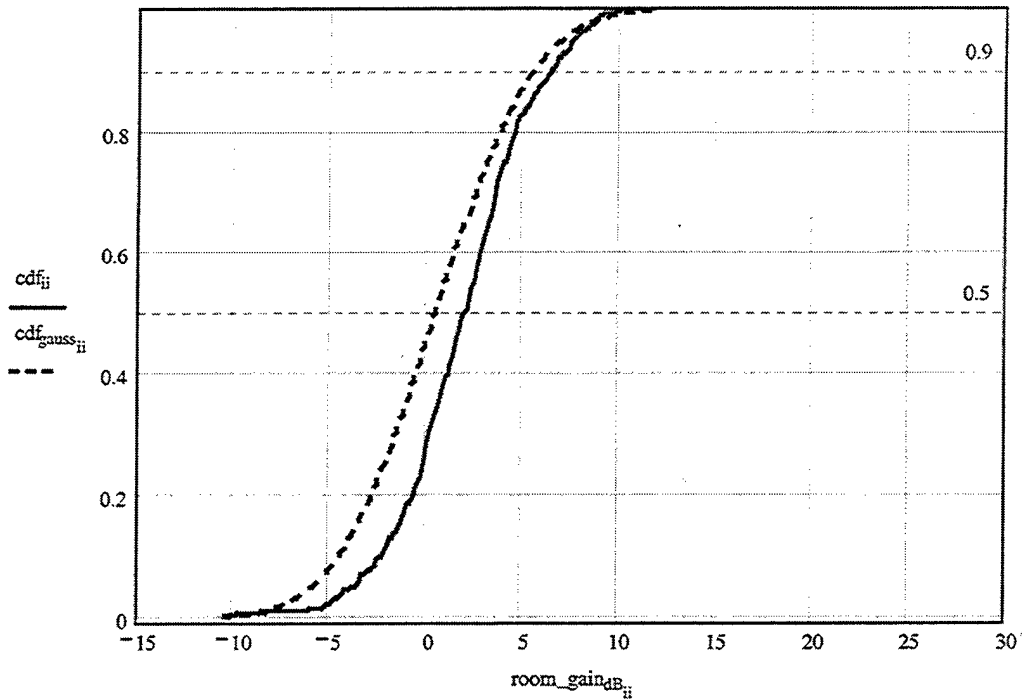
	0	1	2	3	4	5
0	$3.623 \cdot 10^{-3}$	0	0	0	0	$3.293 \cdot 10^{-3}$

$$\text{gauss}^T =$$

	0	1	2	3	4	5
0	$2.077 \cdot 10^{-3}$	$2.249 \cdot 10^{-3}$	$2.433 \cdot 10^{-3}$	$2.631 \cdot 10^{-3}$	$2.842 \cdot 10^{-3}$	$3.067 \cdot 10^{-3}$

$$\text{cdf}_{\text{qq}} := \sum_{m=0}^{\text{qq}} \text{avg_pdf}_m$$

$$\text{cdf}_{\text{gauss}_{ii}} := \text{step} \cdot \left(\sum_{m=0}^{ii} \text{gauss}_m \right)$$



END of MathCAD file used in calculating the excess gain/loss random variables (Forth location)

End of all MathCAD files

LIST OF REFERENCES

1. H. Hashemi, "The Indoor Propagation Channel," *Proceedings of the IEEE*, Vol.81, No.7, July 1993, pp.943-968.
2. D. Molkdar, "Review on Radio Propagation into and within Buildings," *IEE Proceedings-H*, Vol.138, No.1, February 1991, pp.61-73.
3. T.S. Rappaport, *Wireless Communications*, Prentice Hall Inc., Upper Saddle River, New Jersey, 1999.
4. <http://www.radio.gov.uk/busunit/research/antenna/antennas.htm#Contents>
5. J. Andersen, T. Rappaport, and S. Yoshida, "Propagation Measurements and Models for Wireless Communications Channels," *IEEE Communications Magazine*, January 1995, pp.42-49.
6. http://www.deas.harvard.edu/~jones/es151/prop_models/propagation.html#antennafun
7. [http://www.osha-slc.gov/SLTC/radiofrequencyradiation/electromagnetic_fieldmemo/electromagnetic.html#Section 6.](http://www.osha-slc.gov/SLTC/radiofrequencyradiation/electromagnetic_fieldmemo/electromagnetic.html#Section%206)
8. [<http://sss-mag.com/indoor.html>]
9. W. A. Johnson, D. R. Wilton, R. M. Sharpe, "Patch code User's Manual," *Sandia Report San87-2991*, May 1988.
10. M. F. Ibrahim, and J. D. Parsons, "Signal strength prediction in built up areas, part 1: median signal strength," *IEE Proc. F*, 1983, 130, pp.377-384.
11. Y. Okumura, T. Kawano, E. Ohmori, K. Fukuda, "Field strength and its variability in V.H.F. and U.H.F. land mobile radio service," *Review of Communications Lab.*, 1968, 16, pp.825-873.
12. M. Hata, "Empirical formula for propagation loss in land mobile radio services," *IEEE Transactions Vehicular Technology*, 1980, VT-29, pp.317-325.

13. R. J. Bultitude, S. A. Mahmoud, and A. Sullival, "A comparison of indoor propagation characteristics at 910 MHz and 1.75 GHz," *IEEE J. Select Areas Commun.*, vol. 7, pp. 20-30, Jan. 1989.
14. T. S. Rappaport and C. D. McGillem, "UHF fading in factories," *IEEE J. Select Areas Commun.*, vol. 7, pp. 40-48, Jan. 1989.
15. R. Ganesh and K. Pahlavan, "Statistics of short time variation of indoor radio propagation," in *Proc. Int. Conf. Comm. ICC'91*, Denver, CO, June 23-36, 1991, pp. 1-5.
16. H. Hashemi, M. McGuire, T. Vlasschaert and D. Tholl, "Measurements and modeling of temporal variations of the indoor radio propagation channel," *IEEE Transactions Vehicular Technology*, vol 43, pp. 733-737, Aug. 1994.
17. <http://www.imec.be/5/1995/figs/fig72.html>
18. S.R. Saunders, *Antennas and Propagation for Wireless Communication Systems*, John Wiley & Sons, New York, NY, Inc, 1999.
19. R. Grosskopf, "GTD-Based indoor propagation prediction method," *Millennium Conference on Antennas and Propagation AP2000*, Davos, Switzerland, 9-14 April 2000.
20. P. H. Pathak, "Techniques for high-frequency problems," in *Antenna Handbook: Theory, Applications, and Design*, (Y. T. Lo and S. W. Lee, eds.), ch. 4, New York: Van Nostrand Reinhold Co Inc., 1988.
21. P. Selormey and Y. Miyazaki, "Propagation and Interference Characteristics by Group of Buildings in Mobile Communication Channels," *Proceedings of ISAP 2000*, Fukuoka, Japan, August 2000.
22. M.F. Catedra, J. Perez, F. Saez de Adana and O. Gutierrez, "Efficient Ray-Tracing Techniques for Three-Dimensional Analyses of Propagation in Mobile Communications: Application to Picocell and Microcell

Scenarios," *IEEE Antennas and Propagation Magazine*, Vol.40, No.2, April 1998, pp.15-28.

23. M.F. Catedra, J. Perez, F. Saez de Adana and O. Gutierrez, "Efficient Ray-Tracing Techniques for Three-Dimensional Analyses of Propagation in Mobile Communications: Application to Picocell and Microcell Scenarios," *IEEE Antennas and Propagation Magazine*, Vol.40, No.2, April 1998, pp.15-28.
24. W. Honcharenko, H.L. Bertoni and J. Dailing, "Theoretical Prediction of UHF Propagation within Office Buildings," *1st International Conference on Universal Personal Communications Proceedings*, 1992, pp.04.04/1-04.04/4.
25. S.Y. Seidel and T.S. Rappaport, "A Ray Tracing Technique to Predict Path Loss and Delay Spread Inside Buildings," *IEEE Global Communications Conference Proceedings*, 1992, vol.2, pp.649-653.
26. K. W. Cheung, J. H. M. Sau and R. D. Murch, "A New Empirical Model for Indoor Propagation Prediction," *IEEE Transactions on Vehicular Technology*, Vol.47, No.3, August 1998, pp.996-1001.
27. A. Neskovic, Natasa Neskovic and Dodre Paunovic, "Indoor Electric Field Level Prediction Model Based on the Artificial Neural Networks," *IEEE Communications Letters*, Vol.4, No.6, June 2000, pp.190-192.
28. Naval Research Laboratory, *Initial Bistatic Measurements of Electromagnetic Propagation in an Enclosed Ship Environment*, by E.L. Mokole, M. Parent, J. Valenzi, E. Thomas, B.T. Gold, T.T. Street, February 1998.
29. D. B. Newman, Jr. "FCC authorizes spread spectrum," *IEEE Communications Magazine*, pp.46-47, July, 1986.
30. W. Honcharenko, H.L. Bertoni, J.L. Dailing, J. Qian and H.D. Yee, "Mechanisms Governing UHF Propagation on Single Floors in Modern Office Buildings," *IEEE Transactions on Vehicular Technology*, Vol.41, No.4, November 1992, pp.496-504.

31. E.H. Newman and R.J. Marhefka, "Overview of MM and UTD Methods at the Ohio State University," *Proceedings of the IEEE*, Vol.77, No.5, May 1989, pp.700-708.
32. Keller J.B. "A geometrical theory of diffraction In Calculus of variations and its applications," edited by Graves L.M., McGraw Hill Book Co., New York, 1958, pp.27-52.
33. Keller J.B. "Geometrical theory of diffraction," *Jour. Opt. Soc. Amer.*, Vol 52, 1962, pp.116-130.
34. R.J. Marhefka, "Numerical Electromagnetic Code-Basic Scattering Code, NEC-BSC (Version 4.2), User's Manual," Installation Package, Joint Preliminary Report, December 1998, The Ohio State University Electrosience Laboratory, Department of Electrical Engineering, prepared under Contract No. N66001-97-C-6013.
35. D. Ndzi, J. Austin and E. Vilar, "Indoor Channel Characterisation Using Hyper-Resolution Impulse Response," *Millennium Conference on Antennas and Propagation AP2000*, Davos, Switzerland, 9-14 April 2000.
36. J. Lebaric, R. Adler, C. Deyannis and D. Xifaras, *Effects of Fire and Fire Extinguishing on Wireless Communications in the 2.4 GHz ISM Band*, Naval Postgraduate School, Monterey, CA, June 6, 2000.
37. Andre Fourie and Derek Nitch, "SuperNEC: Antenna & Indoor Propagation Simulation Program," *IEEE Antennas & Propagation Magazine*, Vol.42, No.3, June 2000, pp.31-48.
38. Ilias Bolanis, *Prediction of Wireless Communication Systems Performance in Indoor Applications*, Master's Thesis, Naval Postgraduate School, Monterey, CA, December, 2000.
39. H. Hashemi, "The Indoor Propagation Channel," *Proceedings of the IEEE*, Vol.81, No.7, July 1993, pp.943-968.

metallic furniture," *IEEE Transactions on Antennas & Propagation*, Vol.45, No.1, Jan. 1997, pp. 98-106.

41. R.J. Marhefka, "Numerical Electromagnetic Code-Basic Scattering Code, NEC-BSC (Version 3), User's Manual," *Technical Report 718422-3*, 1989, The Ohio State University Electrosience Laboratory, Department of Electrical Engineering, prepared under Contract No. N60530-85-C-0249 for Naval Weapons Center.
42. D.I. Laurenson, A.U.H. Sheikh and S. McLaughlin, "Characterisation of the Indoor Mobile Radio Channel Using a Ray Tracing Technique," *IEEE International Conference on Selected Topics in Wireless Communications*, 1992, pp.65-68.
43. S.R. Saunders, *Antennas and Propagation for Wireless Communication Systems*, John Wiley & Sons, New York, NY, Inc, 1999.

THIS PAGE INTENTIONALLY LEFT BLANK

INITIAL DISTRIBUTION LIST

1. Defense Technical Information Center 2
8725 John J. Kingman Rd., STE 0944
Ft. Belvoir, Virginia 22060-6218
2. Dudley Knox Library 2
Naval Postgraduate School
411 Dyer Road
Monterey, California 93943-5101
3. Engineering and Technology Curriculum Code 34 2
Naval Postgraduate School
700 Dyer Road, Room 115
Monterey, CA 93943-5107
4. Chairman, Code EC 1
Electrical and Computer Engineering Department
Naval Postgraduate School
Monterey, CA 93943-5121
5. Dr. Jovan Lebaric, Code EC/Lb 2
Electrical and Computer Engineering Department
Naval Postgraduate School
Monterey, CA 93943-5121
6. Dr. Richard Adler, Code EC/Ab 1
Electrical and Computer Engineering Department
Naval Postgraduate School
Monterey, CA 93943-5121
7. Hellenic Navy General Staff 2
Department B/2, Stratopedo Papagoy, Mesogeiwn 151,
Holargos, 155-00, Athens,
Greece
8. Dr. Ronald J. Marhefka 1
The Ohio State University Electrosience Laboratory
1320 Kinnear Rd
Columbus, OH 43212-1191
9. LT.J.G John Martinos H.N. 2
Zalokosta 12, Halandri, Athens, TK 15233,
Greece